TASK-RELATED AND RESTING-STATE MOTOR CONNECTIVITY IN AGING AND STROKE INDIVIDUALS

Sara Larivière

Department of Neurology and Neurosurgery

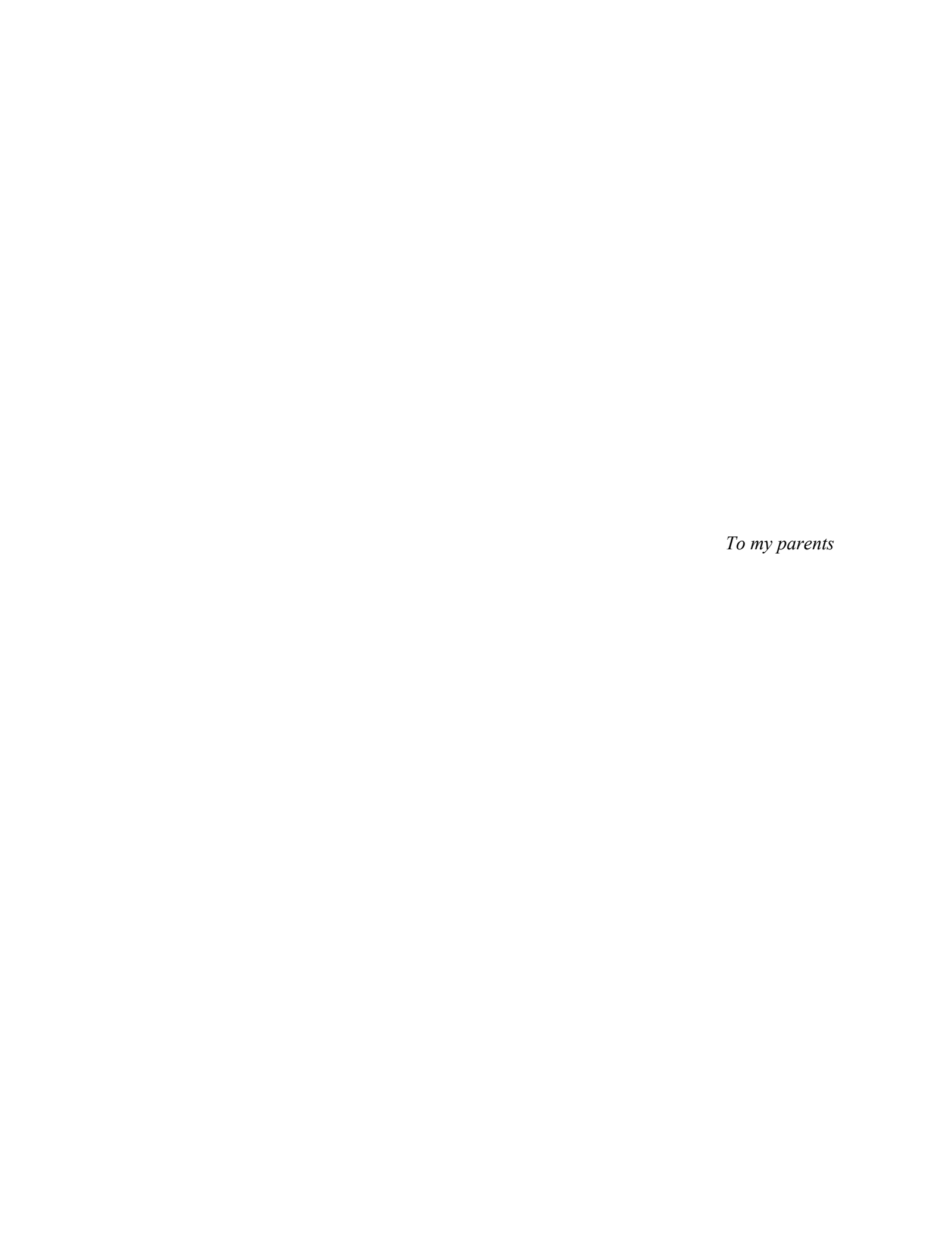
McGill University, Montreal, Canada

August 2017

A thesis submitted to McGill University

in partial fulfillment of the requirements of the degree of Master of Science

©Sara Larivière, 2017



ACKNOWLEDGEMENTS

My sincere appreciation to my supervisors, Marie-Hélène Boudrias and Georgios D. Mitsis, who have provided me with the guidance, direction, and support towards my training and research development.

Special thanks go out to all of the subjects and patients who took part in our research. Their involvement, curiosity, enthusiasm, and endless patience were an essential part of the studies.

Many thanks to my labmates and friends who made the laboratory a fantastic working environment: Fabien Dal Maso, Arna Gosh, Michalis Kassinopoulos, Mohand Khouider, Michael Kleinman, Kyriaki Kostoglou, Gregory Laredo, Prokopis Prokopiou, Jérôme Williams, Alba Xifra-Porxas.

I would like to thank all the people at the MNI, notably: Alexander DeGuise, Vivian Omune, Mirko Sablich, and Katherine Vanka from the IPN for providing ongoing advice and guidance; Elizabeth Bock, David Costa, Ron Lopez, and Louise Marcotte from the BIC for their generous help with the acquisition and processing of imaging data.

Numerous thanks to my committee members, Richard Hoge and David Ostry. Their expertise and wise advice were extremely valuable.

CONTRIBUTIONS OF AUTHORS

The body of work presented in this thesis would not have been made possible without a close collaboration between myself and my M.Sc. supervisors, **Marie-Hélène Boudrias** and **Georgios D. Mitsis**. Listed below are the specific contributions:

Marie-Hélène Boudrias – For experiments 1–3: designed the experiments, helped with participant recruitment, assisted in the interpretation of results, and helped with writing the manuscripts. For experiment 3: collected and provided behavioral and imaging data from stroke patients and control subjects.

Georgios D. Mitsis – For experiments 1 and 2: helped with designing the experiments, assisted in the network connectivity analysis, provided advice on statistical analysis, and helped with the interpretation of results (including experiment 3).

The following list contains the other co-authors, in alphabetical order, who have greatly contributed to the manuscripts:

Michalis Kassinopoulos – Assisted in the implementation of the motor tasks for experiment 1. Assisted in data collection for experiments 1 and 2.

Guiomar Niso – Assisted in the study design and implementation of the motor tasks for experiment 1. Provided advice for the analysis of MEG data for experiments 1 and 2.

Nick S. Ward – Provided behavioral and imaging data from stroke patients and control subjects for experiment 3.

Alba Xifra-Porxas – Participated in the implementation of the motor tasks, helped with participant recruitment, assisted in data collection, as well as helped with the MEG connectivity analyses and interpretation of results for experiments 1 and 2.

ABSTRACT

Background: Motor deficits observed during aging have been shown to be linked with changes in brain structure and functional organization. To date, univariate mapping of functional activity during upper limb movement has mainly focused on changes in the primary motor cortex. However, debate lingers as to how alterations in whole-brain connectivity relate to motor decline observed in elderly subjects. Identification of large-scale connectivity features characterizing the functional reorganization underlying healthy aging could provide insights into understanding residual motor functioning and recovery processes in chronic stroke patients with persistent motor disabilities.

Purpose: Our overarching goal was to investigate the reorganization of functionally-connected networks at rest and during execution of hand movements in aging and stroke individuals.

Methods: The following three experiments are included in this thesis: (1) using a combination of principal component analysis (PCA) and Granger causality on magnetoencephalographic (MEG) data to investigate age-dependent alterations in functional connectivity in whole-brain networks underlying the production of unimanual and bimanual visually-guided isometric hang grips, (2) comparing the effects of performing hand movement on resting-state functional connectivity in young and elderly healthy individuals using envelope correlation on MEG source-reconstructed time series, and (3) assessing functional magnetic resonance imaging (fMRI) connectivity in shared whole-brain networks underlying the production of visually-paced isometric hand grips in individuals with chronic stroke and healthy controls through a combination of multivariate multiple regression and PCA.

Results: Brain reorganization during hand movement in elderly individuals was characterized by overall increased activity in task-specific networks and greater information flow to the left primary motor cortex. Contrastingly, chronic stroke patients with partial hand motor recovery were characterized with overall decreased connectivity

within a large-scale motor network. Alterations in this network appeared to be driven by reduced activity in ipsilesional sensorimotor (M1/S1) regions. The degree of activity within ipsilesional M1/S1 also correlated with motor performance in the stroke group.

Significance: Our findings expanded upon previous research by contributing to the understanding of network-wide brain reorganization during hand movement as well as providing novel insights into motor-task induced connectivity changes in young and healthy elderly individuals. We also showed that elderly individuals employ various compensatory mechanisms during a hand task possibly in an attempt to counteract known structural and neurobiological changes associated with aging by recruiting additional neural resources. Moreover, multivariate task-based network analyses carried out on chronic stroke patients revealed that rehabilitation treatments should target secondary motor areas in order to support residual activity in M1/S1. Collectively, the results reported in this thesis provided useful insights into the neural organization of hand motor control occurring during aging and motor-impaired populations.

RÉSUMÉ

Contexte. La détérioration des performances motrices chez l'humain a été grandement étudiée cependant les changements liés au vieillissement en matière de connectivité fonctionnelle visant les réseaux neuronaux incluant plusieurs régions cérébrales restent jusqu'ici méconnus. En effet, de nombreuses recherches concernant le rôle des aires motrices primaires et secondaires ont été effectuées durant l'exécution des mouvements de la main. Par contre, une meilleure identification des caractéristiques de connectivité fonctionnelle sur l'ensemble des régions du cerveau définissant la réorganisation sousjacente au vieillissement pourrait favoriser la compréhension des mécanismes résiduels ainsi que de la récupération motrice chez les patients atteints d'accident vasculaire cérébrale (AVC) souffrant d'incapacités motrices chroniques.

Objectif. Dans ce contexte, l'objectif principal des études incluses dans ce mémoire était de comparer la connectivité dynamique reliée à la performance motrice auprès de personnes saines jeunes et âgées ainsi que de personnes ayant soufferts d'un AVC lorsqu'ils sont au repos et lorsqu'ils exécutent des mouvements de la main.

Méthodes. Ce mémoire inclus les trois devis suivants : (1) utilisation de l'analyse en composantes principales (ACP) et de la causalité de Granger sur des données de magnétoencéphalographie (MEG) pour étudier les changements en matière de connectivité fonctionnelle dans les réseaux neuronaux reliés au vieillissement et sous-jacents à la production d'une contraction isométrique d'une ou des deux mains, (2) comparaison de la connectivité fonctionnelle du cerveau au repos suite à l'exécution des mouvements de la main mesurée chez de jeunes adultes et des personnes âgés en bonne santé grâce à l'utilisation de la technique d'enveloppe de corrélation des signaux provenant de la MEG et (3) comparaison de la connectivité fonctionnelle dans des réseaux neuronaux sous-jacents à la production de contractions isométriques de la main chez des individus ayant soufferts d'un AVC ainsi que des sujets contrôles sains à l'aide d'une

combinaison de régression multiple multivarié et d'ACP employée sur des données d'imagerie par résonance magnétique fonctionnelle (IRMf).

Résultats. La réorganisation cérébrale associée au vieillissement lors de la production de mouvements de la main est caractérisée par une augmentation globale de l'activité dans les réseaux spécifiques impliqués dans la tâche ainsi que d'une plus grande afférence vers le cortex moteur primaire de l'hémisphère gauche. En revanche, les réseaux sous-jacents aux mouvements de la main chez patients atteints d'un AVC et présentant une récupération motrice partielle de la main étaient caractérisés par une diminution générale de la connectivité principalement dans les aires motrices primaires et secondaires. Les changements observés dans ce réseau semblent être influencés spécifiquement par une activité réduite dans les régions motrices et sensorielles primaires (M1/S1). De plus, une corrélation négative entre le degré d'activité au sein de ces régions et la performance du comportement moteur dans le groupe d'AVC a été observée.

Significativité. Cette recherche contribue à l'avancement des connaissances sur la flexibilité et la réorganisation fonctionnelle des réseaux neuronaux du système moteur humain lors du vieillissement ou en présence de dommages cérébraux qui surviennent lors d'un AVC. Les résultats découlant de ce projet pourront ainsi contribuer au développement d'interventions thérapeutiques individualisées pouvant aider au bien-être de personnes désirant maintenir ou améliorer leurs performances motrices.

ORIGINAL CONTRIBUTIONS

Experiment 1 – This study investigates age-dependent alterations in functional connectivity in whole-brain networks underlying the production of unimanual and bimanual visually-guided isometric hang grips. A combination of principal component analysis and multivariate autoregressive modeling (Granger causality analysis) was used for the first time in this context to assess the direction of information flow within task-based, data-driven functional networks.

Experiment 2 – The effects of performing hand movement on resting-state functional connectivity in healthy young adults and healthy elderly individuals have been largely underexplored. As such, this study uses envelope correlation analyses on resting-state data before and after two different motor tasks to determine whether aging subjects demonstrate different reorganization mechanisms as compared to young adults.

Experiment 3 – This study compares functional connectivity in shared whole-brain networks underlying the production of visually-paced isometric hand grips in individuals with chronic stroke and healthy controls through a unique combination of multivariate multiple regression, principal component analysis, and data-driven, within-network analyses. Moreover, this study assesses the relationship between regional activity levels and motor impairment to derive biomarkers of motor recovery in chronic stroke survivors.

TABLE OF CONTENTS

I Introduction	
1. Introduction	
2. Background ·····	4
II Experiments	10
3. Task-Related Motor Connectivity in Aging	11
3.1 Abstract	13
3.2 Introduction ·····	
3.3 Methods	
3.4 Results · · · · · · · · · · · · · · · · · · ·	
3.5 Discussion ·····	
4. Motor Task-Induced Changes in Resting-State Networks in Aging	35
4.1 Abstract ·····	
4.2 Introduction · · · · · · · · · · · · · · · · · · ·	
4.3 Methods · · · · · · · · · · · · · · · · · · ·	
4.4 Results · · · · · · · · · · · · · · · · · · ·	
4.5 Discussion · · · · · · · · · · · · · · · · · · ·	
5. Task-Related Motor Connectivity in Chronic Stroke ······	50
5.1 Abstract·····	
5.2 Introduction · · · · · · · · · · · · · · · · · · ·	
5.3 Methods · · · · · · · · · · · · · · · · · · ·	
5.4 Results · · · · · · · · · · · · · · · · · · ·	
5.5 Discussion ·····	66
III Conclusions	71
6. Key Findings and Significance	
7. Future Research ·····	75
IV Bibliography	76
V Appendix	93
Appendix A·····	94
Appendix B ······	
	70

ABBREVIATIONS

ANOVA Analysis of variance

atDCS anodal tDCS

BBT Box and block test

BOLD Blood oxygen level-dependent

CBF Cerebral blood flow

CBV Cerebral blood volume

CMRO₂ Metabolic rate of oxygen consumption

DMN Default-mode network

EEG Electroencephalography

FIR Finite impulse response

fMRI Functional MRI

fMRI-CPCA Constrained PCA for fMRI

FrP Frontal pole

FWE Family-wise error

GABA Gamma-aminoutyric acid

HDR Hemodynamic response

LCMV Linearly-constrained minimum variance

MEG Magnetoencephalography

MRS Magnetic resonance spectroscopy

NHPT Nine hole peg test

M1 Primary motor cortex

M1/S1 Primary motor and sensory cortices

MDL Minimum length description

MEG Magnetoencephalography

MMSE Mini-mental state examination

mPFC Medial prefrontal cortex

MRI Magnetic resonance imaging

MRS Magnetic resonance spectroscopy

MVC Maximum voluntary contraction

OFC Orbitofrontal cortex

PASL Pulsed arterial spin labeling
PCA Principal component analysis

PMd Dorsal premotor cortex
PMv Ventral premotor cortex
PPC Posterior parietal cortex

ROI Region of interest

S1 Primary sensory cortex

Secondary sensory cortex

SMA Supplementary motor area

SoS Suborbital sulcus

SVD Singular value decomposition

tDCS Transcranial direct current stimulation

TFCE Threshold-free cluster enhancement

TMS Transcranial magnetic resonance

TR Repetition time

PART I | INTRODUCTION

CHAPTER 1

Introduction

Advancing age has been associated with motor performance decline in humans^{1, 2}. The consequences of such motor decreases have been reported to affect skills that are necessary to perform many tasks of daily life, as for instance, hand motor control (e.g., reaching and grasping objects), bimanual coordination (e.g., tying shoelaces), as well as gait and balance (e.g., walking)^{2, 3}. There is evidence that these age-related movement deficits are associated with neurochemical and structural changes affecting brain structure and function². While the bulk of the current literature has been focused on investigating functional activity changes in individual primary or secondary motor areas, debate lingers as to how alterations in whole-brain connectivity relate to motor decline observed in elderly subjects. This is likely in part due to the lack of large-scale connectivity features that characterize the neural processes underlying aging, which may in turn explain the highly diverse findings reported in literature on motor control and aging^{2, 4, 5}. As such, investigation of whole-brain motor connectivity to identify biological markers associated with motor performance decline appears warranted.

Advances in neuroimaging research, particularly with regards to whole-brain functional connectivity, offer new ways to investigate network-wide consequences of motor performance decline in healthy and diseased populations. The novelty of such approach motivates a shift away from typical connectivity analysis techniques (e.g., region of interest-based approach), and places greater emphasis on multivariate analysis methods which have the ability to capture spatial and temporal task-related and resting-state changes in networks of interconnected brain regions. From a clinical perspective, age is considered to be the most important risk factor for stroke⁶. Gaining a deeper anatomical and functional understanding of the dynamic processes involved in unimanual and

bimanual movements in older adults thus appears crucial in order to improve motor recovery and develop new therapeutic strategies for these patients.

The overarching goal of this thesis was thus to investigate the relation between functional connectivity at rest and during execution of unimanual and bimanual motor control tasks in aging and stroke individuals. Specifically, the objective was threefold: (1) to assess the effects of healthy aging on functional brain networks underlying the production of unimanual and bimanual hand grips, (2) to investigate task-induced connectivity changes on resting brain activity in young and aging individuals, and (3) to identify the impact of chronic stroke on motor network connectivity during a unimanual hand grip task. Altogether, this effort was intended to contribute to the ongoing debate on the neural mechanisms underlying motor connectivity changes during normal aging and to better understand how these changes are associated with motor function decline observed in these individuals. The work presented in this thesis also aimed to provide valuable insights into the mechanisms by which residual motor performance is governed in chronic stroke patients.

CHAPTER 2

BACKGROUND

Age-related neurochemical and structural changes

During normal aging, neurochemical-related changes are diffusely significant in many areas of the human brain, with changes in the dopaminergic system being the most widely studied⁷. Specifically, depletion of the neurotransmitter dopamine and its receptors in the basal ganglia has been evidenced in both post-mortem (i.e., histological staining) and molecular imaging (i.e., positron emission tomography) studies^{7,8}. Furthermore, positive correlations between dopamine transmission levels and fine motor control skills have been previously reported in older adults^{9, 10}. Consequently, it has been proposed that reduction in dopamine release during aging may in fact be caused by alterations in the interaction of dopamine with other neurotransmitters such as glutamate and gamma-aminoutyric acid (GABA)¹¹. In addition to neurochemical changes, gray and white matter brain atrophies are also commonly reported features in aging^{2, 12, 13}. Gray matter volume reduction in primary motor and sensory cortices (M1/S1), for instance, has been consistently associated with normal aging 14-16. Clear age differences in white matter integrity across key motor control structures such as the corpus callosum¹⁷ and the posterior limb of the internal capsule have also been reported¹⁸. Whereas the latter contains a motor pathway known as the corticospinal tract; the former plays a key role in bimanual coordination by allowing both hemispheres to communicate between them¹⁹, in addition to inhibiting input from the ipsilateral motor cortex during unimanual movements²⁰. Many of these studies have also found a positive correlation between the integrity of gray and white matter structures and motor task performance in older adults ^{13, 21, 22}. Based on this concept, it has been theorized that age-related atrophy of motor cortical regions is compensated for by functional activity increases in structurally intact regions^{23, 24}. From a functional standpoint, it seems likely that many of these age-related neurobiological and structural changes also have profound effects on whole-brain motor connectivity. Indeed, the neural mechanisms by which these functional brain changes occur are not fully understood, and may in fact influence the ability of an individual to maintain motor functions.

Age-related neurofunctional mechanisms: two classical theories

Current findings in the literature have paved the way for two prominent theories which aim to explain the nature of the observed age-related changes in the brain. There is on one hand the compensation view which states that, relative to young adults, elderly individuals are able to recruit higher levels of activity across brain regions that are engaged during a specific task, and that this hyperactivity is positively correlated with task performance²⁵. On the other hand, the dedifferentiation hypothesis posits that additional brain regions are recruited in a non-selective fashion, and thus indicates a loss of functional specificity during the performance of a motor task²⁶. Although these theoretical accounts have greatly advanced our understanding of normal aging, it remains largely unknown which of these theories could most closely explain network-wide changes associated with age-related motor decline.

The aging brain at rest: insights from quantitative neuroimaging

Neuroimaging studies on aging have been widely used to investigate the link between age-related motor decline and underlying brain activity. It has been increasingly recognized that decreased motor and cognitive functions in aging may extend beyond activity changes in individual brain regions, and more toward alterations in interconnected networks of multiple motor and non-motor areas²⁷. The advent of graph theory, a branch of mathematics whereby brain networks are represented as a set of nodes (i.e., brain regions) connected by edges (i.e., connections), has been introduced as a novel analysis method for network-level functional connectivity. This whole-brain approach provides a powerful way to quantify important topological properties of brain connectivity²⁸, and as a result can offer new insights into the neural basis of age-related motor decline. Previous resting-state functional magnetic resonance imaging (fMRI) studies using graph theory have shown that network specificity is reduced in elderly^{29, 30}. Consistent with these

results, Geerligs and colleagues²⁷ reported an increase in internetwork connectivity in older individuals, whereas younger adults showed the opposite pattern of connectivity (i.e., high within-network connectivity with few between-network connections). When focusing only on within-network findings, it has been suggested that functional connectivity in older adults is decreased in networks supporting higher-order functions³¹, 32, whereas it is increased in primary sensory networks which are involved in the processing of afferent visual, auditory, and sensorimotor inputs^{32, 33}. In line with this finding of enhanced connectivity, several studies have provided compelling evidence that aging is associated with a decrease in interhemispheric cortico-cortical inhibitory influence, notably between premotor and primary motor areas 34-36. Interestingly, a recent multimodal transcranial direct current stimulation (tDCS), magnetic resonance spectroscopy (MRS), and resting-state fMRI study has shown that anodal tDCS (atDCS), which has the ability to modulate neural activity, can induce reduction of GABA levels within the motor system in older adults³⁷. This was associated with concurrent decreases in resting-state functional coupling during atDCS, including significant M1-M1 interhemispheric decoupling, thereby revealing increased efficiency in brain network functioning due to the stimulation³⁷.

Motor decline in aging: advances and inconsistencies from task-based neuroimaging

Task-based studies are often used to reliably activate a specific brain region or a network of regions associated with a particular cognitive or motor function. Findings from motor task-related studies, however, are highly inconsistent due to the various paradigms and methodological approaches being used. For instance, Noble and colleagues used a voxelwise whole-brain approach to investigate differences in activation related to changes in grip force magnitude in young and older adults³⁸. This study revealed age-related activity increases in several regions, including ventral premotor cortex (PMv), putamen, thalamus, cerebellum, as well as in various areas involved in visuospatial and executive processing³⁸. Conversely, a study investigating the underlying neural correlates of

isometric hand grips using voxelwise metrics reported significant activity increases solely in M1 ipsilateral to the moving hand in elderly subjects⁵. According to the authors, this increase in magnitude of activity was attributable to an age-related inability to dampen interhemispheric inhibition from contralateral to ipsilateral M1⁵. More recently, Park and colleagues used graph theory to study the effects of age on the characteristics of functional brain networks during dominant and nondominant hand grips³⁹. Interestingly, they found that global efficiency in older subjects was diminished only when the task was carried out with their nondominant hand, whereas efficiency of parietal-occipital-cerebellar networks increased with age when the dominant hand was used. These findings likely reflect a compensatory mechanism whereby connectivity within specific networks must be increased in order to maintain overall global efficiency when grasping with the dominant hand. In spite of unravelling marked alterations in individual regions as well as in the topology of whole-brain networks during aging, these task-based studies were limited to a static picture of brain organization. There is a growing body of evidence pointing toward functional connectivity as a highly dynamic process⁴⁰, however this aspect has not yet been fully explored in the context of aging. Investigation of multivariate functional connectivity in network analysis thus appears to be crucial in order to gain a better understanding of the neural underpinnings of aging. As opposed to univariate metrics (which look at activation of single voxels or regions) or bivariate metrics (which compute relationships between pairs of voxels or regions), multivariate analysis methods have the ability to detect networks of interconnected brain areas as well as to provide insights into the dynamics of these interactions in a single model⁴¹.

Electrophysiological changes in aging: evidence from MEG and EEG studies

Magnetoencephalography (MEG) has emerged as a powerful tool to investigate task-related and resting-state dynamic cortical networks in a millisecond time-scale, and as a result may help explain the complex functional changes involved in healthy aging. Notably, MEG captures real-time neuronal activity by measuring extracranial neuromagnetic fields, and as opposed to the similar and most widely used

electroencephalography (EEG), MEG is less sensitive to spatial distortions caused by the brain, skull, and scalp⁴². Using this technique, an increasing number of studies have shown great promise in mapping the spatiotemporal characteristics in the context of aging. For instance, resting-state MEG studies have reported reduced slow oscillatory activity (< 8 Hz) but an increase in faster oscillations (8–30 Hz) in older adults⁴³⁻⁴⁵. These findings are in line with previous work which suggests a speeding of electrophysiological activity among cortical regions in the brain of elderly individuals⁴⁶. With respect to the two competing theories of age-related changes described earlier—the compensation view and the dedifferentiation hypothesis—the speeding of the frequency spectrum may hint toward the presence of a compensatory mechanism that counteracts the decreased nerve conduction velocity due to white matter atrophy present during aging processes⁴³.

One caveat of the current MEG literature is that most of the studies performed until now have solely measured the amplitude and frequency of power, and consequently have failed to examine how the brain integrates information across multiple regions. In fact, studies assessing event-related or resting-state functional connectivity of the whole brain using MEG are relatively sparse. While great efforts have been put towards using multivariate functional connectivity techniques in MEG data analyses of healthy and diseased populations^{47, 48}, to our knowledge these methods have never been employed to study network-wide connectivity patterns underlying the execution of hand movement in aging individuals.

Clinical applications: motor recovery in chronic stroke

Gaining a better understanding of brain reorganization underlying motor performance decline in healthy aging is essential in clinical research. This becomes particularly evident when considering that stroke is the leading cause of long-term disability among older adults worldwide⁴⁹, with persistent hand deficit being one of the key features associated with this condition^{2, 50}. Up to now, the consequences of stroke on brain reorganization have mainly been assessed using univariate seed-based functional

connectivity and consequently remain highly controversial. For instance, this technique has provided evidence for enhanced functional activity in ipsilesional dorsal premotor cortex (PMd)⁵¹, supplementary motor area (SMA)⁵², ipsi- and contralesional M1/S1^{52, 53}, as well as decreased activity in contralesional M1/S1⁵⁴, and anterior cerebellar lobules⁵⁵ have all been reported. Of the few studies that attempted to link blood oxygen leveldependent (BOLD) fMRI alterations to deterioration in motor performance, increases in activity in ipsilesional M1 seemed to be linked to improvements in behavioral performance⁵⁶, while enhanced BOLD activity in contralesional M1 have been shown to have a detrimental effect on hand function ^{57,58}. In line with the latter finding, some authors have postulated that patients with poor recovery were more likely to show greater activation in contralesional motor-related regions relative to control subjects 49, 52, 59. These studies have provided ample evidence of functional remapping of the brain after a stroke but have failed to provide a precise association between different patterns of activity and residual motor performance observed in these patients⁶⁰. At the heart of the problem could be the lack of correlation between functional connectivity changes (e.g., increased or decreased activity) and motor performance. In order to identify accurate biological markers that can predict or improve motor recovery in at-risk populations, it is important to gain a deeper understanding of the network-wide mechanisms involved in ubiquitous movements, and how these mechanisms are affected by normal aging or the presence of a stroke. Our research effort predominantly aims at gaining a better understanding of the reorganization of brain networks underlying motor control in individuals with motor function decline. Ultimately, our findings may lead to the development of personalized treatment strategies using rehabilitation training and/or stimulation protocols (e.g., tDCS) in order to maintain or maximize motor functions in aging or movement-impaired populations.

* * *

PART II | EXPERIMENTS

CHAPTER 3

TASK-RELATED MOTOR CONNECTIVITY IN AGING

Preface

Until recently, researchers have attempted to map brain functions to discrete brain regions. In the past few years, however, efforts have been made to link motor performance decline observed during healthy aging to changes in distributed networks of functionally interconnected brain structures. Consequently, there is a growing interest to better understand how brain reorganization at the network-level takes place during aging in order to support residual motor functions.

Task-activation paradigms have proved to be highly useful to investigate functional networks that are specifically related to hand movements. Notably, numerous studies have shown that performance of isometric hand grips consistently and reliably activates well-characterized brain networks which include primary sensorimotor and visuospatial regions^{5,35,61}. Although these studies have provided valuable information, they often lack information regarding the temporal profile of the networks' engagement. Recent advances in non-invasive neuroimaging techniques, particularly with regard to MEG, can provide spatiotemporal dynamics of brain networks, and thus appears to be particularly suitable to capture fast changes in neural information from cortical functional networks. The development and application of multivariate connectivity methods for the analysis of task-related MEG data is however warranted. For instance, quantification of resting-state MEG connectivity using dynamic and spectral resolution could provide new and biologically meaningful ways to assess network-wide changes in healthy and aging populations.

In this study, we applied principal component analysis and multivariate autoregressive Granger causality on MEG data to compare the organization of functional

brain networks underlying the production of unimanual and bimanual hand grips in elderly individuals to that of young adults. We hypothesized that elderly individuals, relative to young adults, will show hyperactivity in motor networks underlying hand movement. This would reflect a potential compensatory mechanism by which the aging brain counteracts neurobiological changes by recruiting additional neural resources.

* * *

3.1 Abstract

Objective: Motor deficits observed during aging have been shown to be linked with changes in brain structure and function, however, the precise neural reorganization associated with these changes remains widely debated. This study sought to address this gap in the literature by quantifying the organization of brain network connectivity in elderly individuals (n = 11; mean age = 67.5 years), as compared to young adults (n = 12; mean age = 23.7 years), while they performed visually-guided unimanual and bimanual hand grips inside the MEG scanner.

Methods: We combined principal component analysis (PCA) to identify task-specific functional brain networks and multivariate autoregressive Granger causality to explore the direction of information flow within these networks.

Results: Our PCA analysis revealed four brain networks in which elderly individuals had significantly higher activity levels than young adults: a ventral frontoparietal network and a left-dominant motor network engaged during the unimanual task, as well as a left-dominant motor network and a bilateral motor network engaged during the bimanual task. Moreover, our Granger causality analysis demonstrated that elderly individuals, but not young adults, had increased effective connectivity to the left primary motor cortex (M1) during unimanual hand grips. On the other hand, the left temporal pole appeared to play a key role in coordinating bilateral M1s during bimanual hand movement in the young group by receiving cortical information from several parietal regions, however this pattern of connectivity was largely absent in the elderly group.

Conclusions: Maintenance of motor performance and task accuracy in elderly individuals was achieved by a relative hyperactivation of the task-specific motor networks. Network-wide brain reorganization therefore occurs and may reflect a compensatory mechanism by which the aging brain counteracts neurobiological changes by recruiting additional neural resources.

Larivière S, Xifra-Porxas A, Niso G, Kassinopoulos M, Mitsis GD, Boudrias MH. Functional and effective reorganization of the aging brain during unimanual and bimanual hand movements.

This work is to be submitted as:

3.2 Introduction

Aging is commonly associated with progressive cognitive and motor functions decline^{1, 2}. Brain reorganization is thought to occur during aging in order to maintain motor performance despite gray and white matter volume loss 11, 13. Prior studies looking at thinning of the cerebral cortex in aging have reported that gray matter atrophy occurs predominantly in M1 and calcarine sulcus¹⁴. Interestingly, Glasser and Van Essen⁶² recently proposed a new method for mapping myelin content to a cortical surface and reported that regions of heavy myelination include mainly M1 and the occipital lobe⁶², which coincide with those areas of marked gray matter volume loss in healthy aging¹⁴. One of the major theoretical accounts aiming to explain these age-related changes proposes that activity levels within a given motor-related area will be increased in an attempt to compensate for neuronal loss and myelin deterioration²⁵. Alternatively, it is possible that such compensatory mechanisms may be reflected as a shift in the topological organization of whole-brain residual brain networks. Few studies to date, however, have delved into network-wide changes of functional or effective connectivity in the context of aging. Indeed, previous neuroimaging studies have provided an unclear picture of the network-wide mechanisms by which the brain adapts to these structural, myeloarchitectural, and neurochemical changes. One way to address this gap in the aging literature is to probe activity in whole-brain networks that are specifically related to hand movement and to treat the identified connectivity patterns as intrinsically directed (e.g., include information about direction flow among cortical areas in the interpretation of findings).

fMRI techniques, though popular, cannot reliably estimate causal connections at the millisecond time scale due to its slow temporal resolution. On the other hand, MEG has been increasingly recognized as a neuroimaging research tool that has the potential to capture the richness and complexity of brain activation patterns with millisecond temporal resolution. As such, MEG can provide valuable insights into the patterns of effective connectivity among cortical regions involved during the production of hand movements.

Notably, Granger causality analysis performed on MEG time series has rapidly emerged as a powerful approach to examine data-driven effective connectivity. For instance, Gao and colleagues recently utilized a time-varying Granger causality analysis technique to explore the fast changing information flow among somatosensory regions of healthy adults⁶³. Importantly, the authors reported high consistency between their results and well-established anatomical connectivity models of sensorimotor regions, thus providing empirical validation of the Granger causality method⁶³.

In this study, we applied PCA and multivariate autoregressive Granger causality on MEG data to characterize the organization of functional brain networks involved in unimanual and bimanual visually-paced isometric hand grips in healthy young and elderly adults. We hypothesized that functional brain networks in elderly relative to young adults will exhibit reduced global efficiency as indexed by non-optimal levels of connectivity (i.e., hyperactivity). The overly-connected brain networks underlying hand motor control in elderly individuals would possibly reflect a compensatory mechanism by which the aging brain counteracts neurobiological changes by recruiting additional neural resources. We further expected to observe an increase in interhemispheric connectivity in elderly subjects, predominantly in primary and secondary motor, as well as parietal regions identified in the task-based networks. This would suggest that the aging brain is characterized by a decreased lateralization, which is in line with a prevalent theory claiming a loss of hemispheric asymmetry during normal aging 64-66.

3.3 Methods

Participants

We collected MEG data from twelve healthy young adults (mean age = 23.7 years) and eleven healthy elderly individuals (mean age = 67.4 years). Details regarding demographic information and behavioral performance are presented in Table 3.1; both groups were matched on gender and education. Inclusion criteria for all participants were as follow: (1) no present or previous history of a psychiatric condition, (2) aged between

18 to 30 years (young group) and 60 to 75 years (elderly group), and (3) right-handed according to the Edinburgh Handedness Inventory⁶⁷. Exclusion criteria included: (1) contraindications for MRI, or other limitations that would interfere with MRI or MEG data acquisition (e.g., claustrophobia, metal implants), and (2) a Mini-Mental State Examination (MMSE) score \leq 24. Written informed consent was obtained from all participants. The study was approved by the Research Ethics Board of the Montreal Neurological Institute and Hospital, McGill University.

	Young	Elderly
Variable	Subjects	Subjects
Sex (male/female)	8/4	8/3
Handedness (right/left)	12/0	11/0
Age (years) ^a	23.7 (2.9)	67.4 (3.9)
BBT (right) ^b	67.5 (5.5)	57.1 (4.2)
BBT (left) ^b	66.7 (5.5)	56.8 (4.8)
NHPT (right) b	0.58 (0.1)	0.44 (0.04)
NHPT (left) c	0.52 (0.1)	0.41 (0.06)
Grip strength (right)	46.2 (15.1)	39.1 (9.3)
Grip strength (left)	44.1 (16.1)	34.8 (7.9)

Table 3.1: Participants' demographic information and behavioral scores. Standard deviations are in parentheses. BBT, Box and Block Test; NHPT, Nine-Hole Peg Test. ^a = Elderly > Young, p < 0.0001; ^b = Young > Elderly, p < 0.0005; ^c = Young > Elderly, p < 0.01.

Experiment protocol

As detailed in Appendix A, motor performance of both hands was assessed for each participant via measurements of (1) hand grip strength, (2) fine manual dexterity (nine hole peg test; NHPT), and (3) unilateral gross manual dexterity (box and block test; BBT). Motor performance scores for the dominant hand (right hand) and non-dominant hand (left hand) were used in our group comparison.

As depicted in Figure 3.1, all participants underwent three separate 5 min resting-state sessions, interspersed with two isometric hand grip tasks. The first task consisted of 50 unimanual, visually-paced, isometric right-hand grips, in which subjects had to apply force to track a ramp target. Prior to scanning, each subject was asked to grip the manipulandum with maximum force in order to generate their maximum voluntary contraction (MVC). These values were then used to set the subject-specific target forces of 15% and 30% of MVC. In each trial, participants had to maintain a steady force at 15% of MVC for 3 s, followed by a linear increase of 3 s to reach and maintain a steady force at 30% of MVC for 3 s. The second motor task consisted of 50 bimanual, visually-paced, isometric hand grips performed at 15% of MVC (6 s each).

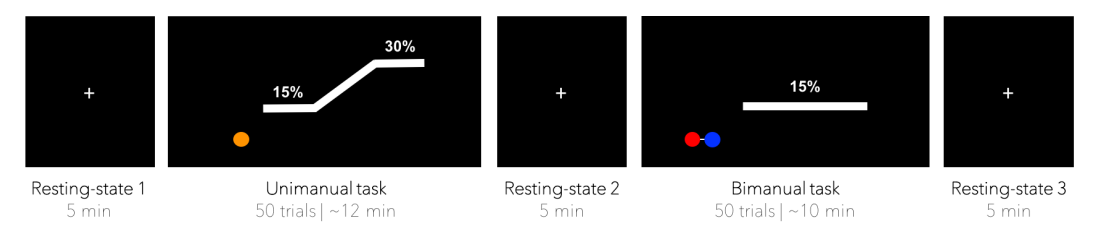


Figure 3.1: Schematic overview of the experiment protocol carried out in the MEG. Subjects performed two hand motor control tasks (unimanual, bimanual) interspersed with three 5 min resting-state sessions. Each motor task consisted of 50 trials with variable interstimulus intervals.

Functional connectivity analysis

Details regarding data acquisition and preprocessing are described in Appendix A. A schematic of the subsequent data analysis pipeline is provided in Figure 3.2. For every participant, the task-related data was down-sampled to 160 Hz and epoched offline with a poststimulus time window of 9000 ms (unimanual task) and 6000 ms (bimanual task) with the first time point (time = 0) corresponding to stimulus onset. A linearly-constrained minimum variance (LCMV) beamformer spatial filtering approach⁶⁸ was then used on the subject-specific task-averaged epoched data to reconstruct a single time series for each of the 148 cortical brain regions defined by the Destrieux sulcogyral-based atlas⁶⁹. For each pre-defined source location (i.e., brain region), activity was estimated at each vertex and subsequently averaged to produce a single time series per brain region. The use of this

brain atlas aids in interpretation and comparison with other modalities while allowing computational power for greater temporal accuracy, the latter being a crucial aspect of functional connectivity that varies as a function of task-timing. Time-frequency decomposition of source time series was then performed using Morlet wavelets⁷⁰ for four frequency bands of interest: theta (5–7 Hz), alpha (8–12 Hz), beta (13–30 Hz), and gamma (31–80 Hz). Frequency-specific source time series of every subject were combined to create four data matrices (one per frequency band), each with columns corresponding to brain regions and rows corresponding to poststimulus time points × subjects. Singular value decomposition (SVD), of which PCA is a special case, was performed on each of the four standardized data matrices. For every component extracted, the resulting decomposition yielded (1) a spatial pattern (i.e., network of interconnected brain regions) accounting for part of the pattern of covariances between spectral power at each brain region, and (2) component scores (i.e., a time series) providing an estimate of the network's engagement at each poststimulus time points. The network-level connectivity analyses of oscillatory power described above were performed separately for each motor task (i.e., unimanual and bimanual).

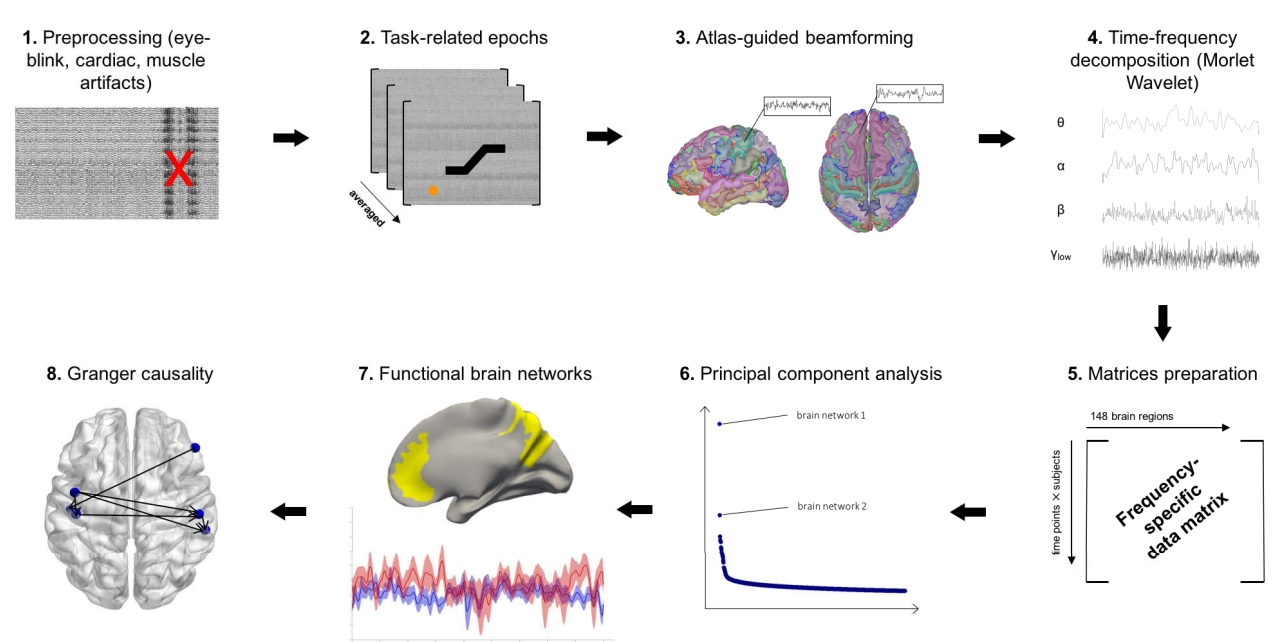


Figure 3.2: Schematic overview of the analysis pipeline used for the task-related MEG data.

An advantage of the proposed method is that it allowed non-static characterization of functional networks that are specifically related to unimanual or bimanual hand grips. This in turn provided new ways to describe brain connectivity underlying ubiquitous motor tasks and thus allowing us to assess how normal aging affects integration of information.

Statistical analysis

To investigate group differences in the activation level of each functional brain network we carried out statistical analyses on the envelope of the component score time series. This was achieved by using the Hilbert transform to extract the amplitude of each network's associated time series. For every unimanual network identified, the Hilbert transform values at each time points and for each subject were submitted to a 1441 × 2 mixed-model analysis of variance (ANOVA), with the within-subjects factor of Poststimulus Time (1441 time points were estimated after stimulus onset), and between-subjects factor of Group (elderly individuals and young adults). Similarly, for the identified bimanual networks, these Hilbert transform values for every subject were submitted to a 962 × 2 mixed-model ANOVA, with the within-subjects factor of Poststimulus Time (962 time points), and between-subjects factor of Group.

Granger causality analysis

Granger causality has been increasingly used to identify the presence of directional interactions (or causal relations) in physiological systems⁷¹. This approach relies on the concept that a causal influence from a source region to a target region can be assumed if past information about the source region (e.g., a time series) improves the prediction of future values of the target region. In other words, Granger causality can provide information as to how information travels from one brain region to another. Here, the Granger causality connectivity analysis was conducted on the task-specific, PCA-derived functional brain networks (i.e., constrained to the dominant 15% of interconnected brain regions within each identified task-based networks) and consisted of two main steps. First,

Granger causality was performed on each subject individually, and binary outcomes were coded 0 for non-significant causal relations (p > 0.05) and 1 for significant causal relations (p < 0.05). The model order parameter of our multivariate autoregressive model was optimized with Minimum Description Length (MDL) criterion and statistical significance of every pairwise causal relation was detected using an F-test. Secondly, significant group-level causality maps (constrained to the significant, subject-level causal relations) were detected using binomial p-value computation for testing proportions. Specifically, for a given causal link, the binomial test uses the mean of all coded binary outcomes within a group (i.e., 0s and 1s) to compute the number of subjects with this significant causal link that is required for this link to be significant at the group-level. As such, the resulting task-based Granger causality maps (Figure 3.9) display the dominant patterns of cortical information flow that were significant both at the subject- and group-levels for every task-specific brain network.

As opposed to neuroimaging modalities with lower temporal resolutions such as fMRI, MEG can resolve neuronal events with millisecond time precision and can thus be used to reliably investigate effective connectivity using Granger causality. In light of this, our primary functional connectivity analysis was complemented by information about the dominant direction of information flow within the identified data-driven brain networks. Taken together, this approach provided a more complete picture of the organization of brain networks during aging.

3.4 Results

Behavioral results

As displayed in Table 3.1, the behavioral scores for each hand were entered into two-sample t tests to compare motor performance between young and elderly individuals. For both hands, young adults performed significantly better than elderly individuals on the BBT and NHPT (ps < 0.01), whereas grip strength did not differ between groups (ps

> 0.09). A significant age difference was also observed between the young group and the elderly group (p < 0.0001).

Here, we defined task accuracy as the difference between the grip force applied and the position of the ramp target; higher accuracy is achieved when participants closely matched the target force (i.e., defined by the middle of the target ramp). We computed the mean accuracy of all trials for every participant (within each task independently), and subsequently tested for significant differences between young and elderly individuals on each task by entering the accuracy values into two-sample t tests. Both groups were matched on task accuracy during the unimanual task (using the dominant right hand; p > 0.3) as well as during the bimanual task (using the dominant right hand and the non-dominant left hand; ps > 0.1).

Functional connectivity results

Inspection of the scree plot of singular values was carried out for each frequency band (theta, alpha, beta, gamma) of the two motor tasks (unimanual, bimanual). Visual inspection of every component (i.e., network) extracted from our task-based analysis was performed. Brain networks which included regions that appeared randomly scattered or that were not clustered into well-documented networks were excluded from the analysis and are not discussed below. This led to the inclusion of three unimanual networks (all in beta) and three bimanual networks (two in beta, one in alpha). The brain regions and estimated time series associated with each network are displayed in Figures 3.3-3.9 and described below.

Functional networks underlying unimanual hand grips

Ventral Frontoparietal Network. This network was the first component extracted from the beta frequency and accounted for 18.3% of task-related variance. Activation in this network was largely lateralized to the right hemisphere and specifically included the temporoparietal cortex, anterior cingulate cortex, occipital cortex, as well as bilateral

anterior inferior frontal cortex (Figure 3.3A). This spatial pattern is highly consistent with that of a frontoparietal attention network known to play a role in detecting behaviorally relevant stimuli and mediating bottom-up processing^{72, 73}. This network was therefore identified as the *ventral frontoparietal network*. The Hilbert transform values (i.e., envelope) of the network's associated time series were entered into a mixed-model ANOVA, and a significant main effect of Poststimulus Time was observed, $F_{1440,30240} = 1.16$, p < 0.001. The Poststimulus Time × Group interaction was also significant, $F_{1440,30240} = 1.19$, p < 0.001, and was caused by increased activity in the elderly group during the sustained hand grip periods (i.e., 0-3 s and 6-9 s; Figure 3.3B).

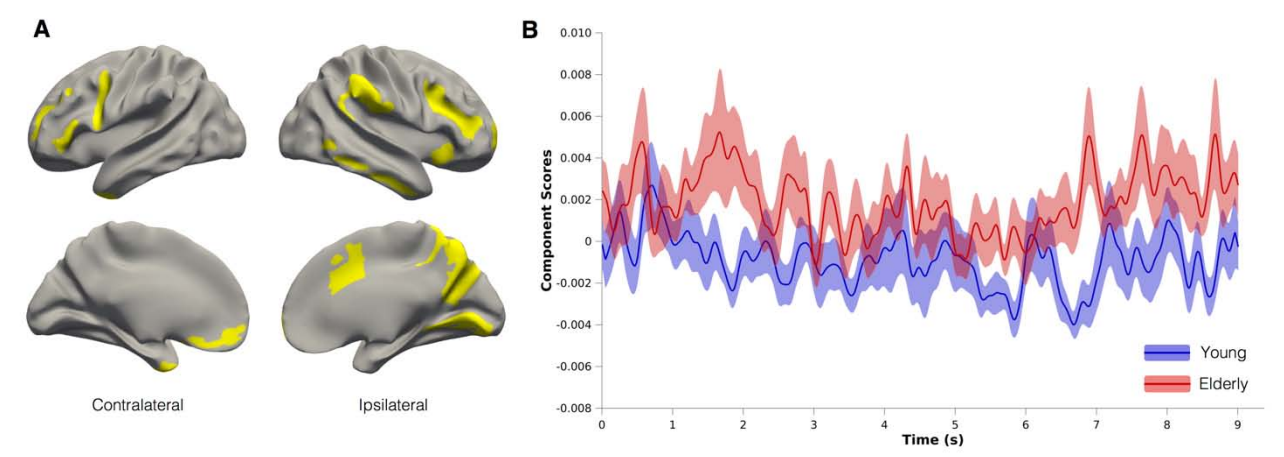


Figure 3.3: The first principal component extracted from the beta frequency (13–30 Hz) for the unimanual task, labelled *Ventral Frontoparietal Network*. (A) Dominant 15% of loadings for this component are displayed, representing a network of strongly interconnected brain regions (B) The estimated time series (i.e., component scores) associated with this network, representing the network's engagement at each poststimulus time points. Shaded regions represent the standard error of the group mean. Contralateral and ipsilateral with respect to the moving (right) hand.

Default-Mode Network. This network was the second component extracted from the beta frequency and accounted for 8.4% of task-related variance. As displayed in Figure 3.4A, activations in this network were found in core regions of the *default-mode network* such as right anterior cingulate cortex, precuneus, inferior temporal cortex, as well as bilateral ventromedial prefrontal and lateral parietal cortices. Although activation of the default-mode network has been predominantly observed under task-free or "resting-state" conditions, recent studies have reported significant deactivation of this network during

attentionally demanding tasks⁷⁴. A known limitation of MEG functional connectivity, however, lies in its inability to distinguish between excitatory and inhibitory connections⁷⁵; it is therefore possible that the default-mode network identified in the current study underlies task-related deactivations. The Hilbert transform values associated with this network were entered into a mixed-model ANOVA; main effects of Poststimulus Time and Group, as well as the interaction, were all not significant (ps > 0.2), suggesting that activity within this network did not differ across time or between groups (Figure 3.4B).

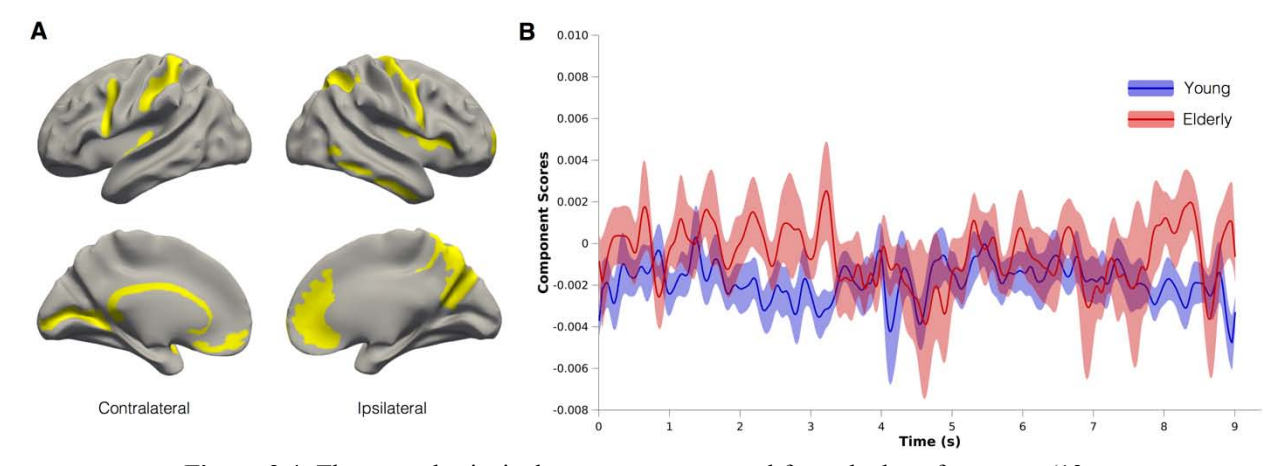


Figure 3.4: The second principal component extracted from the beta frequency (13–30 Hz) for the unimanual task, labelled *Default-Mode Network*. (A) Dominant 15% of loadings for this component are displayed, representing a network of strongly interconnected brain regions (B) The estimated time series (i.e., component scores) associated with this network, representing the network's engagement at each poststimulus time points. Shaded regions represent the standard error of the group mean. Contralateral and ipsilateral with respect to the moving (right) hand.

Motor Network. This network was the third component extracted from the beta frequency and accounted for 5.1% of task-related variance. Activity in this network was observed predominantly in left motor-related regions, notably M1, primary and secondary sensory cortices (S1, S2), and superior frontal gyrus extending into supplementary motor area (SMA). This network also included activation in right S1 as well as superior and inferior parietal lobules. Based on this spatial pattern (Figure 3.5A) this network was labeled the *motor network*. This network showed a significant main effect of Group,

 $F_{1,30240} = 4.12$, p = 0.05, but also a significant Poststimulus Time × Group interaction, $F_{1440,30240} = 1.26$, p < 0.001. As can be seen from Figure 3.5B, both groups showed similar levels of activity, however, relative to the young group, the time series of elderly individuals were characterized by distinct sharp activation peaks which may underlie the significant interaction.

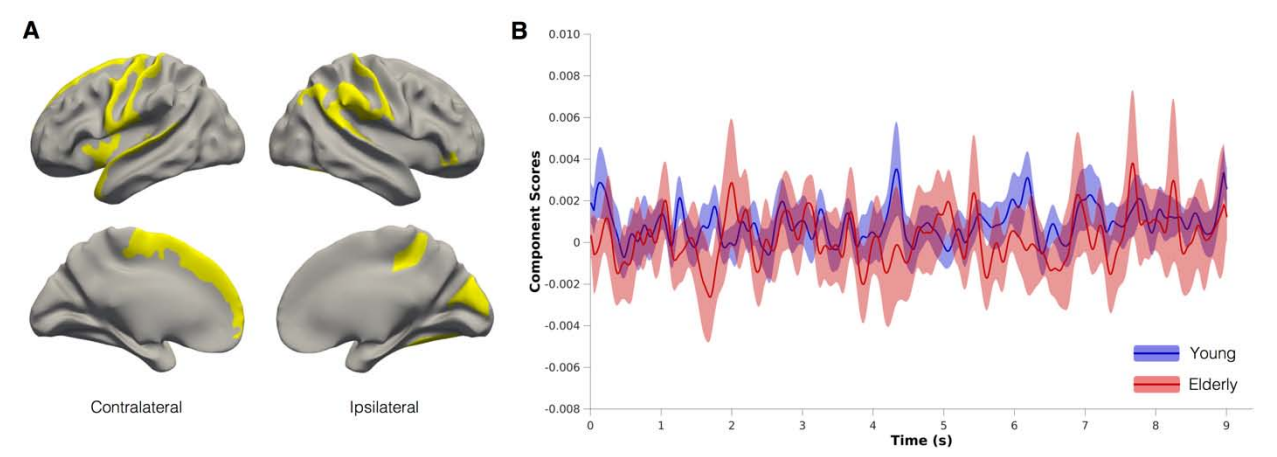


Figure 3.5: The third principal component extracted from the beta frequency (13–30 Hz) for the unimanual task, labelled *Motor Network*. (A) Dominant 15% of loadings for this component are displayed, representing a network of strongly interconnected brain regions (B) The estimated time series (i.e., component scores) associated with this network, representing the network's engagement at each poststimulus time points. Shaded regions represent the standard error of the group mean. Contralateral and ipsilateral with respect to the moving (right) hand.

Functional networks underlying bimanual hand grips

Left-Dominant Motor Network. This network was the first component extracted from the beta frequency and accounted for 19.4% of task-related variance. Activations in this network was mostly lateralized to the left hemisphere, and included M1 extending anteriorly into PMd and PMv, S1, inferior parietal lobule, and bilateral occipital cortex (Figure 3.6A). This component was therefore labelled the Left-Dominant Motor Network. As evidenced in Figure 3.6B and by a significant Poststimulus Time × Group interaction, $F_{961,22125} = 1.10$, p < 0.05, elderly individuals exhibited distinctly higher levels of activity throughout the whole sustained bimanual hand grip relative to young adults.

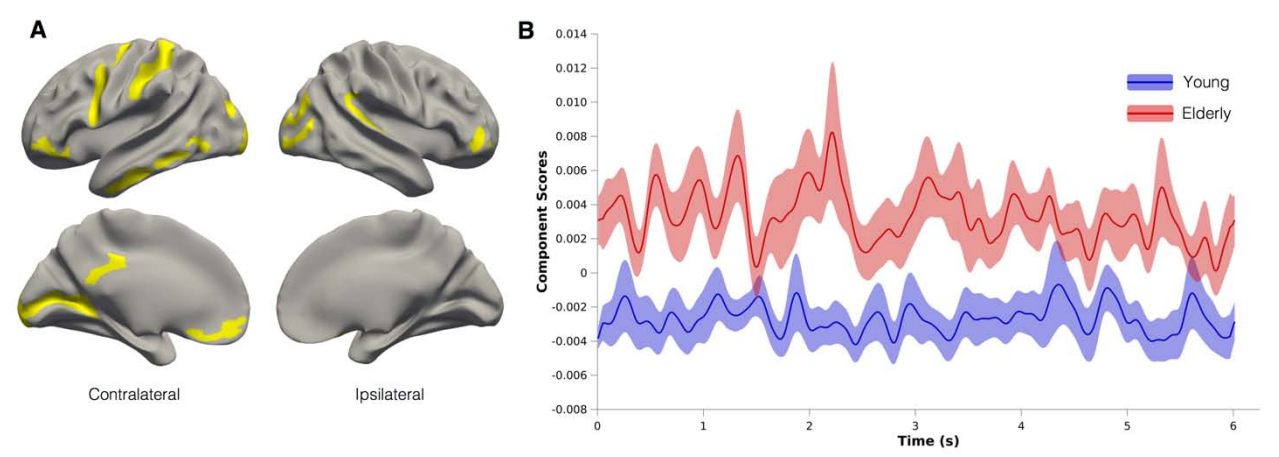


Figure 3.6: The first principal component extracted from the beta frequency (13–30 Hz) for the bimanual task, labelled *Left-Dominant Motor Network*. (**A**) Dominant 15% of loadings for this component are displayed, representing a network of strongly interconnected brain regions (**B**) The estimated time series (i.e., component scores) associated with this network, representing the network's engagement at each poststimulus time points. Shaded regions represent the standard error of the group mean. Contralateral and ipsilateral with respect to the dominant (right) hand.

Bilateral Motor Network. This network was the second component extracted from the beta frequency and accounted for 7.8% of task-related variance. The spatial pattern of interconnected brain regions in this network was characterized by bilateral M1 activations (extending anteriorly into PMd) as well as left S1 and anterolateral parietal cortex (Figure 3.7A). This component was thus identified as the Bilateral Motor Network. A mixed-model ANOVA carried out on the Hilbert transform values of the network's associated time series revealed significant main effects of Poststimulus Time, $F_{961,20181} = 1.16$, p < 0.0005, and Group, $F_{1,20181} = 7.17$, p < 0.05, as well as a significant Poststimulus Time × Group interaction, $F_{961,22125} = 1.15$, p < 0.005. As can be seen from Figure 3.7B, this interaction appears to be caused by an increase in activity levels in the elderly group later in the trial (from 3 to 6 s), whereas young adults exhibit constant levels of activity throughout the entire bimanual hand grip.

Right-Dominant Motor Network. This network was the first component extracted from the alpha frequency and accounted for 25.6% of task-related variance. This component was characterized by a functional network that included activations in and

around right M1, specifically extending anteriorly into PMd and posteriorly into the central sulcus, left inferior parietal cortex, and bilateral occipital cortex (Figure 3.8A). Based on the spatial distribution of the network, this component was labelled the *Right-Dominant Motor* Network. The main effects of Poststimulus Time and Group, as well as the interaction, were all not significant (ps > 0.4), suggesting that activity within this network did not differ across time or between groups (Figure 3.8B).

Granger causality mapping

We investigated the direction of information flow from and to every brain region derived from all six task-based networks extracted from the functional connectivity analysis. Binomial statistics revealed that causal links were significant at the group-level if the links were significant at the individual-level in at least 7 subjects (i.e., 7/12 for the young group and 7/11 for the elderly group), that is: p-value = $P(X \ge 7 \mid p = \mu_{group}) < 0.05$. Here we used a multivariate autoregressive model of order 3, meaning that the time lag between interacting neuronal ensembles was 18.75 ms (i.e., 3/160). Granger causality maps for the unimanual and bimanual networks and for each group are depicted in Figure 3.9A–C and Figure 3.9D–F, respectively.

3.5 Discussion

In the present study, we compared functional brain activity underlying the production of unimanual and bimanual isometric hand grips in young and elderly individuals. Notably, we employed a combination of functional and effectivity multivariate connectivity analyses to derive task-specific brain networks and assess the direction of information flow among cortical areas. The production of unimanual right-hand grips revealed three distinct functional networks extracted from the beta frequency band: a ventral frontoparietal network, a default-mode network, and a motor network.

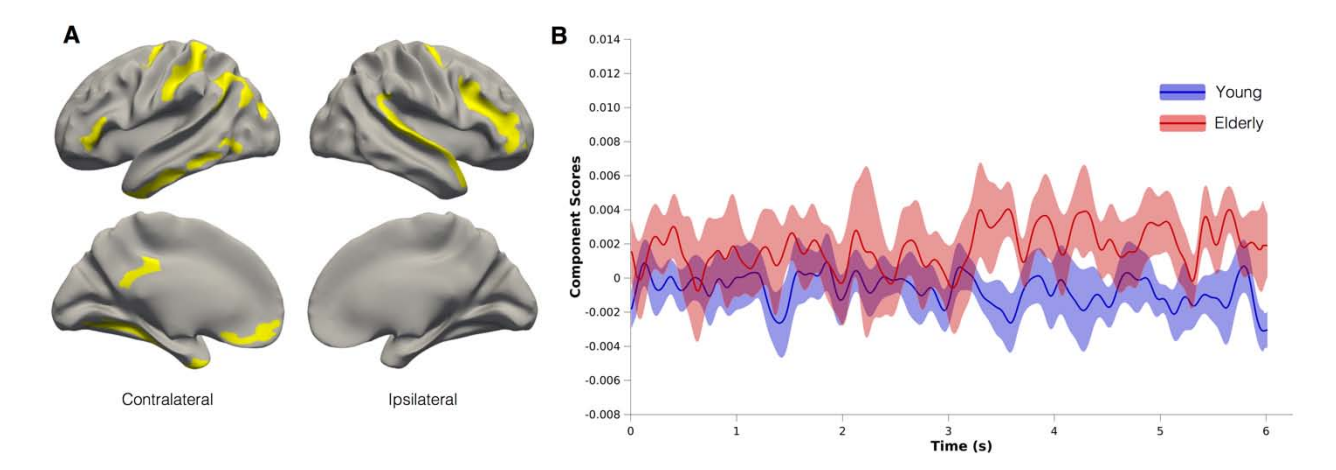


Figure 3.7: The second principal component extracted from the beta frequency (13–30 Hz) for the bimanual task, labelled *Bilateral Motor Network*. (A) Dominant 15% of loadings for this component are displayed, representing a network of strongly interconnected brain regions (B) The estimated time series (i.e., component scores) associated with this network, representing the network's engagement at each poststimulus time points. Shaded regions represent the standard error of the group mean. Contralateral and ipsilateral with respect to the dominant (right) hand.

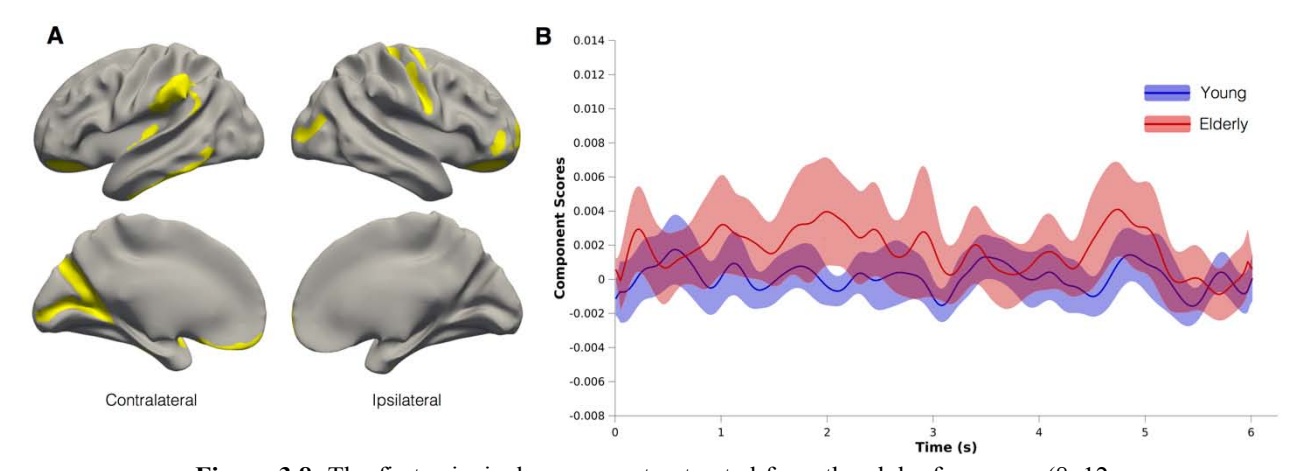


Figure 3.8: The first principal component extracted from the alpha frequency (8–12 Hz) for the bimanual task, labelled *Right-Dominant Motor Network*. (**A**) Dominant 15% of loadings for this component are displayed, representing a network of strongly interconnected brain regions (**B**) The estimated time series (i.e., component scores) associated with this network, representing the network's engagement at each poststimulus time points. Shaded regions represent the standard error of the group mean. Contralateral and ipsilateral with respect to the dominant (right) hand.

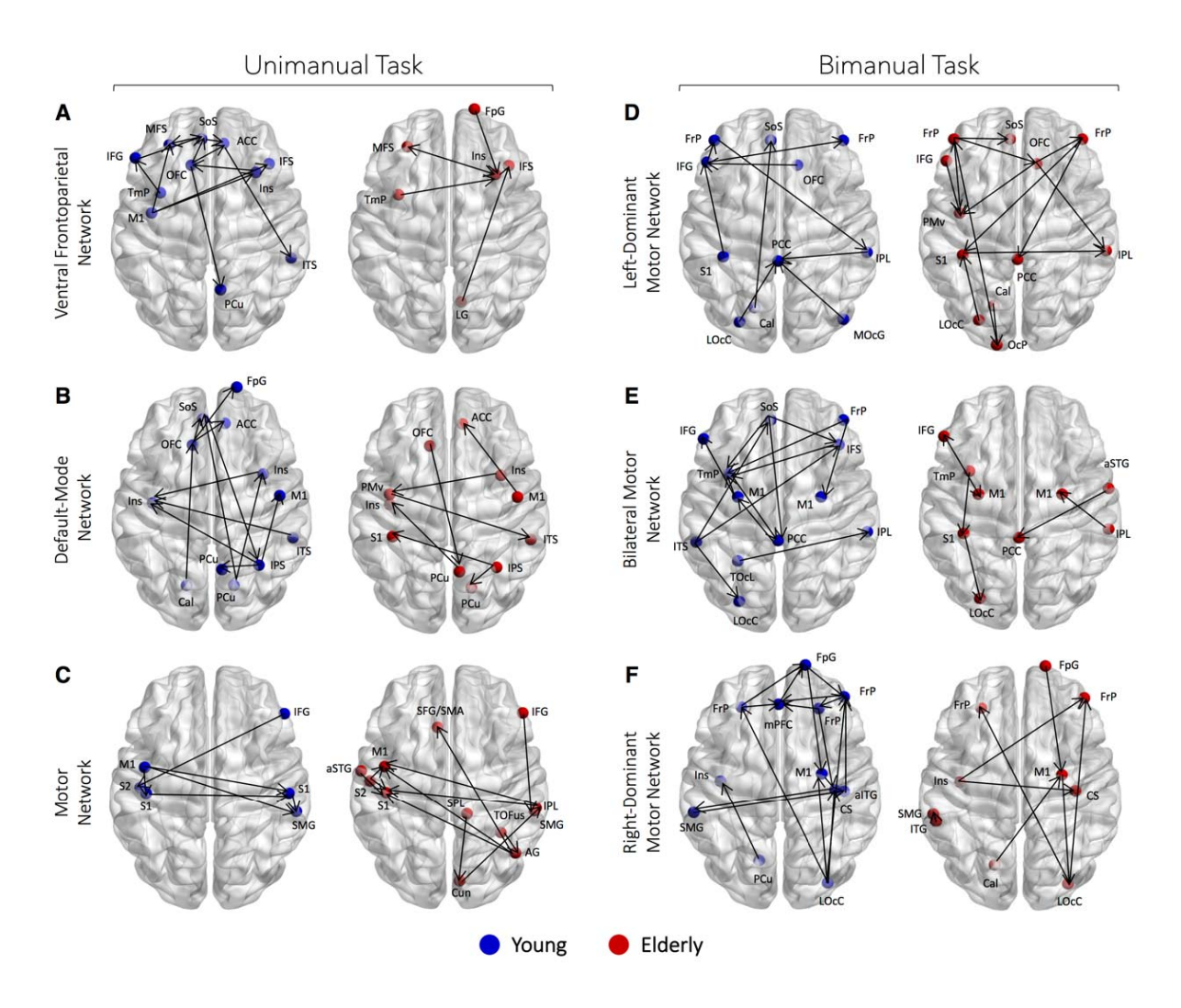


Figure 3.9: Group-specific Granger Causality maps for the unimanual and bimanual task-based brain networks are displayed in (A-C) and (D-F), respectively. Arrows depict the direction of information flow from one cortical region to another that reached statistical significance both at the individual-level and group-level (p < 0.05). Surface brains with blue nodes represent causal maps for the young group and surface brains with red nodes represent causal maps for the elderly group. Abbreviations: angular gyrus (AG), anterior cingulate cortex (ACC), anterior inferior temporal gyrus (aITG), anterior superior temporal gyrus (aSTG), calcarine cortex (Cal), central sulcus (CS), cuneus (Cun), frontal pole (FrP), frontal pole gyrus (FpG), inferior frontal gyrus (IFG), inferior frontal sulcus (IFS), intraparietal sulcus (IPS), inferior temporal sulcus (ITS), insula (Ins), lateral occipital cortex (LOcC), lingual gyrus (LG), medial prefrontal cortex (mPFC), middle frontal sulcus (MFS), middle occipital gyrus (MOcG), occipital pole (OcP), orbitofrontal cortex (OFC), posterior parietal cortex (PCC), precuneus (PCu), primary motor cortex (M1), primary sensory cortex (S1), secondary sensory cortex (S2), suborbital sulcus (SoS), superior frontal gyrus/supplementary motor area (SFG/SMA), superior parietal lobule (SPL), supramarginal gyrus (SMG), temporal pole (TmP), temporooccipital fusiform gyrus (TOFus), temporooccipital lobe (TOcL), ventral premotor (PMv).

Relative to young adults, elderly individuals demonstrated hyperactivity in the ventral frontoparietal and motor networks, whereas activity levels within the default-mode network did not differ between groups. Interestingly, our Granger causality analysis performed on the unimanual task-specific networks demonstrated that elderly individuals had increased input to M1 during unimanual hand grips, which was not observed in young adults. As for the bimanual task, two beta motor networks and one alpha motor network were identified: a left-dominant motor network (beta), a bilateral motor network (beta), and a right-dominant motor network (alpha). As with the unimanual task, elderly showed activity increases in both networks extracted from the beta band during production of bimanual hand grips, however, similar levels of activity were observed on the right-dominant alpha motor network. Altogether, these findings seem to favor the compensatory view of aging, whereby both groups engage similar networks of interconnected brain regions but, as opposed to younger adults, elderly exhibited a greater magnitude of activity in those networks in order to complete the motor tasks with similar accuracy.

Connectivity patterns underlying unimanual right-hand grips

Regions of the ventral frontoparietal network identified in this study have been observed previously in healthy adults, with temporoparietal cortex, anterior cingulate cortex, occipital cortex, as well as bilateral anterior inferior frontal cortex implicated in goal-directed attention processing^{72, 73}. Tasks that demand externalized attention to a visually presented stimulus have been shown to reliably activate regions within the frontoparietal network^{72, 76}, with older adults showing higher activity increases in prefrontal and parietal cortex^{25, 77}. Our findings revealed a similar pattern of connectivity during the isometric hand grip periods (i.e., from 0 to 3s and from 6 to 9s), however, activity levels within this network during the ramp period (i.e., from 3 to 6s) were similar between both young and elderly subjects. This could indicate that attentional demands are significantly increased when subjects are required to maintain an isometric hand grip at a specific force level. Accordingly, the greater cortical activation observed in older adults in the ventral frontoparietal network could be interpreted as a mechanism of attentional

control employed by elderly individuals in an attempt to dampen the processing of task-irrelevant stimuli⁷⁸.

Comparing elderly individuals to young adults on the unimanual motor network, we observed a similar group difference in activity levels to that of the ventral frontoparietal network, with elderly individuals exhibiting activation increases relative to young adults. This motor network was extracted from the beta frequency band and mainly included left pre- and postcentral gyri, occipital cortex, superior frontal gyrus (extending into SMA), as well as right inferior frontal gyrus, inferior and superior parietal lobules. Unlike the attention network in which increased activation was depicted by overall higher oscillatory amplitude, enhanced activity in the motor network was indexed by sharp beta peaks in elderly individuals. According to a computational modelling study on transient neocortical beta rhythms, these sharp beta oscillations reflect greater temporal synchrony in synaptic input on cortical pyramidal neurons⁷⁹. In line with this finding, our Granger causality analysis of the unimanual motor network provides additional evidence for an association between greater synchrony inputs and sharper beta oscillations (i.e., larger amplitude). More specifically, we found that greater cortical information flow to M1 was only present in the elderly group, which notably, was characterized with distinctly higher beta peaks. Combined, these results may therefore be reflective of a compensatory mechanism of the aging brain whereby greater synchrony of excitatory input currents are required in order to counteract structural changes such as myelin reductions in M1. Accordingly, since agerelated myelin deterioration is associated with a slowing of electrical activity^{80, 81}, it could be speculated that sharp beta oscillatory features constitute a neurophysiological mechanism by which activity within the motor network is increased, consequently allowing elderly individuals to achieve similar levels of task accuracy to those of young adults. Future task-based studies may therefore wish to relate network connectivity levels to myelin content and investigate whether a relationship exists between beta oscillatory rhythms and myelin in healthy adults as well as in neurodegenerative disorders or aging populations. Furthermore, the finding of enhanced interhemispheric information flow

between left primary and secondary sensorimotor regions and right parietal regions in elderly subjects observed during the unimanual task in the current study is in agreement with an influential theory of brain reorganization suggesting a loss of asymmetry in connectivity patterns in older adults⁶⁴⁻⁶⁶.

Connectivity patterns underlying bimanual hand grips

Our whole-brain multivariate PCA analysis on the bimanual task data revealed three functional networks of interest: a left-dominant, a right-dominant, as well as a bilateral motor network. Interestingly, movement of each hand independently activated a motor network in its respective dominant hemisphere (e.g., movement of right hand was controlled by a left-dominant motor network, and vice-versa). On the other hand, interhemispheric coordination between these two motor networks appeared to be modulated by a bilateral motor network which included left and right M1 as well as temporofrontal regions. As with the unimanual motor network described earlier, elderly subjects showed significant activity increases relative to young adults on the left-dominant motor network, which suggests an increase in the generation of postsynaptic currents during the performance of bimanual hand grips⁸². A similar pattern of activity was observed on the bilateral motor network, however, significant activity increases in the elderly group were only observed during the second half of the trial. Again, this finding may reflect a compensatory mechanism whereby augmented neuronal activity is recruited in older adults which enable them to sustain an isometric bimanual hand grip for the overall duration of the trial (6 s). The current findings therefore expand upon previous work supporting the view that the dominant hemisphere, as opposed to each contralateral hemisphere independently, controls the organization of bimanual hand movements⁸³ (for a review, see Maes et al.³). Notably, our data suggest a role for a whole-brain, bilateral motor network in the modulation of each lateralized hemisphere's motor network, with the temporal pole acting as an integrative hub for coordination of cortical information flow.

Interestingly, the effective connectivity maps for the bimanual task-based networks revealed that young adults rely more on prefrontal regions, such as the frontal pole (FrP), suborbital sulcus (SoS), orbitofrontal cortex (OFC), and medial prefrontal cortex (mPFC). This pattern of strongly interconnected frontal regions was largely absent in the elderly group, which is in agreement with previous cognitive studies reporting age-related activity decreases in prefrontal regions^{25, 84}. Another striking difference in connectivity patterns between young and older adults lies in the importance of the left temporal pole region in the bilateral motor network. Based on our Granger causality analysis, this brain area appears highly integrated within the network in the young group as it receives cortical information from several parietal and frontal regions (including left M1), but also has a causal influence on the posterior cingulate cortex (PCC) which in turn sends information back to the left M1 (see Figure 3.9E). While the neural organization of the bilateral motor network in young adults seems to be driven by the dominant (left) hemisphere, as previously reported⁸³, bimanual movements in elderly individuals rather appear to be controlled from each contralateral hemisphere independently, with minimal interhemispheric connectivity. This lack of coordination between hemispheres could be attributable to altered white matter integrity of the corpus callosum in older adults, which plays a key role in allowing both hemispheres to communicate during bimanual movements^{17, 19}. Indeed, previous monkey research investigating the interhemispheric connections of the temporal lobes has revealed that the corpus callosum receives extensive fibers from the temporal pole 85. We thus speculate the left temporal pole to be an important substrate for coordination of both hands during bimanual movements and further propose this region to be a central hub responsible for mediating information flow between the two hemispheres. Partly due to their long-distance connectivity and topological centrality supporting integration of multiple regions, cortical hubs are known to be highly biologically costly and as a consequence become highly vulnerable in aging⁸⁶.

Limitations

Multivariate network connectivity analysis techniques for MEG data are sparse and relatively novel hence it is important to note some limitations of the methods used in the current study. First, the low number of participants in each group ($n_{young}=12$, $n_{old}=11$) limited the statistical power of the study, which may have led to an overestimation of the effect size and consequently to increased chances of a Type II error. Reproducibility of these findings should be assessed in a similar, but larger, sample of young and elderly individuals. Second, we investigated group differences in activity levels of commonly shared task-based brain networks which in turn precluded us from determining whether, and how, spatial reorganization occurs during healthy aging. Lastly, the Granger causality approach employed in the current study did not take into account instantaneous or time-varying directional effects which may consequently provide an incomplete description of the causal relations between cortical brain regions in the identified task-based networks⁷¹.

Conclusions

In conclusion, this work illustrates that despite matching levels of task accuracy, elderly individuals were characterized with higher levels of activity in functional brain networks underlying the performance of unimanual and bimanual hand movements. A possible large-scale compensatory mechanism in elderly subjects was observed in the unimanual motor network Granger causality map, in that M1 received input from several parietal regions possibly in an attempt to support residual motor function within this primary motor region. Moreover, findings from the current study suggest a role for a whole-brain, bilateral motor network in the modulation of each lateralized hemisphere's motor network. We further suggested that the left temporal pole region within this network acts as an integrative hub for coordinating cortical information flow from both hemispheres in young adults, but was impaired in elderly individuals. Collectively, these findings suggest that despite functional brain reorganization, elderly individuals have overly activated and disintegrated task-specific motor networks. Taking into account the

high dynamicity of cortical brain networks, an interesting research avenue would be to repeat similar analyses using a time-varying (dynamic) approach.

CHAPTER 4

MOTOR TASK-INDUCED CHANGES IN RESTING-STATE

NETWORKS IN AGING

Preface

A promising paradigm in human neuroimaging research is the study of intrinsically activated brain networks, which can be observed in the absence of external stimuli or explicit tasks. Historically, Biswal and colleagues⁸⁷ were the first to detect the manifestation of spontaneous low-frequency fluctuations in the BOLD signal and successfully identified functional connectivity in the motor network at rest. Over the past years, this so-called resting-state approach has become increasingly popular to investigate alterations in the synchronization of neuronal activity and their relevance to various healthy and diseased populations.

In this project, we collected MEG data at rest before and after two different motor tasks. We then employed envelope correlation to investigate whether resting-state connectivity is modulated by the performance of visually-paced hand grips and whether it affects resting brain activity differently in aging individuals relative to young adults. We hypothesized that an increase in task-related activity, as observed in elderly individuals in our experiments described in previous chapters, would lead to an increase in resting-state connectivity.

The recent advent of resting-state MEG analysis has drawn much attention mainly due to its capability to derive dynamic and spectral information, which is a limitation of fMRI studies. As of now, the analysis methods used for stationary estimation of MEG resting-state connectivity are novel and underdeveloped. This challenge was addressed in a study that compared consistency and reproducibility of several whole-brain network

connectivity metrics on resting-state MEG data⁸⁸. The authors concluded that simple envelope correlation ranks among the most consistent analysis methods as it was found to have good test-retest reliability as well as to minimize spatial leakage artifacts⁸⁸.

* * *

4.1 Abstract

Objective: Resting-state functional connectivity provides a unique way to explore the underlying brain changes associated with aging.

Methods: Using MEG measurements of brain activity acquired from three separate resting-state sessions interspersed with two motor tasks, we studied whether executing unimanual and bimanual hand grips would affect subsequent resting-state functional connectivity patterns differently in aging subjects when compared to young adults. MEG data were collected from twelve young (mean age = 23.7 ± 2.9 years) and eleven elderly subjects (mean age = 67.5 ± 3.9 years). Beamformer-based time series were reconstructed for 148 brain regions and the Hilbert transform was used to extract the instantaneous power from multiple frequency bands. Functional connectivity analysis was then performed by systematically computing pairwise envelope correlations between the source-reconstructed brain regions.

Results: For both groups, we observed enhanced beta connectivity from the first to the second resting-state run (i.e., a unimanual task was performed between the two runs). This connectivity increase was present in networks that govern core attentional, visuospatial, and sensorimotor processes. Furthermore, elderly subjects demonstrated a strong delta connectivity increase at rest following the performance of a unimanual task, which correlated positively with activity of the task-based ventral frontoparietal attention network derived from the unimanual task.

Conclusions: Our findings suggest that elderly individuals maintain the capacity for modulating network-wide brain activity in the beta frequency (13–30 Hz) when switching from an active motor state to a resting-state period. In contrast, elderly individuals show altered slow (1–4 Hz) oscillatory connectivity when attentional demands are high, possibly indicating a marker of healthy neurocognitive aging.

Larivière S, Xifra-Porxas A, Niso G, Kassinopoulos M, Mitsis GD, Boudrias MH. Motor-task induced changes in resting-state MEG networks in aging.

This work is to be submitted as:

4.2 Introduction

Resting-state (i.e., task-free) acquisitions of spontaneous oscillatory neuronal activity are becoming increasingly used to study brain networks in healthy and diseased populations. Notably, resting-state functional connectivity offers a multitude of advantages over task-evoked paradigms, as for instance, better signal to noise ratio⁸⁹, fast and easy implementation, as well as the possibility of studying broader samples of participants with limited cognitive or motor abilities. Furthermore, previous analyses of resting-state data collected from healthy adults have consistently revealed strong congruence between brain networks derived from resting-state and those from task-related studies, as well as with different modalities such as fMRI and MEG⁹⁰⁻⁹³.

As the world rapidly ages, a growing interest is being paid to the relationship between alterations in distributed brain networks and progressive motor or cognitive function declines observed during aging³¹⁻³³. Whereas previous fMRI and MEG restingstate studies have consistently documented a link between hyperactivity of the sensorimotor network and increasing age^{32, 94-96}, age-related cognitive deficits have often been attributed to connectivity decreases in networks encompassing frontal, parietal, and temporal regions, such as the dorsal attention network and the default-mode network^{31, 97}. Here distinctly, we were interested in studying whether functional connectivity patterns associated with performing a series of hand grips are reflected differently in elderly as compared to young adults. To do so, every participant performed a combination of two different visually-guided motor tasks interspersed with three resting-state periods (see Figure 3.1 for a schematic overview of the experiment protocol). Consequently, this allowed us to characterize how the aging brain at rest alters its functional connectivity after performing a hand motor task and accordingly determine whether elderly individuals retain the capacity to modulate network-wide activity influenced by an increase in task demands.

A number of neuroimaging studies have examined alterations in brain functioning in healthy and diseased populations by employing a combination of resting-state and taskactivation paradigms (rest before task 98-100; task before rest 101, 102). It is commonly assumed that the order of task-evoked and resting-state acquisitions in an experiment protocol has negligible effects on data subsequently acquired. Carrying out a task experiment may however induce connectivity changes on subsequently acquired restingstate data and consequently lead to erroneous interpretation of findings (e.g., attribute task-induced connectivity changes to an underlying pathology). In light of such possibility, it is important to go beyond understanding intrinsically organized brain networks at rest, and investigate the effects of performing a task on subsequent restingstate connectivity. Waites and colleagues ¹⁰³ specifically addressed this issue by comparing resting-state functional connectivity before and after a language task and reported enhanced connectivity in frontal and parietal regions after the task, therefore suggesting that resting-state functional connectivity may in fact depend on the prior cognitive state. Similarly, other research groups have studied the modulatory effect of intensive motor learning practice on subsequent resting-state periods, and consistently reported enhanced connectivity in sensorimotor, visual, and cerebellar areas 104-106. Whether performing a ubiquitous hand motor control task can lead to similar functional connectivity changes in MEG resting-state networks, and whether it would affect resting-state connectivity differently in elderly individuals as compared to young adults, represent important questions that remain largely unexplored. Accordingly, resting-state functional connectivity provides a unique way to explore brain rewiring and reorganization mechanisms underlying aging processes such as gray and white matter loss. A better understanding of these mechanisms could therefore provide beneficial insights for the development of novel and individualized rehabilitative treatments. Ultimately, this research avenue could help optimize motor recovery functions in movement-impaired populations such as stroke survivors.

This study sought to assess whether performing unimanual and bimanual hand movements would affect connectivity within large-scale resting-state MEG networks differently in elderly relative to young adults. In other words, we compared resting-state connectivity before (baseline) and after each motor task (unimanual and bimanual) to investigate functional connectivity changes in response to performing a series of visually-paced isometric hand grips. Partially consistent with prior findings^{32, 33}, we expected to observe increased connectivity at baseline (i.e., initial resting-state) in aging individuals relative to young adults across previously documented resting-state networks⁹², which could suggest reduced inhibitory control of cortical input in elderly subjects¹⁰⁷. We further expected that an increase in task-related activity, as observed in elderly individuals (see Chapter 3), would lead to an increase in resting-state connectivity immediately subsequent to the task. This would provide evidence that undergoing a motor task can lead to age-specific functional changes in the brain, thus hinting at a potential for different mechanisms by which the older brain adapts to task demands.

4.3 Methods

Details on participants as well as data acquisition and preprocessing are described in Chapter 3 and Appendix A, respectively. All participants underwent three separate 5-minute resting-state sessions (interspersed with the two motor tasks as described in Chapter 3 and Figure 3.1) and were instructed to keep their eyes open and fixate on a cross.

Data analysis and functional connectivity

The functional connectivity analyses described below were performed separately for each of the three resting-state sessions. A schematic of the subsequent data analysis pipeline is provided in Figure 4.1. For every participant, the resting-state MEG data were down-sampled to 300 Hz and epoched offline in 10 s windows. Epochs in which significant signal artifacts were observed were rejected (see Appendix A) and the remaining "clean" 10 s windows were concatenated across time. The LCMV beamformer

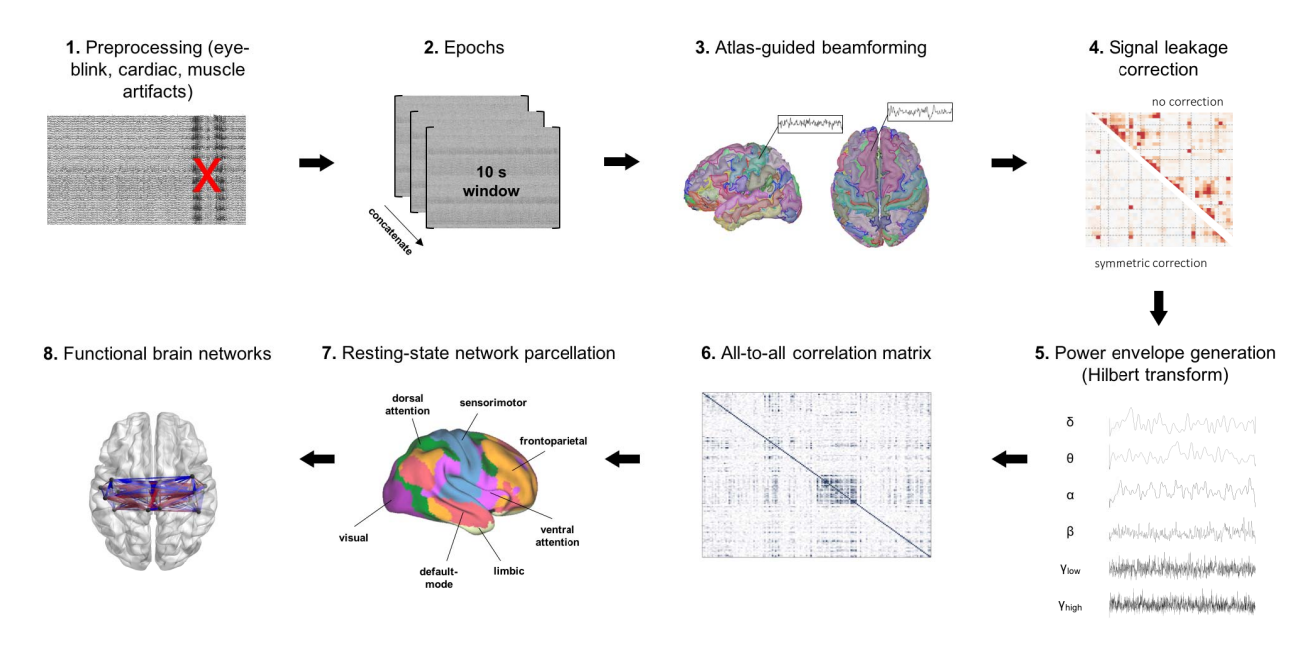


Figure 4.1: Schematic overview of the analysis pipeline used for the resting-state MEG data

spatial filtering approach⁶⁸ was then used on the subject-specific, concatenated data to reconstruct a single time series for all of the 148 cortical brain regions defined by the Destrieux atlas⁶⁹. Each time series was corrected for signal leakage effects (i.e., spurious correlations between the inferred cortical sources) using a symmetric, multivariate correction method intended for all-to-all functional connectivity analysis 108. The Hilbert transform was subsequently used to extract the instantaneous power and phase from six frequency bands of interest: delta (1–4 Hz), theta (5–7 Hz), alpha (8–12 Hz), beta (13–30 Hz), gamma 'low' (31–80 Hz), and gamma 'high' (81–150 Hz). Functional connectivity analysis was performed on each of the six frequency bands by systematically computing pairwise envelope correlations between all 148 source-reconstructed brain regions. The resulting all-to-all connectivity matrices (one per frequency band) were sorted by functional networks according to the recently proposed 7-network brain cortical parcellation estimated by intrinsic functional connectivity using resting-state fMRI data from 1000 healthy adults⁹². This network parcellation provided spatial consistency across all subjects as well as between resting runs, thereby making direct comparison of functional network connectivity possible. Here, functional connectivity was defined as the mean connectivity strength (i.e., the mean of all pairwise correlations) within each of the pre-defined seven resting-state networks. Differences between groups (young vs. elderly), runs (resting-state 1, 2, and 3), and mean connectivity strength for each of the seven resting-state networks were identified by carrying out six $7 \times 3 \times 2$ mixed-model ANOVAs (one per frequency band). Tests of sphericity were carried out for all ANOVAs and Greenhouse-Geisser adjusted degrees of freedom were checked. Original degrees of freedom are reported as any violations of sphericity did not affect the results.

4.4 Results

A significant main effect of Run was observed in two frequency bands, specifically delta ($F_{2,42} = 11.1$, p < 0.005) and beta ($F_{2,42} = 4.7$, p < 0.05), whereas a significant main effect of Network was found in all frequency bands: delta ($F_{6,126} = 14.3$, p < 0.001), theta ($F_{6,126} = 14.3$, p < 0.001), alpha ($F_{6,126} = 56.3$, p < 0.001), beta ($F_{6,126} = 14.3$, p < 0.001), gamma 'low' ($F_{6,126} = 8.8$, p < 0.001), and gamma 'high' ($F_{6,126} = 8.0$, p < 0.001). Significant interactions involving Network, Run, or Group were solely observed in the delta and beta frequency bands and are described below.

Task-induced connectivity changes in the delta frequency band

Slow oscillatory connectivity (1–4 Hz) differed between young and elderly subjects across different resting-state sessions as evidenced by a significant Run × Group interaction, $F_{2,42} = 5.61$, p < .05, $\eta^2_p = 0.21$. Within-subjects contrasts yielded significant group differences from the first to second resting-state run (p < 0.005), and from the second to the third run (p < 0.05). As can be seen from Figure 4.2A, this interaction was caused by elderly subjects exhibiting a large increase in delta connectivity in the second resting-state run (i.e., after the unimanual task) relative to young adults.

Task-induced connectivity changes in the beta frequency band

The beta frequency (13–30 Hz) showed a significant Run × Network interaction, $F_{12.252} = 2.76$, p < .05, $\eta^2_p = 0.12$, indicating that resting-state network connectivity varies

as a function of time (i.e., resting-state run). As can be seen from Figure 4.3A, this interaction can be interpreted by enhanced connectivity from the first to the second resting run (i.e., increased connectivity after the unimanual task), notably in the visual, dorsal attention, and sensorimotor networks. A significant Network × Group interaction was also observed, $F_{6,126} = 3.43$, p < .05, $\eta^2_p = 0.14$, suggesting that elderly subjects demonstrate slightly higher beta oscillatory connectivity than young adults in all resting-state networks (non-significant, ps > 0.36) with the exception of the visual network (p < 0.05; Figure 4.3B).

Correlation with task-based results

In order to relate the delta resting-state findings to the two motor tasks (unimanual, bimanual), we computed correlations between the levels of coordinated activity in each task-related network (Figures 3.3-3.8), and the mean resting-state delta connectivity (z scores averaged across all networks, for each subject). As displayed in Figure 4.2B, an increase in task-related activity in the ventral frontoparietal network (derived from the unimanual task) was positively correlated with larger delta oscillatory connectivity in the subsequent resting-state (second resting run) in older adults only ($r_{\text{elderly}} = 0.49$, p = 0.05). Young adults, however, showed the opposite pattern whereby stronger levels of ventral frontoparietal activity was associated with lower delta connectivity in the following resting-state period ($r_{\text{young}} = -0.60$, p < 0.05). The between-group difference in correlation coefficients reached statistical significance (p < 0.01). The analogous correlations involving the default-mode network and the motor network (unimanual task), as well as the left-dominant, right-dominant, and bilateral motor networks (bimanual task) were not significant.

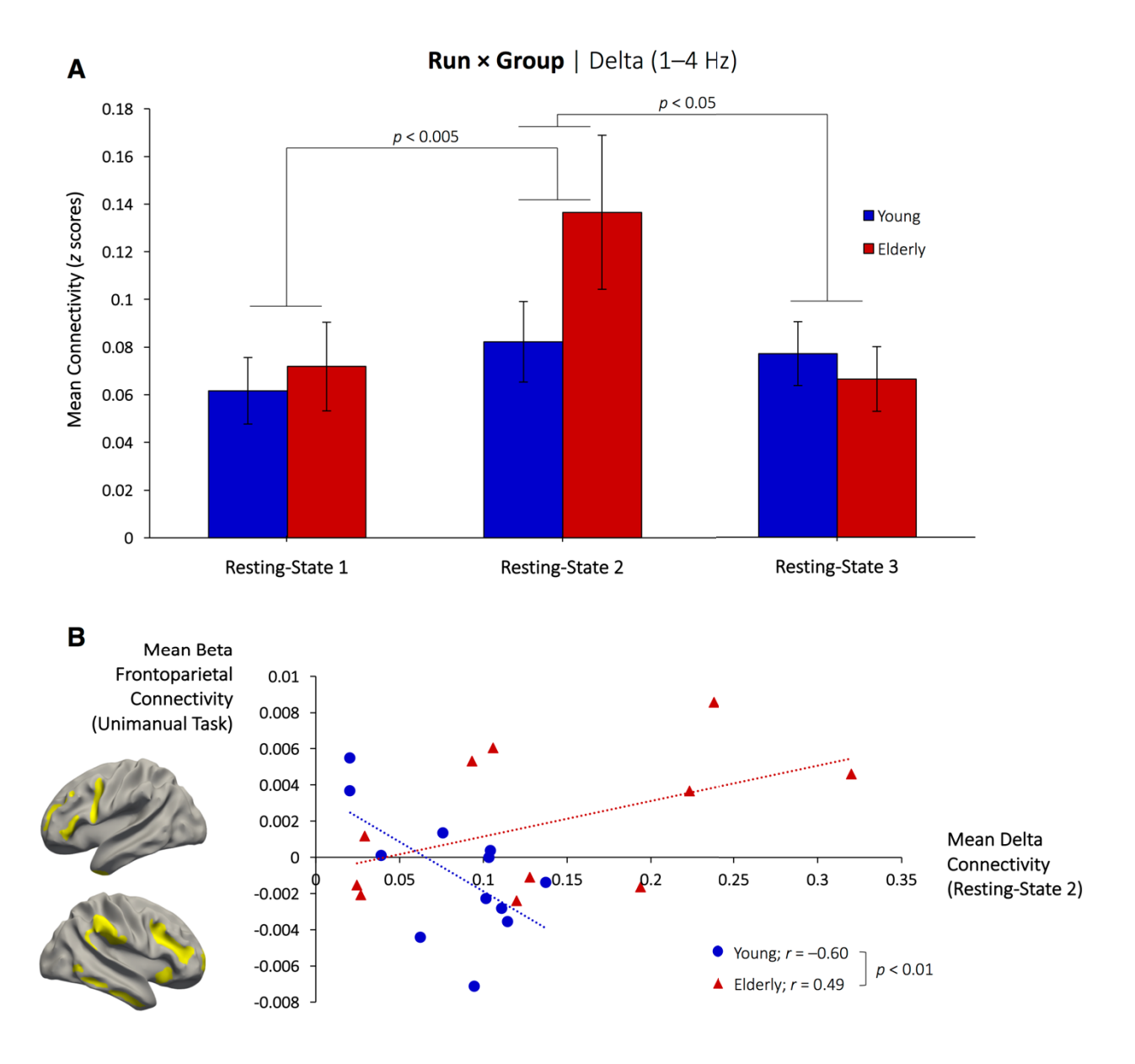


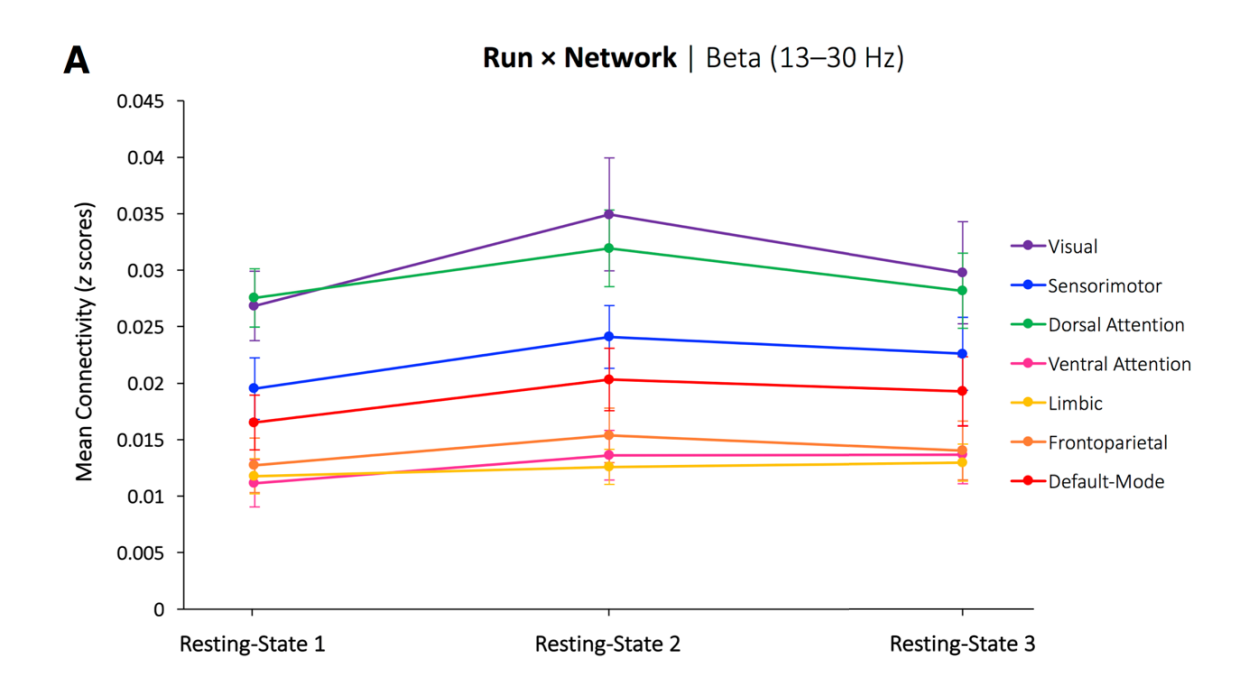
Figure 4.2: (A) Group difference in mean resting-state delta connectivity, averaged across all networks and plotted as a function of resting-state run. (B) Correlation coefficients between the mean beta time series of the ventral frontoparietal network (derived from the unimanual task) and the mean resting-state delta connectivity of the second resting-state run (averaged across all networks). The values on the y-axis represent component scores derived from the task-based PCA (see Chapter 3), whereas the x-axis values represent Pearson's correlation coefficient.

4.5 Discussion

To our knowledge, this is the first MEG study to focus on changes in resting-state functional connectivity in response to performing hand motor tasks. Specifically, we investigated whether performing visually-guided unimanual and bimanual hand grips would affect whole-brain resting-state networks differently in aging subjects as compared to young adults. First, irrespective of age, we observed an increase in beta connectivity immediately following a unimanual motor task. This increase from the first to the second resting-state session was mainly observed in networks that govern core attentional, visuospatial, and sensorimotor processes, and which include regions that were strongly activated during unimanual hand grips (see Chapter 3). Group differences were observed in a slower frequency band; relative to young adults, older individuals exhibited a strong increase in delta connectivity following the unimanual task. We further demonstrated that enhanced delta activity was positively correlated with activity within a task-related ventral frontoparietal network in elderly. Taken together, these results suggest that elderly individuals maintain the capacity to adapt to task demands via network-wide connectivity increases in the beta frequency (13–30 Hz), but have altered slow (1–4 Hz) oscillatory connectivity which could be caused by an increase in attentional demands.

Isometric right-hand grips modulate network-wide beta connectivity increases

In agreement with previous fMRI studies investigating the effects of intensive motor learning on subsequent resting-state brain activity in healthy adults ^{105, 106}, significant connectivity increases were observed following the unimanual task relative to baseline (i.e., the first resting-state session). This enhanced connectivity pattern was present in both young and elderly groups, and was particularly noticeable in resting-state cortical networks that include regions previously engaged during the unimanual task (e.g., visual, dorsal attention, sensorimotor, default-mode networks). Neuromodulation studies using non-invasive brain stimulation protocols such as transcranial magnetic resonance (TMS)



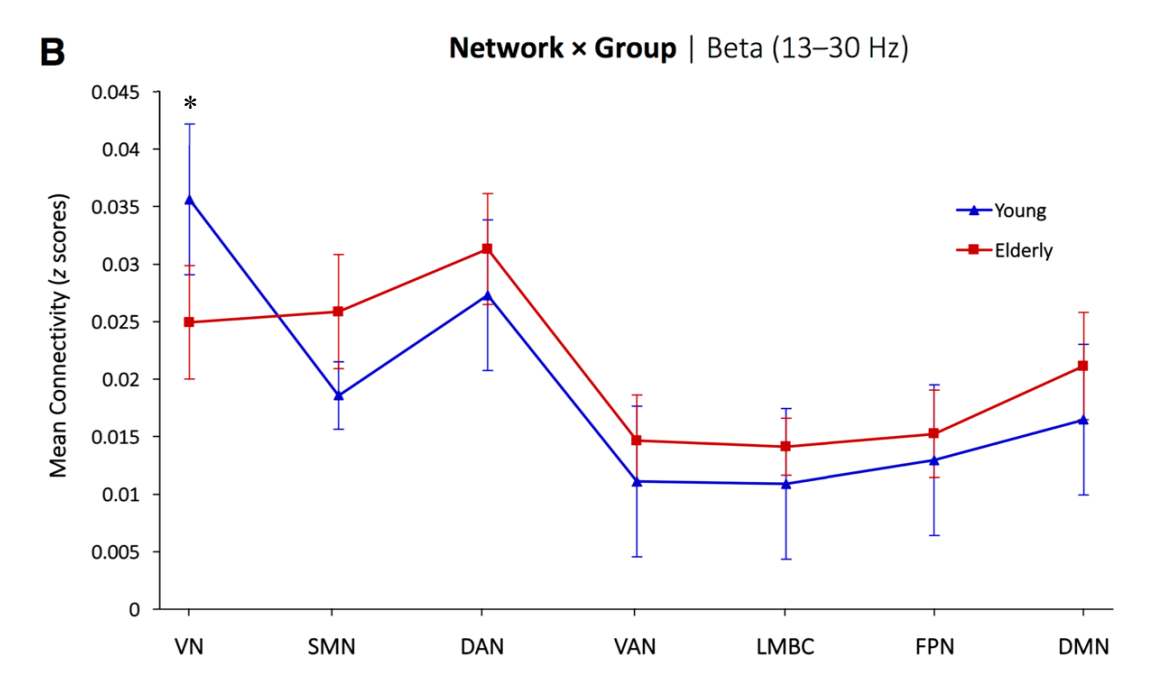


Figure 4.3: (A) Mean beta connectivity differences between resting-state networks, averaged across both groups and plotted as a function of resting-state run. (B) Group differences in mean beta connectivity, averaged across resting-state runs and plotted as a function of resting-state networks. Abbreviations: visual network (VN), sensorimotor network (SMN), dorsal attention network (DAN), ventral attention network (VAN), limbic network (LMBC), frontoparietal network (FPN), default-mode network (DMN). * = p < 0.05.

or tDCS have demonstrated that neuronal flexibility, or any short- or long-term sustained changes in cortical properties, is importantly mediated by GABA receptors 109, 110. Interestingly, despite previously reported neurochemical-related alterations between dopamine and GABA neurotransmitters in older adults¹¹, these individuals exhibited sustained changes in cortical connectivity in response to performing a series of visuallyguided isometric hand grips. Moreover, our current data suggest that ubiquitous hand movements can induce similar neuronal flexibility, observed here as an increase in resting brain connectivity, even in the absence of external stimulation or intensive motor learning. Given the evidence reported herein, we suggest that healthy adults, irrespective of age, retain the capacity for task-induced connectivity changes at a systems level. Specifically, this was evidenced by a significant increase in beta functional connectivity within wholebrain networks subserving functions necessary for the production of unimanual hand grips, as for instance, visuospatial, attentional, and sensorimotor processes. Interestingly, these connectivity changes were not sustained throughout the third resting-state session (i.e., after the bimanual task), which could be explained by the fact that execution of bimanual hand grips activated a combination of beta and alpha motor networks, whereas the unimanual task networks were all identified in the beta frequency. An important consideration for future studies that wish to employ a similar experiment protocol, however, would be to counterbalance the order of the unimanual and bimanual tasks. This would allow for a relationship between connectivity changes and performance of a specific task to be reliably established.

Altered slow oscillatory connectivity in aging relates to attentional demands

Previous studies looking at the role of slow frequencies during healthy aging (e.g., delta; 1–4 Hz or theta 5–8Hz) have been highly inconsistent, reporting increased^{111, 112} and decreased^{113, 114} slow oscillatory power. In this context, our finding of age-related increases in slow wave oscillatory connectivity may expand upon this debate by instead demonstrating that enhanced delta connectivity in fact plays a role in modulating

attentional or cognitive resources in older adults. This interpretation is in line with evidence from cognitive studies which looked at the association between aberrant delta oscillatory activity and healthy aging^{44, 115}. In one such study, Maurits and colleagues¹¹⁵ employed an auditory oddball paradigm to assess the association between EEG coherence and cognitive ability. Partially consistent with our findings, the authors provided evidence that elderly subjects have enhanced interhemispheric delta coherence during a simple cognitive task¹¹⁵. Here distinctly, delta oscillatory connectivity increases were not directly associated with ongoing cognitive processes, but rather represented sustained connectivity likely induced or enhanced by the unimanual task. Alternatively, another study has recently suggested that the phase of slow delta oscillations modulates higher gamma power during attentional reorienting¹¹⁶. The authors further proposed a role for deltagamma phase-amplitude coupling as a neurophysiological mechanism underlying coordination among frontoparietal regions during attentionally demanding tasks¹¹⁶. Although phase-amplitude coupling analysis was not carried out on the current data, we found a significant correlation between intensity levels of the ventral frontoparietal network (extracted from the beta frequency during the unimanual task; see Chapter 3) and the mean delta connectivity strength over the whole brain during the second resting-state session (i.e., following the unimanual task) in the elderly group. Considered alongside cognitive studies in aging^{112, 117}, and in addition to its association to the ventral frontoparietal cortex reported here, the large increase in delta connectivity following the unimanual task could be considered a marker of healthy neurocognitive aging.

Limitations

The large amounts of data generated by MEG recordings often limit large-scale analyses to one high resolution dimension. Temporal accuracy (i.e., high sampling rate), for instance, will be preserved at the cost of spatial accuracy (use of parcels instead of voxels), which in turn may result in a lower ability to localize effects. This limitation was overcome in the current study by using a brain parcellation with 30 or more parcels to reconstruct the source time series, thus allowing higher sensitivity 106. Additionally, one

key assumption of using Yeo et al.'s⁹² atlas-based network parcellation is that the surface registration has accurately aligned individual subjects to the group parcellation map, such that no residual individual differences remain in terms of cortical area locations. Future analyses of the current data could overcome these limitations by (1) repeating the same pairwise envelope correlation on the source-reconstructed MEG time series using a series of different cortical and network parcellation atlases, or (2) identifying cortical areas using a machine learning approach that accounts for individual variability (e.g., areal classifier¹¹⁸).

Conclusions

In summary, this study explored whether performing unimanual and bimanual motor control tasks would affect subsequent resting-state functional connectivity differently in elderly subjects as compared to young adults. Resting-state networks including brain regions that were highly activated during the unimanual task in the beta frequency (e.g., visual, motor, and attention networks) showed enhanced beta oscillatory connectivity after the task in all subjects. Contrastingly, we found that elderly subjects, relative to young adults, had a significant increase in delta connectivity following the unimanual task which was not sustained throughout the third resting run (i.e., after the bimanual task). This large delta connectivity increase was positively correlated with activity of the task-based ventral frontoparietal attention network (derived from the unimanual task), thus suggesting a role for slow oscillations in modulating task-related attentional demands. Collectively, our findings demonstrate that performing hand movements can enhance functional connectivity in the resting brain, specifically in regions that were activated by the task. This work should prompt further studies to assess resting-state connectivity changes induced by a task in motor-impaired populations. The challenge remains to exploit the potential benefits of combined task-related and restingstate protocols to provide a valuable tool for future research and possible rehabilitation strategies aiming to enhance neural flexibility by means of exercise programs targeting hand movement.

CHAPTER 5

TASK-RELATED MOTOR CONNECTIVITY IN CHRONIC

Preface

STROKE

Topics described in previous chapters contribute to our understanding of the underlying neural reorganization and possible compensation mechanisms involved during healthy aging. Notably, we showed that elderly individuals exhibit higher levels of brain activity relative to young adults during hand movement, differ in the underlying effective connectivity patterns (Chapter 3), but nevertheless retain the capacity for neuronal flexibility (Chapter 4). Studies aiming to further our understanding of the brain processes involved during healthy aging are fundamental for stroke research for two main reasons: (1) increasing age ranks among the most common risk factors for ischaemic stroke⁴⁹, and (2) the global population is rapidly aging¹¹⁹.

Despite a high variability in functional motor recovery across different stroke patient subpopulations, rehabilitation strategies continue to employ a 'one size fits all' approach¹²⁰. One reason for this may be that we lack a clear understanding of the biological factors that actively promote poststroke plasticity and recovery. Indeed, according to the International Partnership of Stroke Recovery and Rehabilitation¹²¹, there is an urgent need for better insights into the neural mechanisms guiding stroke recovery. Another pressing issue in stroke research lies in the identification of robust biomarkers of motor recovery, which would allow rehabilitation interventions to target the appropriate brain regions and eventually move towards individually-tailored treatments^{60, 121}.

In this chapter, we compared activity levels of functional brain networks involved during hand movement in chronic stroke patients to those of healthy controls. Notably, we

assessed whether alterations within task-specific networks would lead to the identification of recovery biomarkers in the stroke group. Based on prior findings showing reduced activity in sensorimotor regions of the affected and unaffected hemisphere, we hypothesized that chronic stroke patients would exhibit network-wide decreases in functional connectivity relative to healthy controls. Consequently, we also hypothesized that greater motor impairment would be associated with disruptions within these sensorimotor regions.

* * *

5.1 Abstract

Objective: Studies mapping the patterns of activation in functional brain networks during upper limb recovery after stroke have mainly focused on specific areas such as the ipsi- and contralesional primary motor cortices. Consequently, the contribution of other motor and non-motor areas remains poorly understood. This study sought to identify differences in functional connectivity patterns in whole-brain networks. We wished to expand our knowledge of the brain activity underlying hand motor control in chronic stroke patients in comparison to that of healthy controls.

Methods: Twenty-four healthy control subjects and 17 chronic stroke patients underwent fMRI and performed a series of isometric hand grips with their dominant hand (control subjects) or affected hand (stroke patients). We used task-based multivariate functional connectivity to derive whole-brain networks that underlie hand movement. Permutation testing was then used to identify activity differences within these task-specific networks.

Results: Our whole-brain analysis revealed group differences on two networks: (1) a motor network, in which stroke patients showed overall reduced activation, and (2) a default-mode network, in which healthy subjects demonstrated increased deactivation. Moreover, our within-network analysis showed decreased regional activity in contralateral (to the moving hand) M1/S1, which was specific to the stroke group. With respect to behavioral impairment, we found an association between ipsilesional M1/S1 activity and motor performance in stroke patients.

Conclusions: Following brain damage due to stroke, connectivity within a large-scale motor network was disrupted and appeared to be driven by reduced activity in ipsilesional sensorimotor regions. These findings support the notion that rehabilitation treatments for chronically impaired patients should target secondary motor areas in order to support residual activity in M1/S1.

Larivière S, Ward NS, Boudrias MH. Reduced functional connectivity of the motor network in chronic stroke.

This work is to be submitted as:

5.2 Introduction

Ischemic stroke is a cerebrovascular injury which often results in sensorimotor and cognitive impairments due to brain damage^{50, 122}. Whereas some patients achieve good motor recovery, up to 40% of stroke survivors are left with permanent motor disabilities¹¹⁹, with the majority presenting residual hand deficit⁵⁰. This in turn has dramatic consequences on their daily life activities 123 and represents a major economic burden (estimated at \$2.8 billion a year in Canada for new and chronic stroke patients)¹²⁴. Clinical trials focusing on the manipulation of poststroke plasticity (i.e., changes in spatial distribution or functional brain activation) via stem cell therapy^{125, 126} pharmacotherapy¹²⁷ have so far been unsuccessful in improving motor control in humans. On the other hand, brain imaging studies offer promising avenues in providing more detailed and accurate information about residual motor function than clinical assessment alone 60, 128. As a result, they have the potential to help establishing plausible biological targets for rehabilitation and clinical research¹²⁰. However, the identification of stroke recovery biomarkers, which are defined as characteristics that can have indicative and predictive value for disease state or motor outcome¹²⁹, is still lacking¹²¹ and thus remains an area of active research in neuroimaging 60, 128.

Previous event-related fMRI studies have provided ample evidence for cortical reorganization during recovery of motor function after stroke (for comprehensive reviews, see Lake et al.⁴⁹ and Grefkes and Fink¹³⁰). For instance, Rehme and colleagues¹²⁸ found that enhanced activity in ipsilesional primary motor cortex (M1) during movement of the paretic hand in the acute stage (< 1 week) can accurately predict motor outcome at 4-6 months poststroke. Similarly, another study from Carey et al.¹³¹ looked at the relationship between simple hand movement and cerebral activation. The authors reported that well-recovered chronic stroke patients activated the ipsilesional primary sensorimotor cortex to levels similar to those observed in healthy controls, whereas worse-off patients demonstrated persistent activation decreases in this area¹³¹. On the other hand, reduced functional coupling from ipsilesional SMA and PMd to M1 appear to be characteristics of

worse-off patients¹³². Taken together, these studies suggest that activity levels within the ipsilesional M1 alone is positively correlated with the degree of motor recovery observed after stroke^{56, 133, 134}. Despite a substantial amount of research regarding functional recovery after stroke, current findings are mostly limited to M1.

Recent neuroimaging studies in healthy adults in fact demonstrated that seemingly simple hand movement engages a distributed network of regions which includes, but is not limited to, M1^{39, 135}. Secondary motor areas, particularly PMv, PMd, and SMA, as well as the parietal cortex are also recruited during hand movement ^{136, 137} and may in turn be highly relevant to stroke rehabilitation research. Notably, these regions contain corticospinal neurons ¹³⁸ and as a consequence have the potential of acting on motoneurons which innervate muscles. Secondary motor regions could therefore be ideal biological targets in the context of neurorehabilitation using stimulation protocols, as for instance tDCS. Such treatment strategy could facilitate output to upper limb motoneurons via stimulation of anatomically intact corticospinal regions and accordingly benefit the recovery of some motor function in the affected hand after stroke. The functional capability of the premotor areas to support residual motor function after an infarct, as well as their contribution within large-scale motor networks, however remain unclear.

Despite these alterations in motor connectivity, it is now believed that whole-brain network assessments, as opposed to typically used region of interest (ROI) analyses, can enhance the interpretation of lesion-induced connectivity disruptions following stroke¹³⁹. In light of this, the default-mode network (DMN) has been consistently observed in resting-state studies of stroke patients¹⁴⁰⁻¹⁴². Originally thought to be predominantly associated with self-generated thoughts and mind wandering^{143, 144}, it was recently proposed that the DMN also acts as a global integrator, in that it has the ability to integrate information from multiple sources in order for cognitive and motor tasks to be performed^{145, 146}. Similarly, some authors have theorized the existence of a cognitive-to-motor functional gradient, such that involvement of higher-order brain areas precedes

activation of motor-related regions during purposeful movements^{147, 148}. Whether task-related DMN hyperactivity in stroke patients¹⁴⁹ plays a supportive role during movement of the affected hand, however, has not yet been investigated. Combining a data-driven network method with patient-specific clinical measures of motor impairment could therefore provide a valuable approach to identify robust recovery biomarkers in chronic stroke survivors.

The goal of this study was to compare functional connectivity in whole-brain networks underlying the production of isometric, visually-paced hand grips in individuals with chronic stroke and healthy controls. To derive multiple distinct, simultaneously active task-based functional brain networks with unique hemodynamic response (HDR) shapes, we used a method based on multivariate multiple regression analysis and principal component analysis (Constrained Principal Component Analysis for fMRI or fMRI-CPCA)^{150, 151}. As opposed to univariate analysis techniques, fMRI-CPCA identifies brain networks that are (1) specifically underlying the task (viz., motor control), and (2) shared across all subjects to allow identification of network-wide functional connectivity differences between chronic stroke patients and controls. We further used a nonparametric statistical approach to investigate within-network regional brain activity changes between the two groups. Evidence of activity differences in individual brain regions was examined within the data-driven task-specific brain networks thus avoiding potential bias that may have arisen from choosing a priori regions of interest. To our knowledge, this is the first study to use this approach to examine possible network-wide connectivity alterations during isometric hand movement after stroke. Based on prior findings showing reduced activity in sensorimotor regions of the affected and unaffected hemisphere^{53, 54, 149}, we hypothesized network-wide decreases in functional connectivity across networks involving default-mode as well as primary and secondary motor regions in chronic stroke patients relative to healthy controls. Such connectivity differences would indicate a disruption of neuronal function both at the lesion site and in remote regions. We further hypothesized that reductions in regional brain activity would be associated with poorer motor performance in chronic stroke patients.

5.3 Methods

Participants

A total of 17 chronic stroke patients and 24 healthy control subjects were included in this study. All patients had suffered from first ischemic stroke. Full written consent was obtained from all subjects in accordance with the Declaration of Helsinki. The study was approved by the Joint Ethics Committee of the Institute of Neurology, UCL and NHNN, UCL Hospitals NHS Foundation Trust, London.

	Control	Stroke
Variable	Subjects	Patients
Sex (male/female)	14/10	14/3
Handedness (right/left)	23/1	17/0
Age (years)	46.7 (17.5)	53.2 (12.3)
Time since stroke (months)	_	44.9 (56.6)
Lesion side (right/left)	_	11/6
Hand affected (right/left)	_	6/11
BBT % of unaffected	_	52.1 (26.6)
NHPT % of unaffected	_	40.8 (35.5)
Grip strength % of unaffected	_	56.0 (33.7)

Table 5.1: Participants' demographic information and behavioral scores. Standard deviations are in parentheses. BBT, Box and Block Test; NHPT, Nine-Hole Peg Test.

Experiment protocol

Behavioral assessment. Motor impairment was assessed in stroke patients via measurements of (1) hand grip strength, (2) finger dexterity (NHPT), and (3) unilateral gross manual dexterity (BBT). As depicted in Table 5.1, all three measurements were

corrected within subject as a percentage of their score obtained for the unimpaired hand ¹⁵². These motor scores were then entered into a PCA and the first component was used as a single impairment score per patient, with higher motor score values corresponding to greater motor impairment.

Motor task. While undergoing fMRI, all participants performed a series of 50 visually cued dynamic isometric hand grips, using an MRI compatible manipulandum as described elsewhere⁶⁴. Healthy controls carried out the task with their dominant hand while stroke patients performed the task with their affected (i.e., contralesional) hand. Prior to scanning, each subject gripped the manipulandum with maximum force in order to generate their MVC. These values were then used to set the subject-specific target forces of 10% and 30% of MVC. Throughout the scanning session, each subject performed a total of 50 isometric hand grips, in a randomized order, at a target pressure of 10% or 30% of their MVC. Each hand grip was sustained for 3 s and was followed by a variable interstimulus interval between 3 and 7 s.

Data analysis and functional connectivity

Details regarding data acquisition and preprocessing are described in Appendix B. To allow for direct comparison between groups, images from the right-sided stroke patients were flipped about the midsagittal plane so that the lesioned hemisphere corresponded to the left hemisphere (i.e., contralateral to the hand used). Data from the left-handed control subject were also flipped so to conform to the rest of the control group (i.e., a left-dominant hemisphere).

The data was analyzed using fMRI-CPCA using orthogonal rotation $^{150, 151}$. Briefly, fMRI-CPCA integrates multivariate multiple regression analysis and principal component analysis into a unified framework. This type of analysis required the preparation of two matrices: a $5084 \times 259,423$ data matrix, with rows corresponding to scans (41 subjects \times 124 volumes) and columns corresponding to voxels, and a 5084×492 design matrix, with

rows corresponding to scans and columns corresponding to combinations of conditions (10%, 30%) and poststimulus time points (six time points) for every subject (i.e., 41 subjects × 2 conditions × 6 poststimulus time points). Here, a finite impulse response (FIR) model was used as the design matrix in which binary values were coded 1 in cells where the HDR signal is to be estimated and 0 otherwise, creating mini-boxcar functions. For the current analysis, we modeled six poststimulus time points corresponding to the 1st to 6th full brain scans following stimulus presentation. Multivariate multiple regression of the data matrix onto the design matrix was subsequently performed in order to partition the overall variance into task-related and task-unrelated fluctuations. In the current study, we regressed out the rigid-body parameters prior to regressing other task-unrelated variance. Brain networks were then isolated by performing a principal component analysis on the task-related variance in brain activity, which resulted in independent sources of variance reflecting task-specific brain networks. This method therefore enables derivation of brain networks from variations of the task-related BOLD signal, while also allowing for identification of functional brain networks that vary as a function of task-timing. As opposed to univariate methods, in which BOLD responses in each brain voxel are analyzed independently, fMRI-CPCA allows for the analysis of functionally connected networks of brain regions, and identification of their role in specific cognitive and motor processes as they occur over poststimulus time for different groups.

Statistical analysis

The cognitive and motor functions of each brain network are interpreted by analyzing predictor weights that produce subject- and condition-specific estimated HDR shapes. Specifically, these predictor weights are the weights that were applied to the FIR model used in the current analysis. The resulting functional brain networks can then be interpreted spatially by examining the dominant patterns of intercorrelated voxels, and temporally by looking at their associated HDR shapes. The repetition time (TR) for these data was 3.25 s, which resulted in an estimated BOLD signal over a 19.5 s time period, with the first time point (time = 0) corresponding to stimulus onset. Statistical analyses on

the HDR shapes (i.e., predictor weights) were carried out to test whether each functional network reflected a reliable hemodynamic response as well as to test differences in activation of each functional network between conditions and between groups. These analyses were carried out as four $6 \times 2 \times 2$ mixed-model ANOVAs (four components extracted; see section 5.4), with the within-subjects factors of Poststimulus Time (6 poststimulus time points) and Force (10%, 30%), and the between-subjects factor of Group (healthy controls, stroke patients). Tests of sphericity were carried out for all ANOVAs and Greenhouse-Geisser adjusted degrees of freedom were checked. Original degrees of freedom are reported as any violations of sphericity did not affect the results.

Within-network analysis

We used a nonparametric statistical method (e.g., FSL's Randomise permutation-testing tool, run with 5,000 permutations) to investigate group differences within the identified task-dependent functional brain networks. Activity differences between controls and stroke patients were constrained to the most extreme 10% of voxels (i.e., highest component loadings) for each shared functional network from the fMRI-CPCA output. As such, differences in activation of individual brain regions were examined within the data-driven, task-based brain networks, thus avoiding potential bias that may arise from choosing a priori regions of interest. Significant group differences were identified using threshold-free cluster enhancement (TFCE) and were corrected for multiple comparisons using family-wise error (FWE), $p < .05^{153}$.

5.4 Results

Lesion overlap

The brain lesions of all 17 stroke patients are displayed in Figure 5.1, with purple (superimposed on the brain image) representing voxels damaged in one patient and shades of red indicating areas of greater lesion overlap. The majority of the lesion overlap was found along the corticospinal tract and affected the insula, parietal and central operculum

cortices, precentral gyrus, temporal pole, inferior frontal gyrus, as well as supramarginal gyrus.

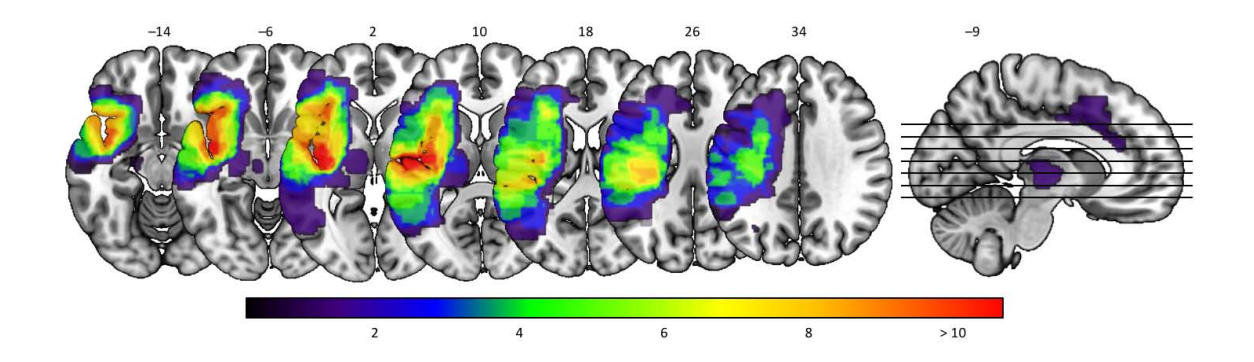


Figure 5.1: Lesion locations in all stroke patients. The heatmap represents the degree of overlap, with the purple end of the spectrum indicating voxels damaged in one patient, and shades of red indicating voxels damaged in a larger number of patients.

Behavioral results

For the stroke group, the percentage of variance of the three motor scores for the first principal component was 82.2%, and so was used as the representative motor impairment score. A higher principal component score represents greater motor impairment. Comparison of control subjects and stroke patients in raw motor performance scores can be found in the Appendix B (Table B1).

Functional connectivity

The scree plot of singular values revealed four predominant components accounting for task-related variance in brain activity. The percentages of task-related variance accounted for by each rotated component were 12.1%, 6.7%, 6.3%, and 4.5% for Components 1–4, respectively. The brain regions associated with Components 1, 2, 3, and 4 are displayed in Figures 5.2–5.5, respectively, with estimated HDR shape of each functional network represented by predictor weights plotted as a function of poststimulus time. Anatomical descriptions for each component are presented in Tables B2–B5.

Component 1: Dorsal Attention Network. The first component was characterized by a functional network of bilateral activations in frontal regions (inferior frontal gyrus, pars opercularis), parietal regions (anterior intraparietal sulcus, inferior and superior parietal lobules), as well as temporal regions (inferior and middle temporal gyri). Activity increases were also observed in the anterior cingulate cortex and cerebellum. Relating Component 1 to the recently proposed 7-network brain parcellation derived from resting state data, 92 the frontal, parietal, and temporal activation peaks were all located on the dorsal attention network. Predictor weights reflecting the estimated HDR for Component 1 were submitted to a mixed-model ANOVA. A significant main effect of Poststimulus Time emerged, $F_{5.195} = 9.31$, p < 0.001, $\eta_p^2 = 0.19$, indicating that this component reflects a reliable HDR shape as opposed to varying randomly around zero. A significant Force × Poststimulus Time interaction was also observed, $F_{5,195} = 2.49$, p < 0.05, $\eta^2_p = 0.06$, and a follow up analysis of simple main effects revealed that more attentional resources were allocated to increasing hand grip force, as indexed by a distinctly higher peak (at 4.9 and 8.1 s; all ps < .05) in the 30% relative to the 10% condition (Figure 5.2B). No significant main effects or interactions involving Group emerged (all ps > 0.10).

Component 2: Visual Network. The second component was characterized by a functional network including bilateral activations in primary visual network and extending laterally into the secondary visual network, extrastriate cortex, as well as ventrally into the inferior temporal cortex. Predictor weights reflecting the estimated HDR for Component 2 were submitted to a mixed-model ANOVA. As with the Dorsal Attention Network (Component 1), this component showed a significant main effect of Poststimulus Time, $F_{5,195} = 15.54$, p < 0.001, $\eta_p^2 = 0.28$, as well as a significant Force × Poststimulus Time interaction, $F_{5,195} = 5.77$, p < 0.001, $\eta_p^2 = 0.13$. A subsequent analysis of simple main effects indicated that this interaction was significant at 1.6, 4.9, 11.4, and 17.9 s (all ps < 0.05), reflecting a slightly earlier and higher HDR shape in the 30% condition relative to the 10% condition (Figure 5.3B). No significant main effects or interactions involving Group was observed (all ps > 0.55).

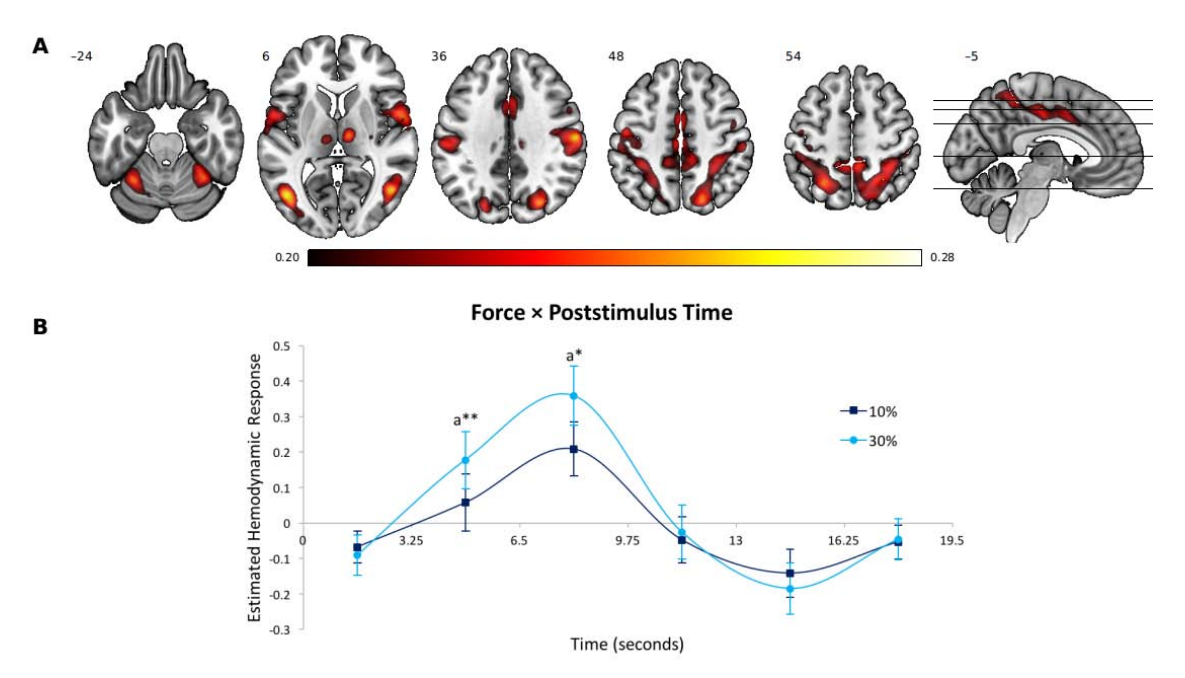


Figure 5.2: (**A**) Dominant 5% of component loadings for the Dorsal Attention Network (Component 1); positive loadings in red, threshold = 0.20, max = 0.28, no negative loadings. MNI Z-axis coordinates are displayed. (**B**) Mean FIR-based predictor weights averaged across groups, plotted as a function of poststimulus time. Error bars are standard errors. $^a = 30\% > 10\%$. $^* = p < 0.05$; $^{**} = p < 0.01$.

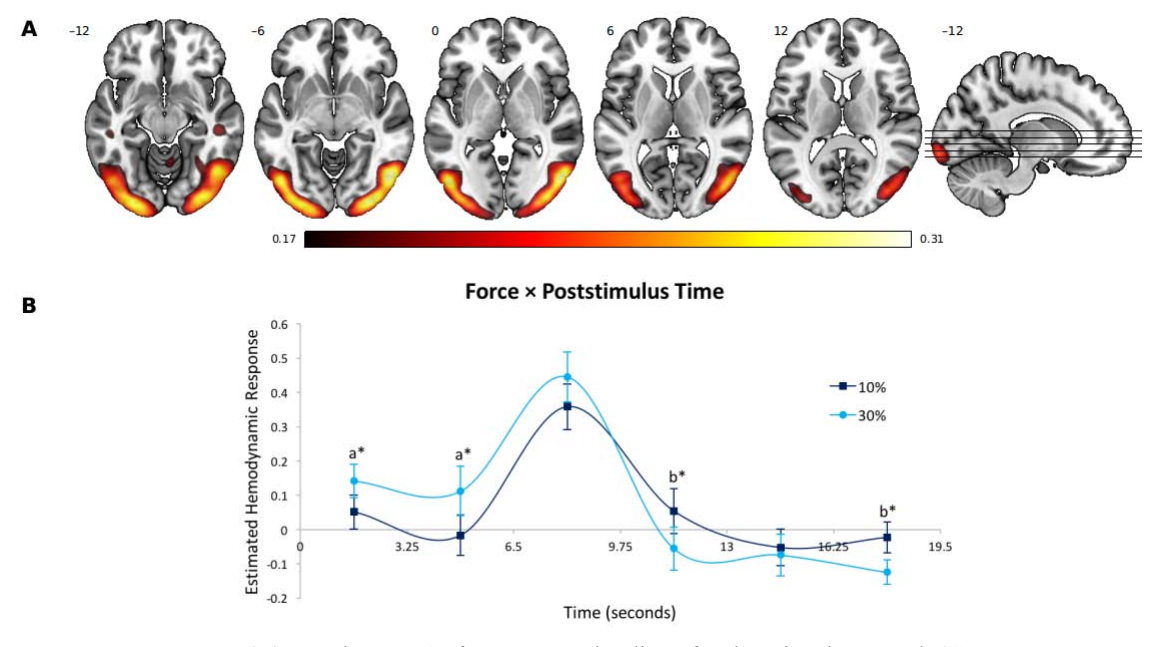


Figure 5.3: (**A**) Dominant 5% of component loadings for the Visual Network (Component 2); positive loadings in red, threshold = 0.17, max = 0.31, no negative loadings. MNI Z-axis coordinates are displayed. (**B**) Mean FIR-based predictor weights averaged across groups, plotted as a function of poststimulus time. Error bars are standard errors. a = 30% > 10%; b = 10% > 30%. * = p < 0.05.

Component 3: Motor Network. The third component was largely dominated by left-lateralized activations in motor regions, specifically M1, SMA, posterior parietal cortex (PPC), as well as PMd and PMv. The spatial distribution of this network is reflective of sensorimotor response processes involved in isometric right-hand grips. This component also included BOLD signal decreases bilaterally in primary visual cortex. Predictor weights reflecting the estimated HDR for Component 3 were entered into a mixed-model ANOVA, and a significant main effect of Poststimulus Time, $F_{5,195} = 39.61$, p < 0.001, $\eta_p^2 = 0.50$, as well as significant Force × Poststimulus Time, $F_{5,195} = 6.68$, p < 0.001, $\eta_p^2 = 0.15$, and Force × Group, $F_{5,195} = 5.13$, p < 0.05, $\eta_p^2 = 0.12$, interactions were observed. Follow up analyses of simple main effects detected a non-significant trend towards a decrease in functional connectivity in regions encompassing the motor network in chronic stroke patients relative to control subjects in the 30% force condition (p = 0.09; Figure 5.4B and C). This indicates that the brain network underlying performance of hand motor movements in stroke patients is characterized by a BOLD response with lower peak magnitude and greater poststimulus undershoot than in controls.

Component 4: Default-Mode Network. The fourth component primarily included BOLD signal decreases in regions associated with the well-documented DMN, ^{154, 155} notably in posterior cingulate cortex, precuneus, and medial prefrontal cortex. Statistical analysis of the predictor weights for Component 4 was carried out as a mixed-model ANOVA, and a significant main effect of Poststimulus Time, $F_{5,195} = 12.43$, p < 0.001, $\eta_p^2 = 0.24$, as well as a significant Poststimulus Time × Group interaction, $F_{5,195} = 7.53$, p < 0.001, $\eta_p^2 = 0.16$, emerged. A subsequent analysis of simple main effects revealed that this interaction was strongest at 8.1 s (p < 0.005), reflecting a significantly higher deactivation peak in the control group relative to the stroke group (Figure 5.5B).

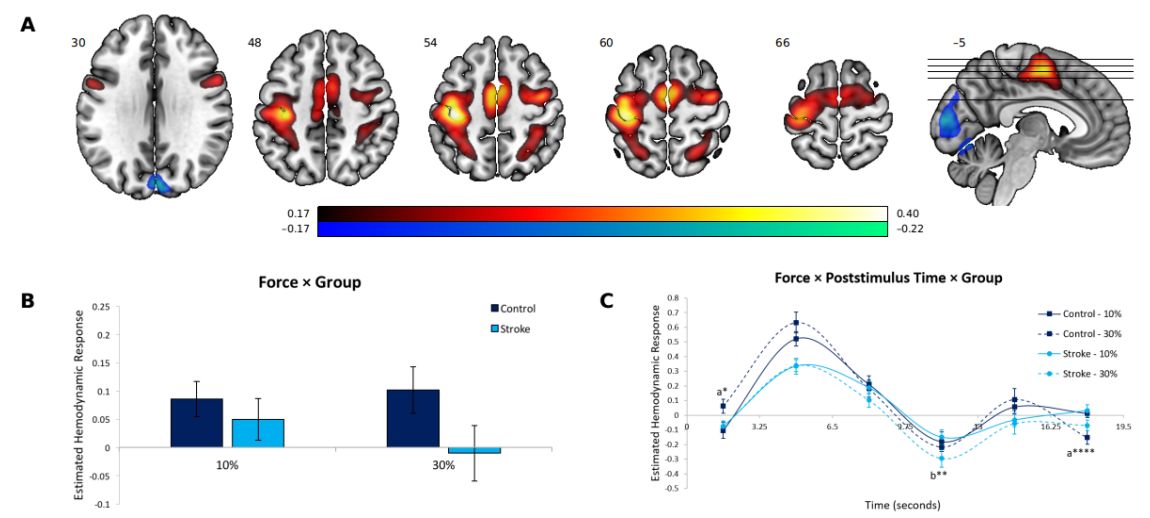


Figure 5.4: (**A**) Dominant 5% of component loadings for the Motor Network (Component 3); positive loadings in red, negative loadings in blue, threshold = ± 0.17 , min = -0.22, max = 0.40. MNI Z-axis coordinates are displayed. (**B**) Mean FIR-based predictor weights averaged across all time points, plotted as a function of condition. (**C**) Mean FIR-based predictor weights for each combination of group and condition, plotted as a function of poststimulus time. $^a = 30\% > 10\%$; $^b = 10\% > 30\%$. $^* = p < 0.05$; $^{**} = p < 0.01$; $^{*****} = p < 0.001$. Error bars are standard errors.

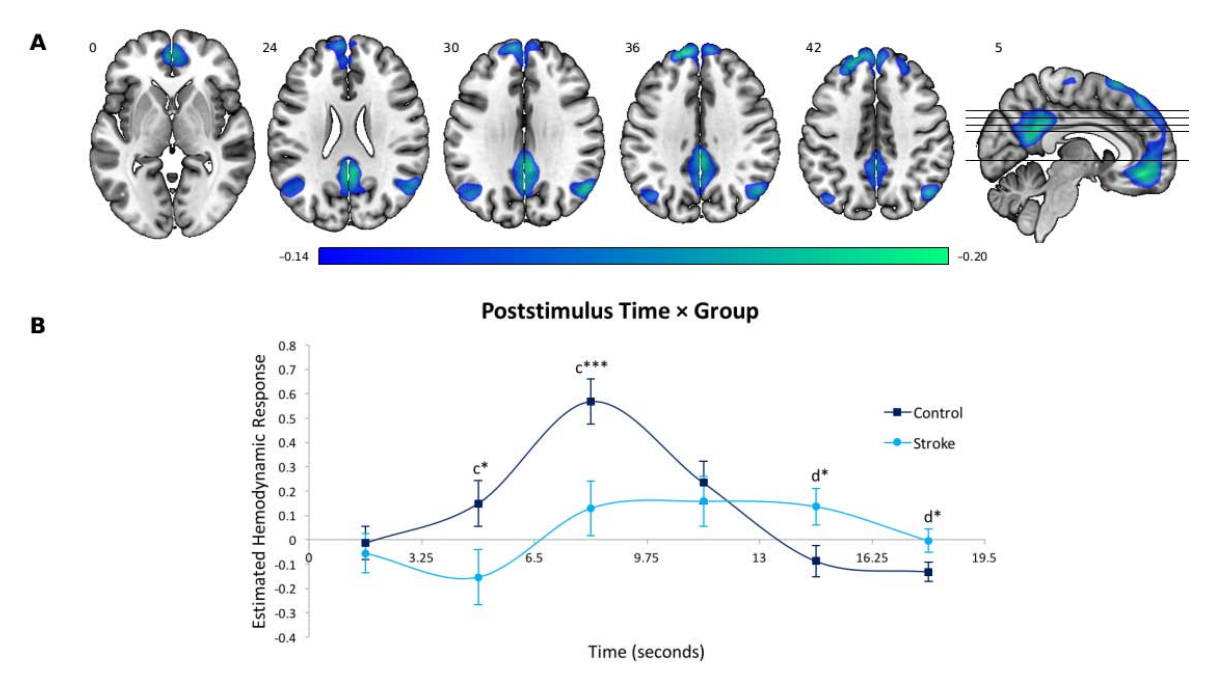


Figure 5.5: (**A**) Dominant 5% of component loadings for the Default-Mode Network (Component 4); negative loadings in blue, threshold = -0.14, min = -0.20, no positive loadings. MNI Z-axis coordinates are displayed. (**B**) Mean FIR-based predictor weights averaged across conditions, plotted as a function of poststimulus time. c = Control > Stroke; d = Stroke > Control. * = p < 0.05; *** = p < 0.005. Error bars are standard errors.

Within-network activity differences

Activation differences between groups within the task-based brain networks derived from fMRI-CPCA were assessed using nonparametric permutation testing. This analysis yielded two distinct clusters of voxels that showed significant activation (or deactivation) increases in control subjects relative to stroke patients: (1) when masked for the motor network (Component 3), a left sensorimotor cluster emerged (i.e., left pre-and postcentral gyri; Figure 5.6A; $p_{corr} < 0.01$); and (2) when masked for the DMN (Component 4), a bilateral precuneus cluster emerged (Figure B1; p < 0.05). In other words, voxels within these regions showed greater intensity (i.e., increased activations and/or increased deactivations) in the control group relative to the stroke group.

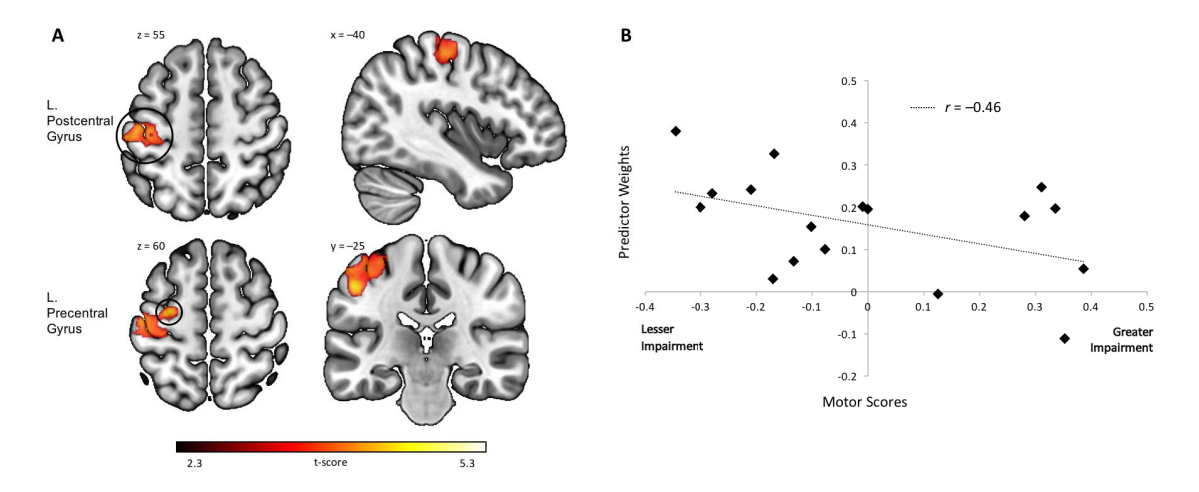


Figure 5.6: (**A**) The within-network analysis masked for the dominant 10% of component loadings for the Motor Network (Component 3) revealed significantly reduced activity in left sensorimotor regions (pre- and postcentral gyri) in stroke patients relative to control subjects ($p_{corr} < 0.01$). (**B**) Negative relationship between left sensorimotor regions and motor impairment scores in stroke patients (p = 0.06).

Relationship between regional activity and motor performance

The relationship between regional brain activity and motor performance in stroke patients was assessed by computing correlations between the predictor weights of the within-network clusters (ipsilesional pre- and postcentral gyri, precuneus) and the PCA motor impairment scores. There was a moderately strong but non-significant trend for a

negative relationship between ipsilesional pre- and postcentral gyri activation and motor impairment scores, r = -0.46, p = 0.06 (Figure 5.6B). Since higher principal component scores equate greater motor impairment, increased brain activity within this sensorimotor cluster appears to be associated with better motor performance. The analogous correlations between motor performance and precuneus deactivations, as well as with functional connectivity within each whole-brain network, age, post-stroke duration, and lesion size were not significant (ps > 0.15).

5.5 Discussion

This study investigated functional connectivity alterations in brain networks underlying visually-paced isometric hand grips in chronic stroke patients relative to control subjects. Of the four functional brain networks identified, group differences were only observed on the motor network and the DMN, in which stroke patients revealed decreased functional connectivity relative to control subjects. A secondary analysis investigating group differences in activation of individual brain regions within these networks showed reduced activity intensity in ipsilesional (contralateral to the hand) preand postcentral gyri, which was characteristic of chronic stroke patients and which also appeared to be associated with motor performance. Groups did not differ on the remaining two networks (dorsal attention and visual networks), however increased activity in these networks was associated with production of higher force levels in all participants. Collectively, these findings suggest that reduced regional brain activity in ipsilesional sensorimotor regions may impair the integrity of the motor network in individuals with stroke, and consequently appears to be an important biological marker of the motor state in chronic stroke patients.

Consistent with existing findings showing regional activity reductions in various motor-related regions^{53, 54, 156}, we observed significant activity decreases in a whole-brain, left-dominant motor network in stroke patients relative to control subjects. Notably, with regard to behavioral performance we found that activity intensity within the ipsilesional

M1/S1 cluster of the task-specific motor network was positively correlated with lower levels of motor impairment, thus hinting at a potential biomarker of the motor state in chronic stroke patients. Interestingly, Borich and colleagues¹⁵⁷ discovered that a certain amount of residual corticospinal tract integrity must be preserved in chronic stroke patients in order to observe meaningful behavioral motor performance changes following motor learning training after stroke. In line with this research, our within-network finding of reduced M1/S1 activity in patients with greater impairment may in fact reflect damage to corticospinal tract fibers originating from the ipsilesional M1. Combined, these findings bear important implications for stroke recovery rehabilitation; the currently employed 'one size fits all' treatment approach may not be beneficial for a substantial proportion of patients characterized with high degree of M1/S1 alterations or corticospinal tract damage. Moreover, our findings suggest that secondary motor areas, notably bilateral SMA, PMv, and PMd, have strong contributions to the task-specific motor network (as indexed by the lighter shades of red/white superimposed on the brain image in Figure 5.4A). Given that the within-network analysis did not reveal any significant group differences in these secondary motor regions, it could indicate that these areas are relatively spared by the infarct and still contain vast amounts of corticospinal motoneurons. In other words, secondary motor areas, alongside bilateral parietal cortices, may represent a brain circuit that becomes critically important in order to support residual motor function and consequently allow chronic stroke patients to perform hand movements.

The association between motor performance and underlying brain activity in the motor network may also provide insights into long-term neurovascular alterations present in chronic stroke patients. In fact, increases in the BOLD response, commonly interpreted as an indirect measure of neural activity, are driven by simultaneous changes in three factors, namely: cerebral blood flow (CBF), cerebral blood volume (CBV), and metabolic rate of oxygen consumption (CMRO₂)^{158, 159}. Interestingly, combined MEG and fMRI studies of chronic stroke patients with good recovery of sensorimotor hand control have previously shown that absent or reduced BOLD activity may not necessarily indicate an

absence of neuronal activity but may instead reflect altered cerebral hemodynamics, as for instance significantly decreased CBF^{160, 161}. Another possible explanation for the lack of concordance between the two modalities could be due to the use of a standard voxelwise fMRI analysis which in itself may not be sensitive enough to detect task-specific BOLD alterations ¹⁶². Here distinctly, we estimated the BOLD impulse response underlying hand movement using a FIR model which, unlike typical hemodynamic response function models, does not require any a priori assumption concerning the shape of the HDR¹⁶³. Consequently, this allowed us to quantify the primary BOLD response as well as the poststimulus undershoot. Whereas the former is classically characterized as neural activity, it has been hypothesized that poststimulus undershoots reflect concurrent reductions in neural activity, CBF, and possibly changes in CBV¹⁶⁴. Although there were no significant differences between patients and controls at peak (i.e., primary BOLD response) in the motor network, stroke patients demonstrated a larger and wider poststimulus undershoot in the highest force level condition. Using pulsed arterial spin labeling (PASL), Brumm et al. 165 found that CBF was significantly reduced in anatomically intact regions in chronic stroke survivors. In line with this finding, we can speculate that modulation of grip force in chronically impaired patients targets suboptimal neurophysiological mechanisms. Quantification of motor connectivity using a model-free approach (e.g., FIR) may therefore help to reveal underlying diffuse cerebral vascular dysregulations in the ischemic brain⁵⁴. Further investigation of the effects of stroke on the biological basis of the BOLD signal as well as the long-term neurovascular consequences of an ischemic lesion could become instrumental in neuroimaging research of cerebrovascular patients.

Increasing evidence suggests that localized brain lesions also disrupt connectivity in large-scale networks subserving higher-order functioning ^{141, 149, 166}. One such network, the dorsal attention network, has been consistently shown to activate during attention-demanding tasks ^{72, 167}. A longitudinal study on stroke patients manifesting attentional deficits (i.e., visuospatial neglect ¹⁶⁸) showed that functional connectivity within the dorsal

attention network was highly disrupted during the acute stage but was fully recovered by the chronic stage⁹⁴. Similarly, when compared to controls, we found no breakdown of functional connectivity in the dorsal attention network in our chronic stroke group, suggesting that such network alterations may be specific to the pathophysiology of neglect during the acute stage. Despite significant impairments in motor performance and motor connectivity, chronic stroke patients in our study maintained the ability to regulate activity of the attention network with increasing levels of grip force. Distinct from the externallyoriented dorsal attention network is the well-documented DMN^{154, 155}. In an elegant paper, Margulies and colleagues¹⁴⁶ described the hierarchical organization of large-scale connectivity in healthy adults by means of connectivity gradients which reflect the dominant differences of connectivity patterns 146, 169. The authors concluded that the DMN and the primary sensory networks (e.g., sensorimotor, visual, and auditory) were anchored on opposite ends of a connectivity gradient spectrum, thus providing evidence that the DMN may play a functional role during tasks that require the integration of information from multiple sensory systems¹⁴⁶. In line with this theory, the inability of stroke patients to deactivate the DMN, as observed in the current study and elsewhere 140-142, may reflect specific disruptions within this connectivity gradient. One hypothesis is that the DMN, being located at the top of a representational hierarchy, recognizes hypoactivity of the motor network and consequently engages its main hubs (e.g., precuneus, medial prefrontal cortex) in an attempt to support residual motor function. Alternatively, DMN hyperactivity, along with the finding of reduced activity in the motor network, may provide evidence that the boundaries between functional systems in the brain become less precise in chronically impaired stroke patients than in healthy adults. In favor of the latter hypothesis, we did not find an association between DMN activity (or precuneus activity alone) with motor performance, therefore suggesting that DMN hyperactivity seen in stroke patients possibly reflects higher-order cognitive impairments. Future studies are needed to characterize the connectivity gradients in stroke, as well as their relation to motor and cognitive performance outcomes, in order to yield additional insights into reorganization of brain networks during recovery.

The four brain networks derived from our multivariate functional connectivity analysis accounted for 30% of task-related variance. It is therefore possible that the remaining sources of variance include subject-specific biomarkers of functional recovery, which our group-level analysis was unable to detect due to the inter-subject variability in brain activation patterns in the stroke group. Arguably, the specificity of our findings to the chronic stroke population could be hampered by the large variability in post-stroke recovery phase (i.e., time after stroke), however excluding the subacute patients (< 4 months) from our analysis did not alter the results. Despite that, we cannot absolutely exclude the influence 'time after stroke' on functional connectivity alterations. In view of these limitations, further studies may wish to track the neural mechanisms underlying ischemic stroke progression longitudinally, from acute to chronic stages.

In summary, the ability to regulate activity of the motor network, notably within ipsilesional sensorimotor regions, appears to play a crucial role in successful hand motor recovery in stroke patients. In other words, the overall motor network connectivity decrease observed in stroke patients may be driven by significant alterations in ipsilesional M1/S1 and possibly underlying corticospinal tract damage. We further proposed that rehabilitation treatments targeting SMA, PMv, and/or PMd may be beneficial in patients with highly impaired ipsilesional M1/S1 as these secondary motor areas seem to be functionally intact and as a result can support residual motor function after and infarct. In addition to quantifying the brain's functional networks involved in hand movement, our whole-brain, task-based functional connectivity analysis lends a foundation that could allow future multimodal studies to integrate non-static properties of brain networks with changes in vascular health in at-risk populations. Taken together, our study establishes the ipsilesional sensorimotor regions as a biomarker of the motor state in chronic stroke patients, which in turn may open up new avenues for maximizing meaningful outcomes by promoting tailored neurorehabilitation approaches for individual patients.

* * *



CHAPTER 6

KEY FINDINGS AND SIGNIFICANCE

The work presented in this thesis includes a combination of MEG and fMRI studies carried out on healthy young and elderly individuals, as well as chronic stroke patients. As opposed to previous research using typical univariate analysis techniques, here we employed a variety of multivariate functional and effective connectivity methods to investigate resting-state and task-specific brain networks in healthy and motor-impaired populations. Our main goal was thus to study the reorganization of functionally-connected brain networks at rest and during execution of hand movements in aging and stroke individuals.

In the first experiment (Chapter 3), we investigated age-dependent alterations in functional connectivity in whole-brain MEG networks underlying the production of unimanual and bimanual visually-guided isometric hang grips using multivariate functional connectivity and Granger causality analysis. Brain network reorganization was observed in elderly individuals in order to maintain motor performance and task accuracy. This pattern was evidenced by overall hyperactivity in task-specific motor network in addition to increased neuronal input to the left primary motor cortex, which likely reflected compensatory mechanisms employed by older adults in order to support residual motor functions.

In the second experiment (Chapter 4), we compared the effects of performing hand movement on resting-state functional connectivity in healthy young and elderly individuals. Envelope correlation analyses were carried out on resting-state MEG data before and after each motor task to study whether aging subjects demonstrate different reorganization mechanisms relative to young adults. We reported beta connectivity increases from the first to the second resting-state session (i.e., after a unimanual task) in

both groups. This connectivity increase was predominantly found in networks that govern core attentional, visuospatial, and sensorimotor processes. Moreover, we demonstrated that elderly subjects were characterized by a strong delta connectivity increase after the unimanual task, which correlated positively with activity of the task-based ventral frontoparietal attention network (derived from the unimanual task). These data suggested that elderly individuals maintain the capacity for task-induced network-wide neuronal flexibility in the beta frequency (13–30 Hz), but have altered slow (1–4 Hz) oscillatory connectivity when attentional demands are high.

In the third experiment (Chapter 5), we compared functional connectivity in shared whole-brain networks underlying the production of visually-paced isometric hand grips in individuals with chronic stroke and healthy controls through a combination of multivariate multiple regression and principal component analysis. We observed overall motor network connectivity decrease in stroke patients which appeared to be driven by significant alterations in ipsilesional M1/S1 and possibly concurrent corticospinal tract damage. As opposed to healthy elderly individuals (in Chapter 3), where greater motor network activity was observed and interpreted as a compensatory mechanism, motor connectivity decreases observed in this experiment suggested that brain damage due to an infarct significantly alters the compensatory mechanisms observed during healthy aging. We therefore reported that stroke patients must instead rely on a residual brain circuit in order to perform a motor task. With respect to behavioral impairment, we also found a negative correlation between activity levels in ipsilesional M1/S1 activity and greater motor impairments in stroke patients. In light of these data, we proposed that rehabilitation treatments targeting SMA, PMv, and/or PMd may be beneficial in patients with highly impaired ipsilesional M1/S1 as these secondary motor areas seemed to be functionally intact and can therefore support residual motor function after and infarct.

These experiments provided valuable insights into the neural mechanisms underlying motor performance decline in both aging and stroke populations. By

combining task-related and resting-state network-level connectivity, our neuroimaging study led to the identification of neural hallmarks of motor aging. Our findings also expanded upon previous research by contributing to the understanding of motor-task induced connectivity changes in young and healthy elderly individuals. This in turn provides an important framework for novel therapeutic interventions that wish to take advantage of context-dependent functional adaptability (e.g., performing a hand motor control task to enhance connectivity). Ultimately, the investigation of motor connectivity contributes to the development of more efficient treatment of other seemingly related neurodegenerative disorders that share similar underlying pathogenesis to that of normal aging or chronic stroke.

CHAPTER 7

FUTURE RESEARCH

MEG proved to be an excellent tool for measuring neural interactions at millisecond time scales, however its use was restricted to the study of cortical activity with limited spatial resolution and therefore precluded the investigation of subcortical structures. Fortunately, the recent emergence of multimodal neuroimaging can lead to increasingly accurate representations of the human brain. Notably, the simultaneous integration of millisecond temporal resolution from EEG and millimeter spatial resolution from fMRI can provide more detailed information about brain connectivity patterns that is unachievable by either modality alone. In light of this, our research team will also collect simultaneous EEG-fMRI data on the same sample of subjects (see Chapter 3) while they undergo two resting-state sessions interspersed with a dynamic visually-paced right-hand grip task.

The rich experimental data that will be provided by our ongoing multimodal study (MEG, simultaneous EEG-fMRI) brings to the fore the importance of advanced connectivity analysis methods that are able to integrate these data in a meaningful manner, including a more accurate characterization of time-varying connectivity. These research efforts will result in obtaining more accurate connectivity-based biomarkers associated with the decrease of performance observed in the aging population.

* * *

PART IV | BIBLIOGRAPHY

Bibliography

- 1. Enoka RM, Christou EA, Hunter SK, et al. Mechanisms that contribute to differences in motor performance between young and old adults. *J Electromyogr Kinesiol*, 13:1-12, 2003.
- **2**. Seidler RD, Bernard JA, Burutolu TB, et al. Motor control and aging: links to agerelated brain structural, functional, and biochemical effects. *Neurosci Biobehav Rev*, 34:721-733, 2010.
- **3**. Maes C, Gooijers J, de Xivry J-JO, Swinnen SP, Boisgontier MP. Two hands, one brain, and aging. *Neurosci Biobehav Rev*, 75:234-256, 2017.
- **4**. Bernard JA, Seidler RD. Evidence for motor cortex dedifferentiation in older adults. *Neurobiol Aging*, 33:1890-1899, 2012.
- **5**. Ward NS, Swayne OB, Newton JM. Age-dependent changes in the neural correlates of force modulation: an fMRI study. *Neurobiol Aging*, 29:1434-1446, 2008.
- **6**. Michael KM, Shaughnessy M. Stroke prevention and management in older adults. *Eur J Cardiovasc Nurs*, 21:S21-S26, 2006.

- 7. Kaasinen V, Rinne JO. Functional imaging studies of dopamine system and cognition in normal aging and Parkinson's disease. *Neurosci Biobehav Rev*, 26:785-793, 2002.
- **8**. Fearnley JM, Lees AJ. Ageing and Parkinson's disease: substantia nigra regional selectivity. *Brain*, 114:2283-2301, 1991.
- **9**. van Dyck CH, Avery RA, MacAvoy MG, et al. Striatal dopamine transporters correlate with simple reaction time in elderly subjects. *Neurobiol Aging*, 29:1237-1246, 2008.
- **10**. Emborg ME, Ma SY, Mufson EJ, et al. Age-related declines in nigral neuronal function correlate with motor impairments in rhesus monkeys. *J Comp Neurol*, 401:253-265, 1998.
- **11.** Mora F, Segovia G, del Arco A. Glutamate–dopamine–GABA interactions in the aging basal ganglia. *Brain Res Rev*, 58:340-353, 2008.
- **12**. Ge Y, Grossman RI, Babb JS, Rabin ML, Mannon LJ, Kolson DL. Age-related total gray matter and white matter changes in normal adult brain. Part I: volumetric MR imaging analysis. *Am J Neuroradiol*, 23:1327-1333, 2002.

- . Sullivan EV, Rohlfing T, Pfefferbaum A. Quantitative fiber tracking of lateral and interhemispheric white matter systems in normal aging: relations to timed performance. *Neurobiol Aging*, 31:464-481, 2010.
- . Salat DH, Buckner RL, Snyder AZ, et al. Thinning of the cerebral cortex in aging. *Cereb Cortex*, 14:721-730, 2004.
- . Good CD, Johnsrude IS, Ashburner J, Henson RN, Fristen K, Frackowiak RS. A voxel-based morphometric study of ageing in 465 normal adult human brains. *Neuroimage*, 14:21-36, 2001.
- . Resnick SM, Pham DL, Kraut MA, Zonderman AB, Davatzikos C. Longitudinal magnetic resonance imaging studies of older adults: a shrinking brain. *J Neurosci*, 23:3295-3301, 2003.
- 17. Ota M, Obata T, Akine Y, et al. Agerelated degeneration of corpus callosum measured with diffusion tensor imaging. *Neuroimage*, 31:1445-1452, 2006.
- . Salat D, Tuch D, Greve D, et al. Agerelated alterations in white matter

- microstructure measured by diffusion tensor imaging. *Neurobiol Aging*, 26:1215-1227, 2005.
- . Kennerley SW, Diedrichsen J, Hazeltine E, Semjen A, Ivry RB. Callosotomy patients exhibit temporal uncoupling during continuous bimanual movements. *Nat Neurosci*, 5:376-381, 2002.
- . Gerloff C, Cohen LG, Floeter MK, Chen R, Corwell B, Hallett M. Inhibitory influence of the ipsilateral motor cortex on responses to stimulation of the human cortex and pyramidal tract. *J Physiol*, 510:249-259, 1998.
- **21**. Kennedy KM, Erickson KI, Rodrigue KM, et al. Age-related differences in regional brain volumes: a comparison of optimized voxel-based morphometry to manual volumetry. *Neurobiol Aging*, 30:1657-1676, 2009.
- . Rosano C, Aizenstein H, Brach J, Longenberger A, Studenski S, Newman AB. Special article gait measures indicate underlying focal gray matter atrophy in the brain of older adults. *J Gerontol A Biol Sci Med Sci*, 63:1380-1388, 2008.

- . Sala-Llonch R, Bartrés-Faz D, Junqué C. Reorganization of brain networks in aging: a review of functional connectivity studies. *Front Psychol*, 6:663, 2015.
- . Rosen AC, Gabrieli JD, Stoub T, Prull MW, O'Hara R, Yesavage J. Relating medial temporal lobe volume to frontal fMRI activation for memory encoding in older adults. *Cortex*, 41:595-602, 2005.
- . Cabeza R, Anderson ND, Locantore JK, McIntosh AR. Aging gracefully: compensatory brain activity in high-performing older adults. *Neuroimage*, 17:1394-1402, 2002.
- **26**. Park DC, Polk TA, Park R, Minear M, Savage A, Smith MR. Aging reduces neural specialization in ventral visual cortex. *Proc Natl Acad Sci USA*, 101:13091-13095, 2004.
- . Geerligs L, Renken RJ, Saliasi E, Maurits NM, Lorist MM. A brain-wide study of agerelated changes in functional connectivity. *Cereb Cortex*, 25:1987-1999, 2015.
- . Boccaletti S, Latora V, Moreno Y, Chavez M, Hwang D-U. Complex networks: Structure and dynamics. *Phys Rep*, 424:175-308, 2006.

- . Achard S, Bullmore E. Efficiency and cost of economical brain functional networks. *PLoS Comput Biol*, 3:e17, 2007.
- . Betzel RF, Byrge L, He Y, Goñi J, Zuo X-N, Sporns O. Changes in structural and functional connectivity among resting-state networks across the human lifespan. *Neuroimage*, 102:345-357, 2014.
- . Zhang H-Y, Chen W-X, Jiao Y, Xu Y, Zhang X-R, Wu J-T. Selective vulnerability related to aging in large-scale resting brain networks. *PloS ONE*, 9:e108807, 2014.
- . Song J, Birn RM, Boly M, et al. Agerelated reorganizational changes in modularity and functional connectivity of human brain networks. *Brain Connect*, 4:662-676, 2014.
- . Tomasi D, Volkow ND. Aging and functional brain networks. *Mol Psychiatry*, 17:549-558, 2012.
- . Zuo X-N, Kelly C, Di Martino A, et al. Growing together and growing apart: regional and sex differences in the lifespan developmental trajectories of functional homotopy. *J Neurosci*, 30:15034-15043, 2010.

- **35**. Boudrias MH, Gonçalves CS, Penny WD, et al. Age-related changes in causal interactions between cortical motor regions during hand grip. *Neuroimage*, 59:3398-3405, 2012.
- **36**. Solesio-Jofre E, Serbruyns L, Woolley DG, Mantini D, Beets IA, Swinnen SP. Aging effects on the resting state motor network and interlimb coordination. *Hum Brain Mapp*, 35:3945-3961, 2014.
- **37**. Antonenko D, Schubert F, Bohm F, et al. tDCS-Induced Modulation of GABA Levels and Resting-State Functional Connectivity in Older Adults. *J Neurosci*, 37:4065-4073, 2017.
- **38**. Noble JW, Eng JJ, Kokotilo KJ, Boyd LA. Aging effects on the control of grip force magnitude: an fMRI study. *Exp Gerontol*, 46:453-461, 2011.
- **39**. Park CH, Boudrias MH, Rossiter H, Ward NS. Age-related changes in the topological architecture of the brain during hand grip. *Neurobiol Aging*, 33:833.e827-833.e837, 2012.
- **40**. Chang C, Glover GH. Time–frequency dynamics of resting-state brain connectivity

- measured with fMRI. *Neuroimage*, 50:81-98, 2010.
- **41**. Astolfi L, Cincotti F, Mattia D, et al. Assessing cortical functional connectivity by linear inverse estimation and directed transfer function: simulations and application to real data. *Clin Neurophysiol*, 116:920-932, 2005.
- **42**. Supek S, Aine CJ. Magnetoencephalography: from signals to dynamic cortical networks. *Springer*, 2014.
- **43**. Kielar A, Deschamps T, Chu RK, et al. Identifying dysfunctional cortex: dissociable effects of stroke and aging on resting state dynamics in MEG and fMRI. *Front Aging Neurosci*, 8:40, 2016.
- **44**. Vlahou EL, Thurm F, Kolassa I-T, Schlee W. Resting-state slow wave power, healthy aging and cognitive performance. *Sci Rep*, 4:5101, 2014.
- **45**. Bruce EN, Bruce MC, Vennelaganti S. Sample entropy tracks changes in EEG power spectrum with sleep state and aging. *J Clin Neurophysiol*, 26:257, 2009.
- **46**. Hong SL, Rebec GV. A new perspective on behavioral inconsistency and neural noise

in aging: compensatory speeding of neural communication. *Front Aging Neurosci*, 4:27, 2012.

- **47**. O'Neill GC, Tewarie PK, Colclough GL, et al. Measurement of dynamic task related functional networks using MEG. *Neuroimage*, 146:667-678, 2017.
- **48**. Brookes MJ, Tewarie PK, Hunt BA, et al. A multi-layer network approach to MEG connectivity analysis. *Neuroimage*, 132:425-438, 2016.
- **49**. Lake EM, Bazzigaluppi P, Stefanovic B. Functional magnetic resonance imaging in chronic ischaemic stroke. *Phil Trans R Soc B*, 371:20150353, 2016.
- **50**. Broeks JG, Lankhorst GJ, Rumping K, Prevo AJH. The long-term outcome of arm function after stroke: results of a follow-up study. *Disabil Rehabil*, 21:357-364, 1999.
- **51**. Fridman EA, Hanakawa T, Chung M, Hummel F, Leiguarda RC, Cohen LG. Reorganization of the human ipsilesional premotor cortex after stroke. *Brain*, 127:747-758, 2004.

- **52**. Cramer SC, Nelles G, Benson RR, et al. A functional MRI study of subjects recovered from hemiparetic stroke. *Stroke*, 28:2518-2527, 1997.
- **53**. Wang L, Yu C, Chen H, et al. Dynamic functional reorganization of the motor execution network after stroke. *Brain*, 133:1224-1238, 2010.
- **54**. Pineiro R, Pendlebury S, Johansen-Berg H, Matthews P. Altered hemodynamic responses in patients after subcortical stroke measured by functional MRI. *Stroke*, 33:103-109, 2002.
- **55**. Favre I, Zeffiro TA, Detante O, Krainik A, Hommel M, Jaillard A. Upper Limb Recovery After Stroke Is Associated With Ipsilesional Primary Motor Cortical Activity A Meta-Analysis. *Stroke*, 45:1077-1083, 2014.
- **56**. Marshall RS, Perera GM, Lazar RM, Krakauer JW, Constantine RC, DeLaPaz RL. Evolution of cortical activation during recovery from corticospinal tract infarction. *Stroke*, 31:656-661, 2000.
- **57**. Lotze M, Markert J, Sauseng P, Hoppe J, Plewnia C, Gerloff C. The role of multiple

- contralesional motor areas for complex hand movements after internal capsular lesion. *J Neurosci*, 26:6096-6102, 2006.
- . Takeuchi N, Chuma T, Matsuo Y, Watanabe I, Ikoma K. Repetitive transcranial magnetic stimulation of contralesional primary motor cortex improves hand function after stroke. *Stroke*, 36:2681-2686, 2005.
- . Ward N, Brown M, Thompson A, Frackowiak R. Neural correlates of motor recovery after stroke: a longitudinal fMRI study. *Brain*, 126:2476-2496, 2003.
- . Kim B, Winstein C. Can neurological biomarkers of brain impairment be used to predict poststroke motor recovery? A systematic review. *Neurorehabil Neural Repair*, 31:3-24, 2017.
- **61**. Ward N, Frackowiak R. Age-related changes in the neural correlates of motor performance. *Brain*, 126:873-888, 2003.
- . Glasser MF, Van Essen DC. Mapping human cortical areas in vivo based on myelin content as revealed by T1-and T2-weighted MRI. *J Neurosci*, 31:11597-11616, 2011.

- . Gao L, Sommerlade L, Coffman B, et al. Granger causal time-dependent source connectivity in the somatosensory network. *Sci Rep*, 5:10399, 2015.
- **64**. Ward N, Frackowiak R. Age-related changes in the neural correlates of motor performance. *Brain*, 126:873-888, 2003.
- . Heuninckx S, Wenderoth N, Debaere F, Peeters R, Swinnen SP. Neural basis of aging: the penetration of cognition into action control. *J Neurosci*, 25:6787-6796, 2005.
- . Heuninckx S, Wenderoth N, Swinnen SP. Systems neuroplasticity in the aging brain: recruiting additional neural resources for successful motor performance in elderly persons. *J Neurosci*, 28:91-99, 2008.
- . Oldfield RC. The assessment and analysis of handedness: the Edinburgh inventory. *Neuropsychologia*, 9:97-113, 1971.
- . Van Veen BD, Buckley KM. Beamforming: A versatile approach to spatial filtering. *IEEE ASSP Mag*, 5:4-24, 1988.
- . Destrieux C, Fischl B, Dale A, Halgren E. Automatic parcellation of human cortical

- gyri and sulci using standard anatomical nomenclature. *Neuroimage*, 53:1-15, 2010.
- . Tallon-Baudry C, Bertrand O. Oscillatory gamma activity in humans and its role in object representation. *Trends Cogn Sci*, 3:151-162, 1999.
- . Schiatti L, Nollo G, Rossato G, Faes L. Extended Granger causality: a new tool to identify the structure of physiological networks. *Physiol Meas*, 36:827, 2015.
- . Corbetta M, Shulman GL. Control of goal-directed and stimulus-driven attention in the brain. *Nat Rev Neurosci*, 3:201-215, 2002.
- . Wen X, Yao L, Liu Y, Ding M. Causal interactions in attention networks predict behavioral performance. *J Neurosci*, 32:1284-1292, 2012.
- . Anticevic A, Cole MW, Murray JD, Corlett PR, Wang X-J, Krystal JH. The role of default network deactivation in cognition and disease. *Trends Cogn Sci*, 16:584-592, 2012.

- . Park H-J, Friston K. Structural and functional brain networks: from connections to cognition. *Science*, 342:1238411, 2013.
- **76.** Spreng RN, Stevens WD, Chamberlain JP, Gilmore AW, Schacter DL. Default network activity, coupled with the frontoparietal control network, supports goal-directed cognition. *Neuroimage*, 53:303-317, 2010.
- 77. Madden DJ, Spaniol J, Whiting WL, et al. Adult age differences in the functional neuroanatomy of visual attention: a combined fMRI and DTI study. *Neurobiol Aging*, 28:459-476, 2007.
- . Milham MP, Erickson KI, Banich MT, et al. Attentional control in the aging brain: insights from an fMRI study of the stroop task. *Brain Cogn*, 49:277-296, 2002.
- . Sherman MA, Lee S, Law R, et al. Neural mechanisms of transient neocortical beta rhythms: Converging evidence from humans, computational modeling, monkeys, and mice. *Proc Natl Acad Sci*, E4885-E4894, 2016.
- . Bartzokis G. Age-related myelin breakdown: a developmental model of

cognitive decline and Alzheimer's disease. *Neurobiol Aging*, 25:5-18, 2004.

- **81**. Tanaka F, Kachi T, Yamada T, Sobue G. Auditory and visual event-related potentials and flash visual evoked potentials in Alzheimer's disease: correlations with Mini-Mental State Examination and Raven's Coloured Progressive Matrices. *J Neurol Sci*, 156:83-88, 1998.
- **82**. Baillet S, Mosher JC, Leahy RM. Electromagnetic brain mapping. *IEEE Signal Process Mag*, 18:14-30, 2001.
- **83**. Serrien DJ, Cassidy MJ, Brown P. The importance of the dominant hemisphere in the organization of bimanual movements. *Hum Brain Mapp*, 18:296-305, 2003.
- **84**. Damoiseaux J, Beckmann C, Arigita ES, et al. Reduced resting-state brain activity in the "default network" in normal aging. *Cereb Cortex*, 18:1856-1864, 2007.
- **85**. Demeter S, Rosene DL, Van Hoesen GW. Fields of origin and pathways of the interhemispheric commissures in the temporal lobe of macaques. *J Comp Neurol*, 302:29-53, 1990.

- **86**. Crossley NA, Mechelli A, Scott J, et al. The hubs of the human connectome are generally implicated in the anatomy of brain disorders. *Brain*, 137:2382-2395, 2014.
- **87**. Biswal B, Zerrin Yetkin F, Haughton VM, Hyde JS. Functional connectivity in the motor cortex of resting human brain using echo-planar mri. *Magn Reson Med*, 34:537-541, 1995.
- **88**. Colclough GL, Woolrich MW, Tewarie P, Brookes MJ, Quinn AJ, Smith SM. How reliable are MEG resting-state connectivity metrics? *Neuroimage*, 138:284-293, 2016.
- **89**. Fox MD, Greicius M. Clinical applications of resting state functional connectivity. *Front Syst Neurosci*, 4:19, 2010.
- **90**. Cole MW, Bassett DS, Power JD, Braver TS, Petersen SE. Intrinsic and task-evoked network architectures of the human brain. *Neuron*, 83:238-251, 2014.
- **91**. Power JD, Cohen AL, Nelson SM, et al. Functional network organization of the human brain. *Neuron*, 72:665-678, 2011.

- **92**. Yeo BT, Krienen FM, Sepulcre J, et al. The organization of the human cerebral cortex estimated by intrinsic functional connectivity. *J Neurophysiol*, 106:1125-1165, 2011.
- **93**. Brookes MJ, Woolrich M, Luckhoo H, et al. Investigating the electrophysiological basis of resting state networks using magnetoencephalography. *Proc Natl Acad Sci*, 108:16783-16788, 2011.
- **94**. He BJ, Snyder AZ, Vincent JL, Epstein A, Shulman GL, Corbetta M. Breakdown of functional connectivity in frontoparietal networks underlies behavioral deficits in spatial neglect. *Neuron*, 53:905-918, 2007.
- **95**. Schäfer CB, Morgan BR, Ye AX, Taylor MJ, Doesburg SM. Oscillations, networks, and their development: MEG connectivity changes with age. *Hum Brain Mapp*, 35:5249-5261, 2014.
- **96**. Schlee W, Leirer V, Kolassa I-T, Weisz N, Elbert T. Age-related changes in neural functional connectivity and its behavioral relevance. *BMC Neurosci*, 13:16, 2012.
- **97**. Vidal-Piñeiro D, Valls-Pedret C, Fernández-Cabello S, et al. Decreased default

- mode network connectivity correlates with age-associated structural and cognitive changes. *Front Aging Neurosci*, 6:256, 2014.
- **98**. Yang Y, Zhong N, Imamura K, et al. Task and resting-state fMRI reveal altered salience responses to positive stimuli in patients with major depressive disorder. *PloS One*, 11:e0155092, 2016.
- **99**. Sheng M, Liu P, Mao D, Ge Y, Lu H. The impact of hyperoxia on brain activity: A resting-state and task-evoked electroencephalography (EEG) study. *PloS One*, 12:e0176610, 2017.
- **100**. Mannell MV, Franco AR, Calhoun VD, Cañive JM, Thoma RJ, Mayer AR. Resting state and task-induced deactivation: A methodological comparison in patients with schizophrenia and healthy controls. *Hum Brain Mapp*, 31:424-437, 2010.
- **101**. De Havas JA, Parimal S, Soon CS, Chee MW. Sleep deprivation reduces default mode network connectivity and anti-correlation during rest and task performance. *Neuroimage*, 59:1745-1751, 2012.
- **102**. Schneider F, Bermpohl F, Heinzel A, et al. The resting brain and our self: self-

relatedness modulates resting state neural activity in cortical midline structures. *Neurosci*, 157:120-131, 2008.

- **103**. Waites AB, Stanislavsky A, Abbott DF, Jackson GD. Effect of prior cognitive state on resting state networks measured with functional connectivity. *Hum Brain Mapp*, 24:59-68, 2005.
- **104**. Sami S, Robertson EM, Miall RC. The time course of task-specific memory consolidation effects in resting state networks. *J Neurosci*, 34:3982-3992, 2014.
- **105**. Vahdat S, Darainy M, Milner TE, Ostry DJ. Functionally specific changes in resting-state sensorimotor networks after motor learning. *J Neurosci*, 31:16907-16915, 2011.
- **106**. Bellec P, Benhajali Y, Carbonell F, et al. Impact of the resolution of brain parcels on connectome-wide association studies in fMRI. *Neuroimage*, 123:212-228, 2015.
- **107**. Leal SL, Yassa MA. Perturbations of neural circuitry in aging, mild cognitive impairment, and Alzheimer's disease. *Ageing Res Rev*, 12:823-831, 2013.

- **108**. Colclough G, Brookes MJ, Smith SM, Woolrich MW. A symmetric multivariate leakage correction for MEG connectomes. *Neuroimage*, 117:439-448, 2015.
- **109**. Zimerman M, Hummel FC. Non-invasive brain stimulation: enhancing motor and cognitive functions in healthy old subjects. *Front Aging Neurosci*, 2:149, 2010.
- **110**. Bashir S, Mizrahi I, Weaver K, Fregni F, Pascual-Leone A. Assessment and modulation of neural plasticity in rehabilitation with transcranial magnetic stimulation. *PM R*, 2:S253-S268, 2010.
- **111**. Rossini PM, Rossi S, Babiloni C, Polich J. Clinical neurophysiology of aging brain: from normal aging to neurodegeneration. *Prog Neurobiol*, 83:375-400, 2007.
- **112**. Finnigan S, Robertson IH. Resting EEG theta power correlates with cognitive performance in healthy older adults. *Int J Psychophysiol*, 48:1083-1087, 2011.
- **113**. Babiloni C, Binetti G, Cassarino A, et al. Sources of cortical rhythms in adults during physiological aging: a multicentric EEG study. *Hum Brain Mapp*, 27:162-172, 2006.

- **114**. Leirer VM, Wienbruch C, Kolassa S, Schlee W, Elbert T, Kolassa I-T. Changes in cortical slow wave activity in healthy aging. *Brain Imaging Behav*, 5:222-228, 2011.
- 115. Maurits NM, Scheeringa R, van der Hoeven JH, de Jong R. EEG coherence obtained from an auditory oddball task increases with age. *J Clin Neurophysiol*, 23:395-403, 2006.
- 116. Szczepanski SM, Crone NE, Kuperman RA, Auguste KI, Parvizi J, Knight RT. Dynamic changes in phase-amplitude coupling facilitate spatial attention control in fronto-parietal cortex. *PLoS Biol*, 12:e1001936, 2014.
- **117**. Caplan JB, Bottomley M, Kang P, Dixon RA. Distinguishing rhythmic from non-rhythmic brain activity during rest in healthy neurocognitive aging. *Neuroimage*, 112:341-352, 2015.
- **118**. Glasser MF, Coalson TS, Robinson EC, et al. A multi-modal parcellation of human cerebral cortex. *Nature*, 536:171-178, 2016.
- **119**. Krueger H, Koot J, Hall RE, O'callaghan C, Bayley M, Corbett D. Prevalence of Individuals Experiencing the

- Effects of Stroke in Canada. *Stroke*, 46:2226-2231, 2015.
- **120**. Ward NS. Restoring brain function after stroke—bridging the gap between animals and humans. *Nat Rev Neurol*, 13:244-255, 2017.
- **121**. Bernhardt J, Borschmann K, Boyd L, et al. Moving rehabilitation research forward: Developing consensus statements for rehabilitation and recovery research. *Intl J Stroke*, 11:454-458, 2016.
- **122**. Desmond DW, Moroney JT, Sano M, Stern Y. Recovery of cognitive function after stroke. *Stroke*, 27:1798-1803, 1996.
- **123**. Crichton SL, Bray BD, McKevitt C, Rudd AG, Wolfe CD. Patient outcomes up to 15 years after stroke: survival, disability, quality of life, cognition and mental health. *J Neurol Neurosurg Psychiatry*, 87:1091-1098, 2016.
- **124**. Mittmann N, Seung SJ, Hill MD, et al. Impact of disability status on ischemic stroke costs in Canada in the first year. *Can J Neurol Sci*, 39:793-800, 2012.

- **125**. Kalladka D, Sinden J, Pollock K, et al. Human neural stem cells in patients with chronic ischaemic stroke (PISCES): a phase 1, first-in-man study. *Lancet*, 388:787-796, 2016.
- **126**. Azad TD, Veeravagu A, Steinberg GK. Neurorestoration after stroke. *Neurosurg Focus*, 40:E2, 2016.
- **127**. Chollet F, Tardy J, Albucher J-F, et al. Fluoxetine for motor recovery after acute ischaemic stroke (FLAME): a randomised placebo-controlled trial. *Lancet Neurol*, 10:123-130, 2011.
- **128**. Rehme AK, Volz LJ, Feis DL, Eickhoff SB, Fink GR, Grefkes C. Individual prediction of chronic motor outcome in the acute post-stroke stage: Behavioral parameters versus functional imaging. *Hum Brain Mapp*, 36:4553-4565, 2015.
- **129**. Strimbu K, Tavel JA. What are biomarkers? *Curr Opin HIV AIDS*, 5:463, 2010.
- **130**. Grefkes C, Fink GR. Reorganization of cerebral networks after stroke: new insights from neuroimaging with connectivity approaches. *Brain*, 134:1264-1276, 2011.

- **131**. Carey LM, Abbott DF, Egan GF, et al. Evolution of brain activation with good and poor motor recovery after stroke. *Neurorehabil Neural Repair*, 20:24-41, 2006.
- **132**. Rehme AK, Eickhoff SB, Wang LE, Fink GR, Grefkes C. Dynamic causal modeling of cortical activity from the acute to the chronic stage after stroke. *Neuroimage*, 55:1147-1158, 2011.
- **133**. Rehme AK, Eickhoff SB, Rottschy C, Fink GR, Grefkes C. Activation likelihood estimation meta-analysis of motor-related neural activity after stroke. *Neuroimage*, 59:2771-2782, 2012.
- **134**. Favre I, Zeffiro TA, Detante O, Krainik A, Hommel M, Jaillard A. Upper Limb Recovery After Stroke Is Associated With Ipsilesional Primary Motor Cortical Activity. *Stroke*, 45:1077-1083, 2014.
- **135**. Stewart JC, Dewanjee P, Shariff U, Cramer SC. Dorsal premotor activity and connectivity relate to action selection performance after stroke. Hum Brain Mapp, 37:1816-1830, 2016.
- **136**. Roland PE, Larsen B, Lassen NA, Skinhoj E. Supplementary motor area and

other cortical areas in organization of voluntary movements in man. J *Neurophysiol*, 43:118-136, 1980.

- **137**. Nirkko A, Ozdoba C, Redmond S, et al. Different ipsilateral representations for distal and proximal movements in the sensorimotor cortex: activation and deactivation patterns. *Neuroimage*, 13:825-835, 2001.
- **138**. Galea MP, Darian-Smith I. Multiple corticospinal neuron populations in the macaque monkey are specified by their unique cortical origins, spinal terminations, and connections. *Cereb Cortex*, 4:166-194, 1994.
- **139**. Westlake KP, Nagarajan SS. Functional connectivity in relation to motor performance and recovery after stroke. *Front Syst Neurosci*, 5:8, 2011.
- **140**. Liu J, Qin W, Wang H, et al. Altered spontaneous activity in the default-mode network and cognitive decline in chronic subcortical stroke. *J Neurol Sci*, 347:193-198, 2014.
- **141**. Tuladhar AM, Snaphaan L, Shumskaya E, et al. Default mode network connectivity in stroke patients. *PLoS One*, 8:e66556, 2013.

- **142**. Park JY, Kim YH, Chang WH, et al. Significance of longitudinal changes in the default-mode network for cognitive recovery after stroke. *Eur J Neurosci*, 40:2715-2722, 2014.
- **143**. Mason MF, Norton MI, Van Horn JD, Wegner DM, Grafton ST, Macrae CN. Wandering minds: the default network and stimulus-independent thought. *Science*, 315:393-395, 2007.
- **144**. Gusnard DA, Raichle ME. Searching for a baseline: functional imaging and the resting human brain. *Nat Rev Neurosci*, 2:685-694, 2001.
- **145**. Vatansever D, Menon DK, Manktelow AE, Sahakian BJ, Stamatakis EA. Default mode dynamics for global functional integration. *J Neurosci*, 35:15254-15262, 2015.
- **146**. Margulies DS, Ghosh SS, Goulas A, et al. Situating the default-mode network along a principal gradient of macroscale cortical organization. *Proc Natl Acad Sci*, 113:12574-12579, 2016.
- **147**. Abe M, Hanakawa T. Functional coupling underlying motor and cognitive

functions of the dorsal premotor cortex. *Behav Brain Res*, 198:13-23, 2009.

- **148**. Kantak SS, Stinear JW, Buch ER, Cohen LG. Rewiring the brain potential role of the premotor cortex in motor control, learning, and recovery of function following brain injury. *Neurorehabil Neural Repair*, 26:282-292, 2012.
- **149**. Dacosta-Aguayo R, Graña M, Iturria-Medina Y, et al. Impairment of functional integration of the default mode network correlates with cognitive outcome at three months after stroke. *Hum Brain Mapp*, 36:577-590, 2015.
- **150**. Metzak P, Feredoes E, Takane Y, et al. Constrained principal component analysis reveals functionally connected load-dependent networks involved in multiple stages of working memory. *Hum Brain Mapp*, 32:856-871, 2011.
- **151**. Woodward TS, Feredoes E, Metzak PD, Takane Y, Manoach DS. Epoch-specific functional networks involved in working memory. *Neuroimage*, 65:529-539, 2013.
- **152**. Sunderland A, Tinson D, Bradley L, Hewer RL. Arm function after stroke. An

evaluation of grip strength as a measure of recovery and a prognostic indicator. *J Neurol Neurosurg Psychiatry*, 52:1267-1272, 1989.

- **153**. Smith SM, Nichols TE. Threshold-free cluster enhancement: addressing problems of smoothing, threshold dependence and localisation in cluster inference. *Neuroimage*, 44:83-98, 2009.
- **154**. Buckner RL, Andrews-Hanna JR, Schacter DL. The brain's default network. *Ann N Y Acad Sci*, 1124:1-38, 2008.
- **155**. Raichle ME, MacLeod AM, Snyder AZ, Powers WJ, Gusnard DA, Shulman GL. A default mode of brain function. *Proc Natl Acad Sci*, 98:676-682, 2001.
- **156**. Wadden KP, Woodward TS, Metzak PD, et al. Compensatory motor network connectivity is associated with motor sequence learning after subcortical stroke. *Behav Brain Res*, 286:136-145, 2015.
- **157**. Borich MR, Brown KE, Boyd LA. Motor skill learning is associated with diffusion characteristics of white matter in individuals with chronic stroke. *J Neurol Phys Ther*, 38:151, 2014.

- . Buxton RB, Uludağ K, Dubowitz DJ, Liu TT. Modeling the hemodynamic response to brain activation. *Neuroimage*, 23:S220-S233, 2004.
- . Goense JB, Logothetis NK. Neurophysiology of the BOLD fMRI signal in awake monkeys. *Curr Biol*, 18:631-640, 2008.
- . Altamura C, Torquati K, Zappasodi F, et al. fMRI-vs-MEG evaluation of post-stroke interhemispheric asymmetries in primary sensorimotor hand areas. *Exp Neurol*, 204:631-639, 2007.
- **161**. Rossini P, Altamura C, Ferretti A, et al. Does cerebrovascular disease affect the coupling between neuronal activity and local haemodynamics? *Brain*, 127:99-110, 2004.
- . Rowe J. Connectivity analysis is essential to understand neurological disorders. *Front Syst Neurosci*, 4:144, 2010.
- **163**. Henson R, Rugg MD, Friston KJ. The choice of basis functions in event-related fMRI. *Neuroimage*, 13:149-149, 2001.
- . Mullinger KJ, Mayhew SD, Bagshaw AP, Bowtell R, Francis ST. Poststimulus

- undershoots in cerebral blood flow and BOLD fMRI responses are modulated by poststimulus neuronal activity. *Proc Natl Acad Sci*, 110:13636-13641, 2013.
- . Brumm KP, Perthen JE, Liu TT, Haist F, Ayalon L, Love T. An arterial spin labeling investigation of cerebral blood flow deficits in chronic stroke survivors. *Neuroimage*, 51:995-1005, 2010.
- . Corbetta M, Kincade MJ, Lewis C, Snyder AZ, Sapir A. Neural basis and recovery of spatial attention deficits in spatial neglect. *Nat Neurosci*, 8:1603, 2005.
- . Spreng RN, Sepulcre J, Turner GR, Stevens WD, Schacter DL. Intrinsic architecture underlying the relations among the default, dorsal attention, and frontoparietal control networks of the human brain. *J Cognitive Neurosci*, 25:74-86, 2013.
- . Nijboer TC, Kollen BJ, Kwakkel G. Time course of visuospatial neglect early after stroke: a longitudinal cohort study. *Cortex*, 49:2021-2027, 2013.
- . Coifman RR, Lafon S, Lee AB, et al. Geometric diffusions as a tool for harmonic analysis and structure definition of data:

Diffusion maps. *Proc Natl Acad Sci USA*, 102:7426-7431, 2005.

PART V | APPENDIX

APPENDIX A

Behavioral data acquisition

Grip strength was measured using a hand-held dynamometer, and the maximum value of three trials was taken as the maximum grip strength for each hand. Fine motor skills were measured using the NHPT; we calculated the time it took to place all the pegs into the nine holes and subsequently remove them (scores were recorded as pegs per second for each hand). Unilateral gross manual dexterity was assessed using the BBT which measures the number of blocks transferred from one side of the box to the other in 60 s (scores were recorded for each hand separately).

Data acquisition and preprocessing

Prior to the MEG data acquisition, three head position indicator (HPI) coils were placed on each participant's head and three anatomical fiducials were recorded at the nasion and preauricular points. Fiducial points, HPI coils, and scalp points defining each subject's head shape were acquired using a 3D digitiser (Polhemus Inc., Vermont). MEG data were continuously acquired using a 275 channel CTF system at a sampling rate of 2400 Hz. Head movement within the scanner was continuously measured throughout the recordings by periodically energising the HPI coils.

Following the MEG recording, all participants underwent a whole-brain structural MRI scan acquired using a 1.5T Siemens Sonata (spoiled gradient recalled sequence: 8-channel coil; repetition time = 27 ms; echo time = 9.2 ms; $1 \times 1 \times 1 \text{ mm}$ voxels; flip angle = 30° ; field of view = $256 \times 240 \text{ mm}$). Coregistration of the MEG data to the MRI structural images was achieved by registering the three reference fiducial points and the digitized head surface to the head surface extracted from the MRI scan.

The MEG data recordings were applied a third-order synthetic gradient, band-pass filtered offline (1–80 Hz for task-related MEG data and 1–150 Hz for resting-state MEG data), included a notch filter at 60 Hz and 120 Hz, and down sampled to 160 Hz (task) and 300 Hz (rest). Visual inspection of each recording was performed and segments of data containing an excessive amount of artifacts (e.g., muscle movement) were discarded. Signal-space projection was subsequently used to remove heartbeat and eye-blink artifacts identified using electrocardiogram and electrooculogram data.

APPENDIX B

Data acquisition and preprocessing

Imaging was performed on a 3T TRIO scanner (Siemens, Erlangen, Germany) using a 12-channel head coil. All subjects underwent a single scanning session during which all functional images were collected using a T2*-weighted MRI transverse echo-planar images (EPI) with the following parameters: 130 functional volumes consisting of 48 axial slices; thickness/gap = 2.5 mm; matrix = 64×64 ; repetition time (TR) = 3250 ms; echo time (TE) = 30 ms; voxel size = $3 \times 3 \times 3$ mm; flip angle (FA) = 90° ; field of view (FOV) = 192 mm. The first six volumes were discarded to allow for T1 equilibrium effects, and data from the remaining 124 volumes were used in the analysis. A high resolution T1-weighted anatomical image (176 partitions; matrix = 256×240 ; TR = 7.92ms; TE = 2.48ms; $1.3 \times 1.3 \times 1.3$ mm voxels; FA = 16° ; FOV = 256×240 mm) and a field map (TE1 = 10 ms and TE2 = 12.46 ms, $3 \times 3 \times 2$ mm resolution, 1 mm gap) were also acquired.

The data were preprocessed using Statistical Parametric Mapping 8 (SPM8; Wellcome Trust Centre for Neuroimaging, UK). For each subject, all functional images were realigned and unwarped to account for movement artefacts, co-registered to the subject's structural image, normalized to the Montreal Neurological Institute echo planar imaging template (voxel size = $2 \times 2 \times 2$ mm), and spatially smoothed using an $8 \times 8 \times 8$ mm full width at half maximum Gaussian filter. No participants included in the current study showed motion correction that exceeded 4 mm or degrees on any axis.

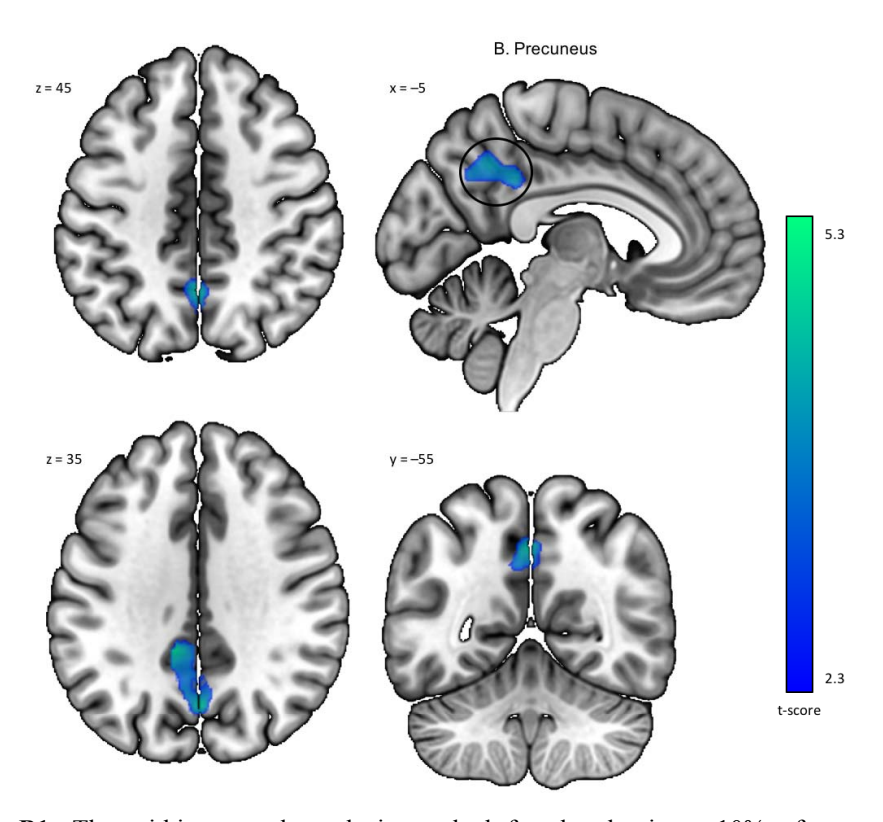


Figure B1: The within-network analysis masked for the dominant 10% of component loadings for the Default-Mode Network (Component 4) revealed significantly reduced deactivity in bilateral precuneus in stroke patients relative to control subjects ($p_{corr} < 0.05$).

	Control	Stroke
Test	Subjects	Patients
BBT^a	63.75 (11.5)	27.06 (16.8)
$NHPT^a$	0.74 (0.1)	0.26 (0.24)
Grip strength ^a	82.87 (25.6)	36.98 (29.4)

Table B1: Behavioral results. Standard deviations in parentheses. BBT, Box and Block Test (number of blocks transferred in a minute); NHPT, Nine Hole Peg Test (pegs/s); grip strength (kg). a Control > Stroke, p < 0.001.

Cortical regions	Cluster volume		BAs for	Peak MNI coordinates		
	(mm ³)	(voxels)	peak locations	х	у	z
Positive loadings				,		
Cluster 1: bilateral	79,464	9933				
Precuneus			7	0	-46	60
Superior parietal lobule			7	-30	-48	60
Anterior intraparietal sulcus			7	-34	-40	44
Cingulate gyrus, posterior division			23	0	-20	44
Cingulate gyrus, anterior division			24	2	12	38
Postcentral gyrus			2	-54	-22	40
Central opercular cortex			43	-58	-20	18
Inferior frontal gyrus, pars opercularis			44	56	10	4
Cluster 1: right hemisphere Lateral occipital cortex, superior division			39	28	-74	34
Cluster 2: left hemisphere	10,672	1334				
Lateral occipital cortex, inferior division			37	-44	-70	2
Cerebellum – Lobule VI			n/a	-26	-60	-20
Cluster 3: right hemisphere	4736	592				
Cerebellum – Lobule VI			n/a	28	-60	-20
Cluster 4: left hemisphere	4144	518				
Lateral occipital cortex, superior division			39	-22	-76	32
Cluster 5: right hemisphere	1640	205				
Putamen	1040	203	n/a	26	0	-10
			11/4	20	Ü	10
Cluster 6: right hemisphere	760	95				
Thalamus			n/a	10	-16	6
Cluster 7: left hemisphere	512	64				
Primary visual cortex		· ·	17	-14	-72	10
I Illiary visual cortex			1 /	-14	-12	10

Table B2. Cluster volumes for the most extreme 5% of Component 1 loadings, Montreal Neurological Institute (MNI) coordinates, and Brodmann area (BA) for the peak locations within each cluster.

Cortical regions	Cluster volume		BAs for	Peak MNI coordinates		
	(mm^3)	(voxels)	peak locations	x	y	z
Positive loadings		1			I	
Cluster 1: right hemisphere Lateral occipital cortex, superior division Lateral occipital cortex, inferior division Occipital fusiform gyrus Primary visual cortex Inferior temporal gyrus, temporooccipital part Temporal occipital fusiform cortex	30,552	3819	19 18 18 17 19	36 44 28 24 48 30	-84 -84 -86 -100 -56 -54	16 0 -10 -10 -16 -12
Cluster 2: left hemisphere Lateral occipital cortex, superior division Lateral occipital cortex, inferior division Occipital fusiform gyrus Primary visual cortex Inferior temporal gyrus, temporooccipital part Temporal occipital fusiform cortex	25,080	3135	19 18 18 17 19	-30 -42 -28 -16 -52 -44	-88 -88 -86 -98 -60	12 -4 -14 -14 -12 -14
Cluster 3: left hemisphere Middle frontal gyrus Superior parietal lobule Postcentral gyrus	18,624	2328	6 7 1	-36 -36 -46	-2 -42 -28	64 64 64
Cluster 4: right hemisphere Inferior temporal gyrus, posterior division Inferior temporal gyrus, anterior division	14,328	1791	37 20	52 52	-28 -4	-20 -40
Cluster 5: left hemisphere Inferior temporal gyrus, posterior division Inferior temporal gyrus, anterior division Temporal fusiform cortex	5792	724	37 20 37	-50 -50 -36	-28 -10 -20	-16 -38 -28
Cluster 6: right hemisphere Cerebellum – Lobule VI Cerebellum – Lobule V	4032	504	n/a n/a	26 8	-54 -54	-26 -14
Cluster 7: right hemisphere Superior parietal lobule	1856	232	7	36	-44	66
Cluster 8: right hemisphere Precentral gyrus	1408	176	6	36	-4	66

Table B3. Cluster volumes for the most extreme 5% of Component 2 loadings, Montreal Neurological Institute (MNI) coordinates, and Brodmann area (BA) for the peak locations within each cluster.

Cortical regions	Cluster volume		BAs for	Peak MNI coordinates		
	(mm^3)	(voxels)	peak locations	x	y	Z
Positive loadings				<u>"</u>		
Cluster 1: bilateral	66,528	8316				
Supplementary motor cortex			6	0	-6	62
Precentral gyrus			6	-30	-10	62
Precentral gyrus			4	-2	-22	52
Superior frontal gyrus			6	18	-6	68
Cluster 1: left hemisphere				40	2.4	7 0
Postcentral gyrus			1	-42	-24	58
Postcentral gyrus			2	-40 20	-38	56
Postcentral gyrus			3 7	−28 −34	-32	56 58
Superior parietal lobule			/	-34	-48	38
Cluster 1: right hemisphere						
Precentral gyrus			6	52	4	38
Cluster 2: right hemisphere	8392	1049				
Superior parietal lobule			7	36	-38	52
Lateral occipital cortex, superior division			7	24	-58	52
Postcentral gyrus			2	52	-20	42
Cluster 3: left hemisphere	2760	345				
Precentral gyrus			6	-54	2	38
Precentral gyrus			44	-54	6	24
Negative loadings						
Cluster 1: bilateral	26,032	3254				
Visual cortex	,	5-U.	18	4	-84	22
Primary visual cortex			17	4	-90	2
Cerebellum – Crus I			n/a	34	-64	-26
Cerebellum – Vermis VI			n/a	2	-78	-26

Table B4. Cluster volumes for the most extreme 5% of Component 3 loadings, Montreal Neurological Institute (MNI) coordinates, and Brodmann area (BA) for the peak locations within each cluster.

Cortical regions	Cluster volume		BAs for	Peak MNI coordinates		
	(mm^3)	(voxels)	peak locations	x	y	z
Negative loadings				<u> </u>		
Cluster 1: bilateral Superior frontal gyrus Dorsomedial prefrontal cortex Ventromedial prefrontal cortex Orbitofrontal cortex	54,256	6782	9 9 10 11	-10 -4 0	38 58 54 44	54 28 6 -14
Cluster 2: bilateral Precuneus Cingulate gyrus, posterior division	17,400	2175	7 23	2 2	-56 -40	38 30
Cluster 3: right hemisphere Middle temporal gyrus, posterior division Middle temporal gyrus, anterior division	6488	811	21 38	56 56	-16 4	-14 -30
Cluster 4: right hemisphere Lateral occipital cortex, superior division	5632	704	7	56	-62	30
Cluster 5: left hemisphere Lateral occipital cortex, superior division	4264	533	7	-48	-66	30
Cluster 6: left hemisphere Middle temporal gyrus, posterior division Middle temporal gyrus, anterior division	4024	503	21 38	-54 -54	-30 -6	-10 -22
Cluster 7: right hemisphere Orbitofrontal cortex	3248	406	47	38	38	-16
Cluster 8: left hemisphere Hippocampus	2368	296	n/a	-26	-18	-18
Cluster 9: right hemisphere Hippocampus	2176	272	n/a	28	-18	-18
Cluster 10: left hemisphere Orbitofrontal cortex	2024	253	47	-36	32	-16

Table B5. Cluster volumes for the most extreme 5% of Component 4 loadings, Montreal Neurological Institute (MNI) coordinates, and Brodmann area (BA) for the peak locations within each cluster.